ACTA PHARMACEUTICA
SCIENCIA

International Journal in Pharmaceutical Sciences, Published Quarterly

ACTA PHARMACEUTICA SCIENCIA

Contents

Aims and Scope of Acta Pharmaceutica Sciencia

Acta Pharmaceutica Sciencia is a continuation of the former "Eczacılık Bülteni" which was first published in 1953 by Prof. Dr. Kasım Cemal GÜVEN's editorship. At that time, "Eczacılık Bülteni" hosted scientific papers from the School of Medicine-Pharmacy at Istanbul University, Turkey.

In 1984, the name of the journal was changed to "Acta Pharmaceutica Turcica" and it became a journal for national and international manuscripts, in all fields of pharmaceutical sciences in both English and Turkish. (1984-1995, edited by Prof. Dr. Kasım Cemal GÜVEN, 1995-2001, edited by Prof. Dr. Erden GÜLER, 2002-2011, edited by Prof. Dr. Kasım Cemal GÜVEN)

Since 2006, the journal has been published only in English with the name, "Acta Pharmaceutica Sciencia" which represents internationally accepted high-level scientific standards. The journal has been published quarterly except for an interval from 2002 to 2009 in which its issues were released at intervals of four months. The publication was also temporarily discontinued at the end of 2011 but since 2016, Acta Pharmaceutica Sciencia has continued publication with the reestablished Editorial Board and also with the support of you as precious scientists.

Yours Faithfully

Prof. Dr. Şeref DEMİRAYAK

Editor

Development of Directly Compressible Excipients from Phoenix dactylifera (Date) Mucilage and Microcrystalline Cellulose using Co-Processing Techniques

Olufunke D. Akin-Ajani[1], Tolulope O. Ajala[1]*, Uchenna M. Okoli[1], Ozioma Okonta[1]

1 University of Ibadan, Faculty of Pharmacy, Department of Pharmaceutics & Industrial Pharmacy, Ibadan, Nigeria.

ABSTRACT

The objective of this study was to harness the excipient potential of date mucilage by co-grinding and co-fusing with avicel for enhanced performance in the direct-compression of metronidazole.

Co-grinding and co-fusing of parent polymers were done using established methods and excipients were used in the direct-compression of metronidazole tablets.

The shape and surface morphology of the particles of date mucilage (DAM) and co-processed excipients were generally granular, rough and irregular. There was a significant improvement in the disintegration of tablets prepared using the co-processed excipients in comparison to that prepared using DAM alone. The disintegration time for tablets prepared using co-fused excipients was lower than that of co-grinded additives although the differences were not significant (p > 0.05).

Generally, the co-processed excipients improved the mechanical and disintegration properties of the tablets produced compared to tablets prepared using DAM alone and could be further developed as direct-compression excipients.

Keywords: Date mucilage, avicel, co-processing, metronidazole tablets.

INTRODUCTION

Excipient functionality has been expanded by direct compression process and the need to use high-speed equipment in tablet manufacturing. The increase in the speed of tableting machinery requires the use of excipients that can offer high weight consistency and good compressibility[1]. In addition, new drug moieties with unpredictable physicochemical and stability properties are constantly being introduced and existing adjuvants like microcrystalline cellulose loses compaction

upon wet granulation and demonstrates poor die filling as a result of agglomeration[2]. There is therefore a need to search for newer excipients or prepare novel ones from existing forms. Furthermore, direct compression is the preferred method for the preparation of tablets due to reduced processing steps, faster processing, usefulness for substances having high moisture sensitivity and cost[3].

One of the methods of obtaining functional excipients having direct-compression properties with inherent ability to demonstrate the properties of two or more excipients is co-processing. IPEC[4] has described a co-processed additive as any excipient obtained by combining two or more materials together using physical methods to modify their properties without any chemical alteration. The starting materials may be compendia or non-compendia excipients. Co-processed excipients are prepared by incorporating one excipient into the particle structure of another, using processes such as co-drying, co-grinding and co-fusion. Co-processing is involved with particle manipulation of two or more existing excipients in which the interaction occurs at sub-particulate level yielding simple physical mixtures and no chemical changes are expected to occur[5]. A synergy is obtained between the particles of the participant excipients with ultimate functionality improvements, concealing undesirable properties[5]. Co-processing has been found to be easy, cost-effective and has also been used to improve stability, wettability, solubility and gelling properties of food and pharmaceutical excipients[6]. For example, Cellactose® is a co-processed product from the combination of cellulose (25 %) and lactose monohydrate (75 %); it has good flowability and good compactibility. The compactibility has been attributed to a synergistic effect of consolidation by fragmentation of lactose and plastic deformation of cellulose[7]. It has been pointed out that cellactose® exhibits dual consolidation behaviour since it contains a fragmenting component (lactose) and a substance (cellulose) that consolidates mainly by plastic deformation[8]. Furthermore, co-processed excipients find application in drug delivery systems by enhancing the pharmaceutical properties of the dosage forms such as accurate dosing hence improving therapeutic efficacy and further patient compliance[9].

Phoenix dactylifera popularly known as date (also called Nakhla and 'tree of life' by the Arabs, Nigerian local name in Hausa-Dabino) is a member of the palm family Arecaceae or Palmae[10]. It has been reported that date palm has its origin in countries with a coastline on the Persian Gulf such as Kuwait, Omar, Qatar, Bahrain, Iraq, Saudi Arabia and UAE[11].

The date palm *(Phoenix dactylifera L.)* is one of the oldest cultivated fruit trees and has been used as staple food in the Middle East for over 6000 years[12]. Dates and their constituents show a role in the prevention of diseases through anti-oxidant[13], anti-inflammatory and anti-bacterial activity[14]. Rahmani et al., also report-

ed the therapeutic effects of date fruits in the prevention of cancer via modulation of anti-tumour activity[15]. Dates can be classified as foods with low glycaemic index most likely due to the high amount of fructose[16]. This has made date fruit a useful aid in diabetic management and its use has been reported to reduce HbA1c[16]. *Phoenix dactylifera* is known to contain high concentration of polysaccharides, proteins, fats and edible fibre[17].

The presence of polysaccharides, safety, availability and usefulness as food has made dates to be of interest in excipient development for pharmaceuticals. Ngwuluka et al., studied the binding potentials of the dried and milled pulp of the fruit[18] but the excipient potentials of date fruit mucilage have remained largely unharnessed. Mucilage is the polymeric slimy material which is a normal product of cell wall and is readily available in certain fruits. Ajala et al., studied the binding potentials of *Chrysophylum albidum* fruit mucilage and reported that it induces faster onset of plastic deformation and higher amount of total plastic deformation but produced tablets with lower tensile strength and faster drug release properties than methylcellulose[19]. In this study, the mucilage of date fruit was extracted and purified by established methods[20] and preliminary studies on the tableted mucilage showed very hard tablets with disintegration times greater than 1 h. Co-processing of this novel mucilage with microcrystalline cellulose was explored using co-grinding and co-fusion methods in order to improve the disintegration properties. The products of the co-processing techniques were then used for direct compression of metronidazole tablets.

METHODOLOGY

Materials

Metronidazole powder was obtained from Suixian Hengtai Biotechnology Co., Ltd. China Mainland; Microcrystalline cellulose (Avicel® PH-101) was obtained from FPC Bio polymer, USA; all other reagents were of analytical grade.

Extraction and purification of mucilage from dried date fruits

The method of *Ajala et al*, was used with modification[19]. Dried fruits of *Phoenix dactylifera* were deseeded, cut into pieces and soaked in chloroform-water Double Strength for 36 h. This was then sieved with a muslin cloth to remove the extraneous matter. Ethanol (90 %$^v/_v$) was then used to precipitate the mucilage and further purification was done using di-ethyl ether. The mucilage was then dried at 40 °C in a hot air oven and coded DAM i.e. date mucilage.

Co-processing of excipients

The co-excipients were prepared using two methods (co-grinding and co-fusion) as described below: Date mucilage (DAM) and avicel® (AV) were weighed according

to the proportional quantities (25:75, 33:67 and 50:50) in the respective batch. The weighed quantities of the DAM and AV were triturated together using a porcelain mortar and pestle for 10 min to ensure uniform size reduction and powder mixing. The resulting product was further screened using a sieve of mesh size 0.25 mm to reduce the particle size. The method was repeated for each batch to obtain the co-grinded excipients and coded DAMAV. For the co-fused excipients, a weighed amount of DAM according to the proportions (25 %) calculated was made into a paste using distilled water. Appropriate quantity (75 %) of AV was also premixed with distilled water and added to the dispersed DAM in aliquots. The mixture was stirred occasionally on a water bath until a homogenous mixture was observed. This process was repeated for the remaining batches (33:67 and 50:50). The paste obtained was spread evenly on a slab and dried in a hot air oven (Model 77-9083, Techmel & Techmel, China) at 50 °C. It was later pulverized with mortar and pestle and the particle size was further reduced by using a sieve of mesh size 0.25 mm.

Swelling capacity

Co-processed excipients (5 g) were transferred into a 50 mL measuring cylinder and the volume occupied was noted. Distilled water was then added gradually making up to 50 mL with thorough agitation for 5 min. The dispersion was allowed to stand for 24 h. The sedimentation volume was measured and swelling capacity was calculated using equation 1.

Swelling capacity = $\frac{V2 - V1}{V1} * 100$

(V_1: initial volume, V_2: final volume) (1)

Determination of particle density

The particle density of the excipients was determined by the liquid-pycnometer method using xylene as the displacement liquid[21]. An empty 50 mL pycnometer bottle with its lid was weighed empty (W), it was then overfilled with xylene and covered with the lid, wiped off the excess and weighed (W1). The sample of excipient (2 g) was weighed (W3) and transferred into the pycnometer bottle, covered with the lid and excess xylene wiped off the surface of the bottle. This was weighed again (W4). The particle density was then calculated using equation 2.

Particle density = $\frac{W2 * W3}{50\{(W3-W4)+(W2-W)\}}$ (2)

Determination of bulk and tapped densities

The bulk density of the excipients was determined by weighing 10 g of the sample and transferring it at an angle of 45° through a funnel into a 100 mL glass measuring cylinder with a diameter of 3.0 cm The height reached by the powder was recorded and the volume and density were then calculated[22].

Bulk density = $\dfrac{m}{\pi r^2 h}$ (3)

where:

m = weight of the sample in the cylinder,

r = radius of the cylinder,

h = height of the sample in the cylinder.

The method of Reus-Medina[23] was used in evaluating the tapped volume and density using a weighed quantity (10 g) of the excipients. Tapping rate was standardized with 38 taps per minute and a total of 250 taps was applied to the material in a graduated glass cylinder. The height, h (cm) of the powder bed and the internal radius, r (cm) of the measuring cylinder were utilized in the computation of the volumes obtained.

The Carr's index[24] and Hausner's ratio[25] were computed from the bulk and tapped densities using the formula below in equations below:

Carr's index = $\dfrac{\text{Tapped density-Bulk density}}{\text{Tapped density}}$ *100   (4)

Hausner's ratio = $\dfrac{\text{Tapped volume}}{\text{Bulk volume}}$ (5)

Determination of angle of repose

Weighed quantities of each excipient (5 g) were poured slowly through a funnel under the force of gravity to form a conical heap[26]. The angle of repose was then calculated as:

Angle of repose $(\tan \theta) = \dfrac{h}{r}$ (6)

Where

h= height of powder heap

r = radius of the cylinder used.

Preparation of powder mix and tablets

Powder mixtures for tablet compression were prepared using drug-excipient ratio of 1:1. The weighed quantities of excipient and metronidazole were mixed for 5 min in a porcelain mortar. It was then transferred into screw-capped bottles and placed in the rotomixer (VSF3843C Forster equipment Co. Ltd, Whetstone, Leicester, England) for 10 min to ensure efficient mixing.

The powder mixtures produced above were compressed into tablets using a single punch Carver hydraulic hand press (Model C, Carver Inc., Menomonee Falls, Wis-

consin, USA) at different pressures. Tablets of 400 mg were compressed for 30 secs at varying pressures using a die of 10.5 mm in diameter. Magnesium stearate dispersion (1 %$^w/_v$) in acetone was used to lubricate the die and punch surfaces before compressing the tablets. Compressed tablets were stored in a dessicator containing silica gel for 24 h before conducting tablet evaluation.

Mechanical Properties

The crushing strength-friability ratios (Cs/Fr) of the tablets were calculated from the values of crushing strength and friability.

The crushing strength (Cs) test was carried out using a hardness tester (MHT-100, Model P&M 01, Pharma Alliance Group, Indonesia). Five tablets were selected at random from each batch. Each tablet was placed between the anvil and the spindle of the hardness tester. The force at which the tablet cracked into two halves was then recorded, and the mean from each batch was calculated.

The friability (Fr) test for tablets was carried out using a friabilator (DBK instruments, Mumbai-6, model 40FTA01, India). Ten tablets (10) were selected at random from each batch, weighed with the aid of a weighing balance and then transferred into the drum of a friabilator. The device was operated at a speed of 25 rpm for 4 min. The tablets were removed, dusted, reweighed and the percentage loss calculated.

Disintegration time

The disintegration test was carried out using the DBK disintegration testing apparatus (Type 40TDA01, India). Six tablets were selected at random from each batch and placed on the mesh of the disintegrating apparatus, the disintegration time (Dt) of the tablets was determined in distilled water at 37 ± 0.5 °C. The time taken for tablet to disintegrate and pass through the mesh was recorded.

Disintegration efficiency ratio

The disintegration efficiency ratio (DER)[27] for the tablets was calculated as a ratio of Cs, Fr and Dt as shown in the equation the equation below:

$$DER = \frac{Cs/Fr}{Dt} \quad (7)$$

where

Cs: crushing strength

Fr: friability

Dt: disintegration time.

Compression behavior of the excipients

The compression behavior of the excipients was evaluated using Heckel equation and the plots of LN{1/(1-D)} versus applied pressure for co-grinded and co-fused excipients and the parent polymers are expressed in Figures 8 & 9 while parameters derived from the plots are presented in Table 5.

Statistical analysis

Most of the tests were done in triplicate but crushing strength, friability and disintegration time tests had n=5, 10 and 6 respectively. The results were reported as mean ± SD except where values were derived by calculation like Cs/Fr and DER. Comparison of means were done using the students't-test and significance levels determined at $p < 0.05$.

RESULTS AND DISCUSSION

Co-processing of date mucilage and Avicel® produced co-excipients which were used for direct compression of metronidazole tablets. The material properties of the parent polymers (date mucilage and Avicel®) and co-excipients are presented in Tables 1 and 2 respectively. The densities for DAM were greater than that of AV. Both materials had poor flow as shown from the Carr's index and angle of repose; although the Hausner's ratio for DAM seemed to show that its flow improved compared to that of AV but other parameters did not confirm this. The particle density of co-grinded excipients reduced with increased amount of DAM while tapped density generally increased, however, bulk density showed no trend. The co-fused excipients showed increased pattern for bulk and tapped densities with increasing quantities of DAM while the particle density showed no particular trend. The Carr's index and Hausner's ratio for both co-grinded and co-fused excipients also showed no particular order. In addition, DAM had significantly higher ($p < 0.01$) swelling index compared to AV.

Table 1. Material properties of date mucilage and Avicel® used to prepare co-processed excipients

Parameter	DAM	AV
Particle density	1.307 ± 0.023	1.136 ± 0.034
Bulk density	0.571 ± 0.001	0.357 ± 0.004
Tapped density	0.634 ± 0.031	0.534 ± 0.042
Carr's index	25.034 ± 1.203	33.180 ± 2.034
Hausner's ratio	1.109 ± 0.233	1.496 ± 0.745
Angle of repose	69.650 ± 2.045	54.210 ± 3.002
Swelling index	92.170 ± 1.356	13.001 ± 2.114

The scanning electron micrographs (SEM) of Avicel® is not shown being a standard material which is well known and has been reported to be irregular in shape[28]. The SEM of DAM is shown in Figure 1, while that of co-grinded and co-fused excipients is shown in Figures 2 and 3 respectively. The shape and surface morphology of the particles were generally granular and rough and DAM showed irregularly shaped particles with rough surfaces. Adetunji et al.,[29] co-processed *Cedrela odorata* gum with plantain starch and microcrystalline cellulose in order to enhance the material, flow and compressional properties. The study reported that the co-processed excipients produced varying degrees of sphericity identified as oval, cylindrical or irregular.

In this study, the particle shape of the parent polymers was irregular and the co-processed excipients generally exhibited irregular shapes. However, the co-fused excipients offered some degree of sphericity which reduced as the concentration of DAM increased. This agrees with the study of Rahmati et al.,[30] which reported that the methods employed in particle processing affects the morphological outcome of the resulting excipients.
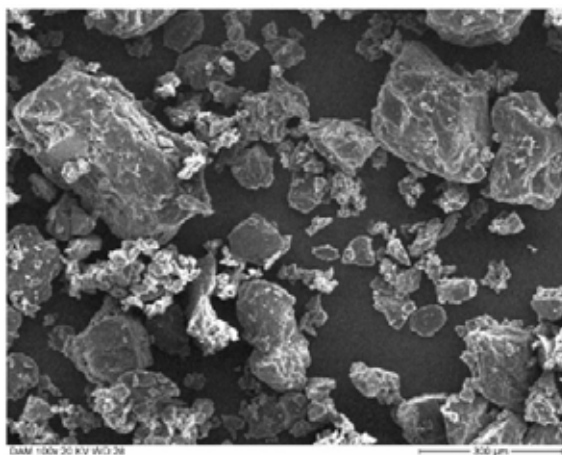
Figure 1. SEM of Date mucilage (DAM) X100.
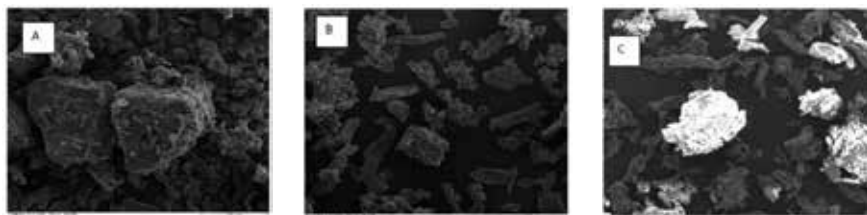
Figure 2. SEM of co-processed excipients prepared using co-grinding method (A-25% DAM, B-33% DAM, C-50% DAM) X150
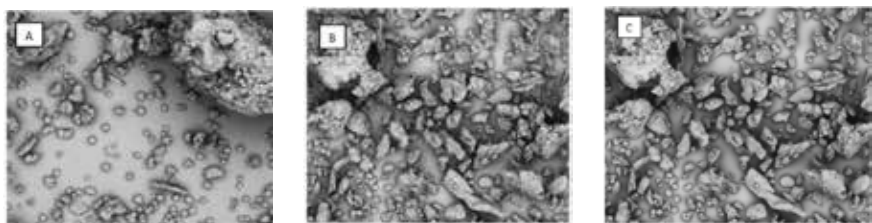
Figure 3. SEM of co-processed excipients prepared using co-fusion method (A-25% DAM, B-33% DAM, C-50% DAM) X200

Table 2. Material properties of co-processed excipients

Parameter	Amount of DAM (%$^w/_w$)	Amount of AV (%$^w/_w$)	Method of co-processing	
			Co-grinding	Co-fusion
Particle density	25.0	75.0	1.663 ± 0.018	1.562 ± 0.006
	33.0	67.0	1.504 ± 0.030	1.733 ± 0.001
	50.0	50.0	1.408 ± 0.009	1.541 ± 0.001
Bulk density	25.0	75.0	0.297 ± 0.001	0.349 ± 0.004
	33.0	67.0	0.276 ± 0.003	0.411 ± 0.007
	50.0	50.0	0.399 ± 0.001	0.481 ± 0.008
Tapped density	25.0	75.0	0.361 ± 0.002	0.478 ± 0.006
	33.0	67.0	0.360 ± 0.005	0.524 ± 0.013
	50.0	50.0	0.506 ± 0.007	0.649 ± 0.006
Carr's index	25.0	75.0	11.81 ± 0.042	26.881 ± 0.071
	33.0	67.0	23.28 ± 0.021	27.36 ± 0.219
	50.0	50.0	21.14 ± 0.071	25.822 ± 0.078
Hausner's ratio	25.0	75.0	0.812 ± 0.005	0.731 ± 0.023
	33.0	67.0	0.761 ± 0.008	0.785 ± 0.006
	50.0	50.0	0.789 ± 0.002	0.741 ± 0.009
Angle of repose	25.0	75.0	59.62 ± 0.011	66.381± 0.113
	33.0	67.0	59.870 ± 0.042	57.322 ± 0.071
	50.0	50.0	60.500 ± 0.092	56.102 ± 0.069
Swelling index	25.0	75.0	162.600 ± 0.177	134.403 ± 0.048
	33.0	67.0	86.670 ± 0.042	150.003 ± 0.227
	50.0	50.0	82.700 ± 0.007	275.001 ± 0.527

The mechanical and disintegration properties of metronidazole tablets prepared using co-grinded and co-fused excipients are presented in Tables 3 and 4 respectively while Figures 4 and 5 showed the effect of relative density on crushing strength of tablets made from co-grinded and co-fused excipients; and Figures 6 and 7 showed the effect of relative density on the friability of tablets prepared from co-grinded and co-fused excipients respectively. The crushing strength of tablets produced using co-grinded and co-fused excipients increased with relative density. Generally, the Cs of tablets produced using co-grinded (CG) excipient was higher than that of co-fused (CF) while Avicel® produced tablets with higher Cs in comparison with that of the co-grinded excipient (AV > CG > CF). It was observed that the relative density of tablets prepared using 100 % DAM were higher than that for other excipients. This could be because as seen in Table 1, the density of DAM is greater than that of AV and its presence within the tablet could confer higher density to them. It also implies that using DAM alone as a direct-compression excipient will require higher compaction forces to produce tablets with appreciable crushing strength compared to Avicel® which requires low compression pressure to impact higher hardness on tablets. The lowest values of Cs were obtained with excipient containing 50 % DAM irrespective of co-processing method while those containing 25 and 33 % DAM had higher crushing strength. This indicates that when stronger tablets are required, lower concentrations (< 50 %) of DAM in the co-excipient will be more valuable. Tablets produced with 100 % DAM and 100 % AV generally had acceptable friability which were significantly ($p<0.05$) lower compared to the co-processed excipients. The friability values in all cases reduced with increase in relative density. The ranking of friability among co-grinded excipients was 25 % DAM < 50 % DAM < 33 % DAM while for co-fused excipients, the order was 33 % DAM < 25 % DAM < 50 % DAM. The strength and weakness of the tablets were influenced by the concentration of DAM and the method of co-processing adopted.

Figure 4. Crushing strength against relative density for metronidazole tablets prepared using co-grinded excipient (♦ 25% DAM, ■ 33% DAM, ▲50% DAM, ○100% DAM, ●100% AV).
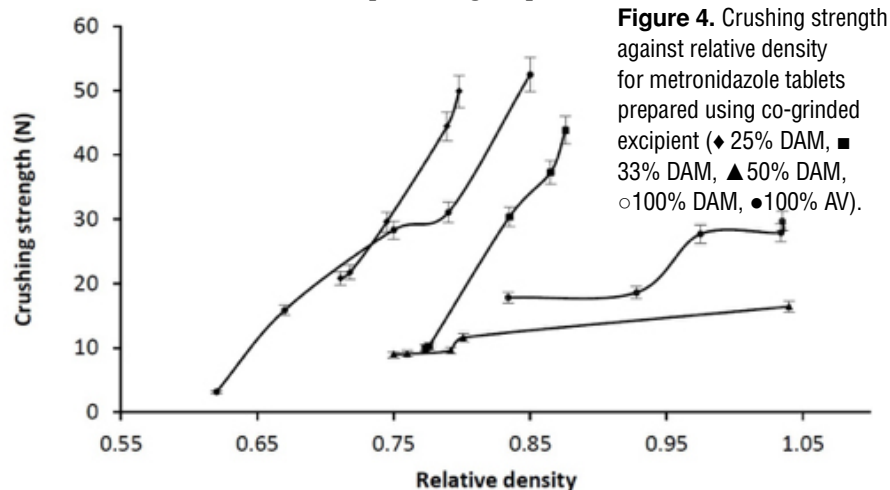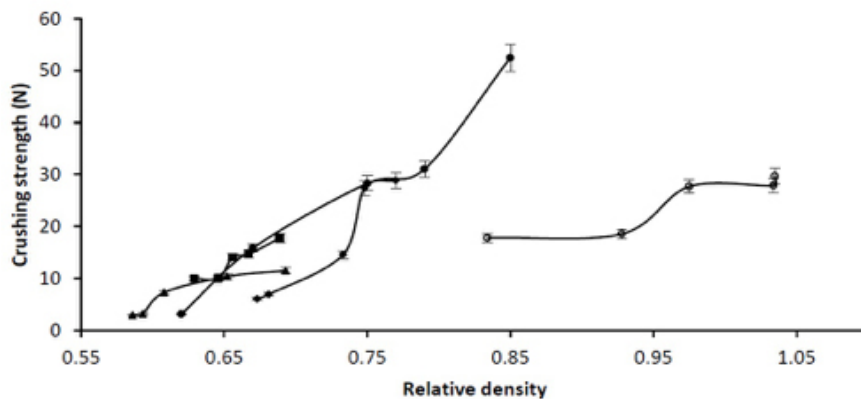
Figure 5. Crushing strength against relative density for metronidazole tablets prepared using co-fused excipient (♦ 25% DAM, ■ 33% DAM, ▲50% DAM, ○100% DAM, ●100% AV).
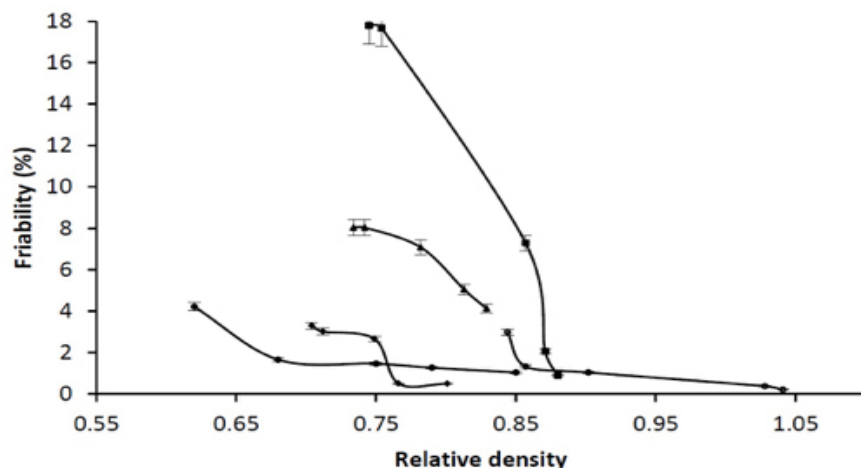
Figure 6. Friability against relative density for metronidazole tablets prepared using co-grinded excipient (♦ 25% DAM, ■ 33% DAM, ▲50% DAM, ○100% DAM, ●100% AV).
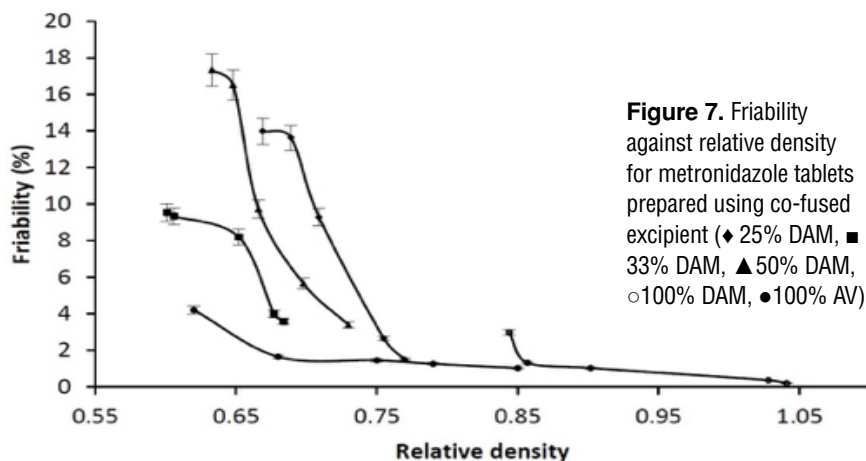
Figure 7. Friability against relative density for metronidazole tablets prepared using co-fused excipient (♦ 25% DAM, ■ 33% DAM, ▲50% DAM, ○100% DAM, ●100% AV).

Table 3. Mechanical and disintegration properties of metronidazole tablets prepared using co-grinded excipient

Applied pressure	Amount of DAM (%$^w/_w$)	Amount of AV (%$^w/_w$)	Cs/Fr	Dt (min)	DER
56.62	0.0	100.0	9.606	0.210 ± 0.010	45.743
84.92			19.397	1.120 ± 0.004	17.319
99.08			24.659	1.220 ± 0.006	20.212
113.23			50.951	1.540 ± 0.010	33.085
56.62	25.0	75.0	16.699	0.211 ± 0.003	79.142
84.92			23.307	0.262 ± 0.001	88.958
99.08			34.707	0.267 ± 0.001	129.989
113.23			45.762	0.300 ± 0.001	152.540
56.62	33.0	67.0	5.189	0.367 ± 0.001	14.139
84.92			17.572	0.383 ± 0.001	45.880
99.08			30.806	0.392 ± 0.002	78.587
113.23			49.801	0.500 ± 0.033	99.602
56.62	50.0	50.0	2.135	0.288 ± 0.004	7.413
84.92			3.542	0.393 ± 0.002	9.013
99.08			10.642	0.417 ± 0.001	25.520
113.23			26.934	0.419 ± 0.016	64.282
56.62	100.0	0.0	8.990	17.560 ± 0.015	0.512
84.92			14.091	25.340 ± 0.056	0.556
99.08			26.893	25.670 ± 0.059	1.048
113.23			75.405	39.410 ± 0.065	1.913

Table 4. Mechanical and disintegration properties of metronidazole tablets prepared using co-fused excipient

Applied pressure	Amount of DAM (%$^w/_w$)	Amount of AV (%$^w/_w$)	Cs/Fr	Dt	DER
56.62	0.0	100.0	9.606	0.210 ± 0.010	45.743
84.92			19.397	1.120 ± 0.004	17.319
99.08			24.659	1.220 ± 0.006	20.212
113.23			50.951	1.540 ± 0.010	33.085
56.62	25.0	75.0	1.915	0.200 ± 0.002	9.575
84.92			7.565	0.200 ± 0.001	37.825
99.08			35.621	0.222 ± 0.008	160.455
113.23			41.286	0.227 ± 0.007	181.877
56.62	33.0	67.0	12.287	0.201 ± 0.002	61.129
84.92			15.161	0.300 ± 0.030	50.537
99.08			36.75	0.318 ± 0.001	115.566
113.23			49.444	0.330 ± 0.002	149.830
56.62	50.0	50.0	0.388	0.233 ± 0.023	1.665
84.92			3.712	0.300 ± 0.015	12.373
99.08			9.204	0.320 ± 0.004	28.763
113.23			33.906	0.330 ± 0.001	102.745
56.62	100.0	0.0	8.990	17.560 ± 0.015	0.512
84.92			14.091	25.340 ± 0.056	0.556
99.08			26.893	25.670 ± 0.059	1.048
113.23			75.405	39.410 ± 0.065	1.913

Generally, the mechanical properties depicted by Cs/Fr increased with increase in applied pressure and tablets prepared with co-grinded excipient containing 33 % DAM had the highest values at the highest pressure, while 50 % showed the least at all pressures. For the Cs/Fr, the concentration of DAM in the co-processed product increased the tablet mechanical property up to a point and a further increase to 50 % reduced it. An increase from zero percent date mucilage to 25 % caused a significant increase in tablet strength except at the highest pressure. Tablets prepared with 100 % DAM all failed the disintegration time test but co-processing with AV yielded disintegration times less than 1 min showing a significant improvement on the disintegration profile of the tablets. Disintegration efficiency ratio is a measure of the balance between mechanical and disintegration properties of tablets[27]. The DER of tablets prepared using 0 % DAM reduced with compression pressure except for the highest pressure while other concentrations increased with increase in applied pressure. Co-grinded excipient containing 25 % DAM showed optimal DER while 50 % showed least. Generally, tablets containing 100 % DAM showed significantly lower ($p < 0.01$) values of DER compared to the other concentrations.

The mechanical and disintegration properties of metronidazole tablets prepared using co-fused excipients are presented in Table 4. Generally, the mechanical properties of tablets prepared using co-fused excipients as expressed by Cs/Fr increased with increase in applied pressure. At the highest pressure, the ranking of Cs/Fr was 100 % DAM > 100 % AV > 33 % DAM >25 % DAM > 50 % DAM. At all pressures, co-fused excipients containing 50 % DAM showed the least mechanical property which was significantly lower ($p<0.05$) in comparison with that of the parent excipients. There was a significant improvement in the disintegration of tablets prepared using the co-processed excipients in comparison to that prepared using DAM 100 %. The disintegration time for tablets prepared using co-fused excipients was lower than that of co-grinded additives although the differences were not significant ($p > 0.05$). Generally, the disintegration time increased with an increase in applied pressure. Ramya and Chowdary[31] prepared coprocessed excipients of pregelatinised starch-polyethylene glycol 1500-Aerosil and evaluated its application as directly compressible vehicle in tablet formulations. The authors reported that all the tablets disintegrated rapidly within 15-30 sec. The results of this current study agree with that of Ramya and Chowdary[31] by yielding fast disintegration times of 12.66 to 30 sec for cogrinded and 12.00 to 19.8 sec for cofused excipients. Generally, co-processing impacted this property as DAM alone failed the disintegration time test while avicel alone produced 12.60 – 92.40 secs as disintegration times.

The DER for tablets compressed at lowest and highest pressures had least DER

when 50 % DAM was present in the co-fused excipient. Among the tablets, those produced with co-fused excipients containing 25 % DAM showed the strongest DER while those produced with 100 % DAM had extremely low DER showing a poor balance of mechanical and release properties. Generally, the co-processed excipients improved the mechanical and disintegration properties of the tablets produced compared to tablets prepared using DAM alone.

Furthermore, the compressional characteristics of the co-processed excipients as shown in Figures 8 and 9 revealed linearity at two segments. The initial segment indicates rearrangement and fragmentation of the component particles. The second segment shows deformation by plasticity. It has been pointed out that cellactose® exhibits dual consolidation behaviour since it contains a fragmenting component (lactose) and a substance (cellulose) that consolidates mainly by plastic deformation[8]. The co-processed excipients therefore showed similarity to previously reported cellactose® in compression properties[8]. However, the parent polymers showed plots typical of single component systems.
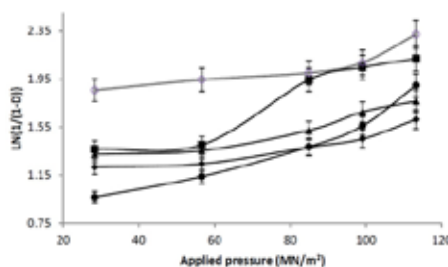
Figure 8. Heckel plots for metronidazole tablets prepared using co-grinded excipient (♦ 25% DAM, ■ 33% DAM, ▲50% DAM, ○100% DAM, ●100% AV).
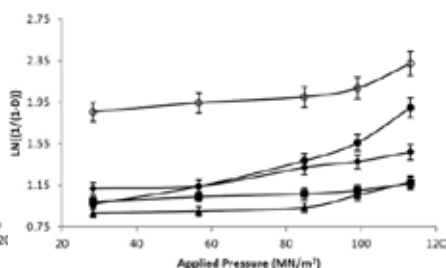
Figure 9. Heckel plots for metronidazole tablets prepared using co-fused excipient (♦ 25% DAM, ■ 33% DAM, ▲50% DAM, ○100% DAM, ●100% AV).

The parameters derived from the Heckel plots are shown in Table 5. The values of the relative density at zero pressure, D_o, which represents the degree of packing in the die as a result of die filling, increased generally with increase in the concentration of DAM in the co-excipients irrespective of production method. Co-fused excipients showed higher D_o than the co-grinded implying a higher degree of packing for formulations containing the co-excipients prepared by co-fusion.

Table 5. Parameters derived from Heckel plots for metronidazole tablets prepared using the co-excipients

Co-processing method	Amount of DAM (%$^w/_w$)	Amount of AV (%$^w/_w$)	D_o	P_y (MN/m²)	D_a	D_b
Co-grinding	0.0	100.0	0.357	103.093	0.620	0.263
	25.0	75.0	0.297	204.082	0.673	0.376
	33.0	67.0	0.276	769.231	0.617	0.341
	50.0	50.0	0.399	909.091	0.593	0.194
	100.0	0.0	0.571	384.615	0.834	0.263
Co-fusion	0.0	100.0	0.357	103.093	0.620	0.263
	25.0	75.0	0.349	175.439	0.681	0.332
	33.0	67.0	0.411	769.231	0.646	0.235
	50.0	50.0	0.481	116.279	0.593	0.112
	100.0	0.0	0.571	384.615	0.834	0.263

The mean yield pressure (Py) for the metronidazole tablet formulations were calculated from the slope of the linear region of the Heckel plots having correlation coefficient > 0.990, and the intercept, A, was determined from its extrapolation[32]. The mean yield pressure, Py, is inversely related to the ability of the metronidazole formulations to deform plastically when pressure is applied. Among the cogrinded excipients, P_y reduced as the concentration of DAM in the co-excipients reduced giving a ranking of 50 % >33% > 25%. However, the Py for 33 % was significantly higher than when 100 % DAM was used. Generally, cofused excipients offered significantly lower (p<0.05) values of P_y. Lower values of P_y implies faster onset of plastic deformation and the cofused excipients in this case would deform more readily under pressure on a high-speed tablet machine[33], compared to the cogrinded types. Avicel (0 % DAM) showed the least P_y and this is not surprising since it's a direct-compresion excipient. In addition, 33 % cofused and co-grinded excipients has same P_y indicating same deformation pattern irrespective of production method.

The total degree of packing achieved at zero and low pressures is referred to as total relative precompression density, D_a. The values increased with reduced concentrations of DAM without significant differences (p > 0.05) between excipients prepared using both methods of co-processing. DAM however had the highest D_a, suggesting a display of higher total degree of packing.

The phase of particle rearrangement in the early stages of tablet compression is called the relative density at low pressure, D_b and indicates the degree of frag-

mentation of particles[33]. Akin- Ajani et al[32]., has reported that fragmentation of particles can occur concurrently with plastic and elastic deformation during compression. The D_b of the excipients generally reduced with increase in the concentration of DAM using both methods of co-processing. Interestingly, the parent polymers both had equal D_b values probably implying same level of rearrangement of particles. Higher values of Db indicate improved particle re-arrangement showing that 25 % co-grinded and 33% co-fused excipients would offer optimal re-arrangements of particles or granules during compression. The compaction results obtained here agrees with the study of Odeku and Patani[34] on dika nut mucilage extracted and used as an excipient in metronidazole tablet formulations.

CONCLUSION

The excipients developed in this study using co-grinding and co-fusion methods of co-processing enabled the direct compression of metronidazole which is a poorly compressible drug. The co-processed excipients also improved the disintegration time and disintegration efficiency ratio of metronidazole tablets compared to date mucilage alone. Co-excipients prepared by co-fusion method showed faster disintegration and onset of plasticity compared to the ones from co-grinded method. For both methods, co-excipients containing 25 % DAM showed optimal disintegration properties while 33 % showed optimal mechanical properties. The co-excipients may therefore be further developed as direct-compression excipients for poorly compressible active agents especially when tablets requiring fast disintegration are needed.

ACKNOWLEDGMENT

REFERENCES

1. Carlin, B. Direct compression and the role of filler-binders. In: Augsburger, L.L., Augsburger, L.L., Hoag, S.W., Hoag, S.W. (Eds.), Pharmaceutical Dosage Forms: Tablets. *Informa*, **2008,** 173–216.

2. Tobyn M.J, McCarthy G.P, Staniforth J.N, Edge S. Physicochemical Comparison between Microcrystalline Cellulose and Solidified Microcrystalline Cellulose. *Int. J. Pharm.* **1998,** 169 (2), 183–194.

3. Shangraw R.F, Demarest, D.A. Survey of Current Practices in the Formulation and Manufacture of Tablets and Capsules. Pharm. Technol. **1993,** 17, 32-44.

4. International Pharmaceutical Excipients Council). Co-Processed Excipient Guide for Pharmaceutical Excipients. First Version. www.ipecamericas.org **2017,** pp. 6-7.

5. Reimerdes, D. The Near Future of Tablet Excipients. *Manufacturing Chemist.* **1993,** 64 (7), 14–15.

6. Modliszewski, J.J.; Ballard, D.A. Co-processed Galactomannan–Glucomannan. US Patent No.

5,498,436 to FMC Corporation (Philadelphia, PA) **1996.**

7. Garr, J. S., and Rubinstein, M. H., Compaction Properties of a Cellulose-Lactose Direct Compression Excipient, *Pharm. Tech. Int.,* **1991,** 3, 24-27.

8. Armstrong, N. A., Roscheisen, G., and Al-Aghbar, M. R Cellactose as a Tablet Diluent, *Manuf. Chem.,* **1996,** 67, 25-26.

9. Ahuja R. K, Dhari1 J, Goel1 A, Kumar V, Sharma R   Co-processing of excipients: a review on excipient development for fast dissolving tablet. *International Journal of Pharma Professional's Research,* **2015,** 6 (3), 1264-1274.

10. Zohary D, Hopf M. Domestication of Plants in the Old World-Date Palm *Phoenix dactylifera.* 2nd edition. Oxford: Clarendon; **1993.**

11. Anwar, M.A Phoenix dactylifera l: A Bibliometric study of the literature on date palm *Malaysian Journal of Library & Information Science,* **2006,** 11 (2), 41-60.

12. Sulieman, A., Elhafise, I., Abdelrahim, A. Comparative study on five Sudanese date (*Phoenix dactylifera* L.) fruit cultivars. *Food Nut Sci.* **2012,** 3, 1245–1251.

13. Mansouri, A.; Embarek, G.; Kokkalou, E.; Kefalas, P. Phenolic profile and antioxidant activity of the Algerian ripe date palm fruit (*Phoenix dactylifera*). *Food Chem.* **2005,** 89, 411–420.

14. Saddiq, A.A., Bawazir A.E. Antimicrobial activity of date palm (*Phoenix dactylifera*) pits extracts and its role in reducing the side effect of methyl prednisolone on some neurotransmitter content in the brain, hormone testosterone in adulthood. *Acta Hort.* **2010,** 882, 665–690.

15. Rahmani, A.H.; Aly S.M.; Ali, H.; Babiker, A.Y.; Srikar, S.; Khan, A.A. Therapeutic effects of date fruits (*Phoenix dactylifera*) in the prevention of diseases via modulation of anti-inflammatory, anti-oxidant and anti-tumour activity. *Int J Clin Exp Med.* **2014,** 7 (3), 483–491.

16. Miller, C. J.; Dunn, E. V,; Hashim, I. B. The glycaemic index of dates and date/yoghurt mixed meals. Are dates 'the candy that grows on trees'? *Eur. J. Clin. Nutr.* **2003,** 57, 427-30.

17. Al-Shahib, W.; Marshall, R. J.; The fruit of Date palm possible use for the best food for the future. Intern. *J Food Sci. Nutri.* **2003,** 54 (4), 247-253.

18. Ngwuluka, N. C.; Idiakhoa, B. A.; Nep, E. I.; Ogaji, I.; Okafor I. S. Formulation and evaluation of paracetamol tablets manufactured using the dried fruit of *Phoenix dactylifera* Linn as an excipient. *Research in Pharmaceutical Biotechnology,* **2010,** 2(3), 25-32.

19. Ajala, T. O, Akin-Ajani D. O, Ihuoma-Chidi, C., Odeku O. A. *Chrysophyllum albidum* mucilage as a binding agent in paracetamol tablet formulations. *Journal of Pharmaceutical Investigation.* **2016,** 46 (6), 565-573.

20. Bamiro, O.A.; Sinha, V.R.; Kumar, R.; Odeku, O. A. Characterization and evaluation of *Terminalia* randii gum as a binder in carvedilol tablet formulation. *Acta Pharm Sci.* **2010,** 52, 254-262.

21. Itiola, O. A. Compressional characteristics of three starches and the mechanical properties of their tablets. *Pharmacy World Journal.* **1991,** 8, 91-94.

22. Mohammadi, M.S., Harnby N. Bulk density modelling as a means of typifying the microstructure and flow characteristics of cohesive powders. *Powder Technol.* **1997,** 92 (1), 1-8.

23. Reus-Medina, M., Lanz, M., Kumar, V., Leuenberger, H. Comparative evaluation of the powder properties and compression behavior of a new cellulose-based direct compression excipient and Avicel PH-102. *J. Pharm. Pharmacy.* **2004,** 56 (8), 951-956.

24. Schwartz, J.B., Martin, E.T., Deliner, E.J. Intragranular starch: Comparison of starch U.S.P and modified corn starch. *J. Pharm. Sci,* **1975,** 64, 328-332.

25. Herman J, Remon JP, Dehydrophilic matrices for controlled oral delivery I. Production and characterization of thermally modified starches. *Intern. J. Pharm.* **1989;** 56, 51–63.

26. Okunlola, A.; Odeku, O.A. Compressional characteristics and tableting properties of starches obtained from four dioscorea species. *Farmacia.* **2009,** 57(6), 756–770.

27. Akin-Ajani, O. D.; Itiola, O. A.; Odeku, O. A. Evaluation of the disintegrant properties of native and modified forms of fonio and sweet potato starches. *Starch/Stärke.* **2016,** 68 (1-2), 169-174.

28. Thoorens, G.; Krier, F.; Leclercq, B.; Carlin, B.; Evrard, B. Microcrystalline cellulose, a direct compression binder in a quality by design environment—A review. *International Journal of Pharmaceutics.* **2014,** 473, 64–72.

29. Adetunji, O.A.; Odeniyi, M.A. Material and Compression Properties of *Cedrela odorata* Gum Co-Processed with Plantain Starch and Microcrystalline Cellulose. *Polim. Med.* **2016,** 46 (1), 35–43.

30. Rahmati, M.R.; Vatanara, A.; Parsian, A.R. Effect of formulation ingredients on the physical characteristics of salmeterol xinafoate microparticles tailored by spray freeze drying. Adv. *Powder Technol.* **2013,** 24, 36–42.

31. Ramya, K.; Chowdary, K. P. R. Preparation, characterization and evaluation of a new coprocessed excipient as directly compressible vehicle in tablet formulation. *Journal of Global Trends in Pharmaceutical Sciences.* **2013,** 4 (4), 1322-1328.

32. Akin-Ajani, O.D.; Itiola, O.A.; Odeku, O.A. Effect of acid modification on the material and compaction properties of fonio and sweet potato starches. *Starch/Stärke.* **2014,** 66, 749–759.

33. Dare, K.; Akin-Ajani, DO, Odeku OA, Itiola OA, Odusote OM). Effects of pigeon pea and plantain starches on the compressional, mechanical and disintegration properties of paracetamol tablets. *Drug Dev Ind Pharm.* **2006,** 32, 357–365.

34. Odeku, O.A.; Patani, B.O. Evaluation of dika nut mucilage (Irvingia gabonensis) as binding agent in metronidazole tablet formulations. *Pharm Dev Technol.* **2005,** 10, 439–446.

ADULT-PEDIATRIC BONE MARROW AND STEM CELL TRANSPLANTATION CENTER

Those who hold on to life...

A promising method of treatment by modern medicine:
Stem cell – bone marrow transplantation

BONE MARROW AND STEM CELL TRANSPLANTATİON İS PERFORMED BY
OUR EXPERİENCED ACADEMİC STAFF İN OUR CENTER EQUİPPED WİTH
LATEST-STATE OF THE ART TECHNOLOGY.

▶ MULTIPLE MYELOMA ▶ LYMPHOMA (HEMATOLOGIC LYMPH GLAND CANCER)
▶ ACUTE LEUKEMIA (BLOOD CANCER) ▶ CHRONIC LEUKEMIA ▶ BONE MARROW
DEFICIENCY ▶ APLASTIC ANEMIA ▶ MDS - BONE MARROW DEFICIENCY IN THE ELDERLY

MEDIPOL
CALL
CENTER | +90 **444 70 44**
International WhatsApp Line:
+90 549 794 13 45
www.internationalmedipol.com

MEDİPOL
MEGA
MEDİPOL
MEGA
HOSPITAL
COMPLEX

UNIVERSITY · HOSPITAL

medipolsaglik   edipolsaglik   edipolsaglik   MedipolSaglik

Solid Lipid Nanoparticles:
A Promising Technology for Delivery of Poorly Water-Soluble Drugs

Shailendra Bhatt[1]*, Jaibharti Sharma[1], Manishkumar Singh[1], Vipin Saini[2]

1 MM College of Pharmacy, Pharmaceutics, Ambala, India.
2 MM University, Solan, India.

ABSTRACT

Oral administration of drugs having low water solubility is hampered by various enzymatic barriers present in gastrointestinal (GI) tract. Lipid nanoparticles based on solid matrix have emerged as a potential drug delivery system to improve the absorption and bioavailability of several drugs, especially lipophilic compounds. Solid lipid nanoparticles (SLN) are reported as the most promising technology for oral administration and offered several advantages over conventional dosages formulations including, enhancement in solubility, stability, permeability, and bioavailability with minimal side effects. In this review, we have highlighted recent advances in the development of SLN for the oral, parenteral, rectal, and topical administration of various drugs. We have also summarized the applications of SLN in the treatment of various diseases like tuberculosis, cancer, diabetes, and several nervous system related disorders.

Keywords: Bioavailability, SLN, permeability, target delivery

INTRODUCTION

The most demanding research area in pharmaceutical field is target delivery of a drug to a specific organ. Whenever a drug is formulated, the dosage form is chosen according to its physicochemical and biological properties. It is inconvenient to take some drugs in simple dosage form because of their low aqueous solubility and low permeability across the cell membrane. Controlled drug delivery system, either dissolution-controlled or diffusion-controlled is used for the delivery of such drugs[1]. For the controlled delivery of a drug, colloidal systems such as liposomes, micelles and nanoparticles have been developed. Recently, nanotechnology has made some considerable advances in controlled drug delivery systems including

sustained release, timed release, extended release, and targeted release of a drug. The predominance of nanoparticles over the other drug delivery systems enables them to use for drug targeting. Nanoparticles are 10-100nm in size in which drug is either dispersed or entrapped in a matrix, encapsulated as the solid solution or may be adsorbed on the surface[2].The nanoparticles are designed to provide intimate contact with GI epithelium, prolong residence time and allow permeation across the cell membrane. A pre-systemic metabolism of a drug can be avoided by using nanoparticles[3]. Lipid nanoparticles are safe to use as they contain lipids, which are included in the category of generally recognized as safe (GRAS).

Solid Lipid Nanoparticles

Solid lipid nanoparticles are an advanced and rapidly budding field of nanotechnology with several applications in pharmaceutical science. SLN were developed first in 1991. These are the colloidal carriers possesses an average diameter of 10 to 1000nm. They composed of single lipid core matrix dispersed in an aqueous surfactant solution. The carriers like liposomes, polymeric micelles, and porous solids can also be used to enhance the aqueous solubility of a drug. But SLN not only helps to increase the solubility of a drug but also offers target release of drugs. SLN can be used as a carrier for lipophilic as well as hydrophilic drugs[4]. SLN provides stability to the solid lipid matrix and overcomes the disadvantages of liposomes, which includes stability problems[5]. Instead of polymeric nanoparticles, SLN are found to be more compatible with the biological system. Exclusive properties of SLN such as smaller size, larger surface area and interaction of phases at the interface make them valuable candidate[2]. The release of encapsulated compounds is controlled by solid lipid matrix, which also improves the stability of incorporated lipophilic ingredients. The type of lipids, surfactants and their concentration in the formulation of SLN adjust the particle size, drug loading, and release behavior of drugs[5]. The physicochemical characteristics of the solid lipid phase, such as reduced mobility of the drug in solid matrix, micro phase separation and enhanced absorption of poorly water-soluble drugs offer potentially beneficial effects. **The release of a lipophilic drug from SLN was found to be better than compare to the emulsion.** SLN also improves the solubility and bioavailability of lipophilic drugs[6]. SLN possess controlled drug release through lipid matrix and protect the drug from gastric degradation[7]. They improve the stability of those drugs which are sensitive to light, environment, pH, and oxidation[8]. The incorporated drugs can be protected against enzymatic degradation[6]. SLN enhance the intracellular uptake of drugs and deliver them at defined rates[8].

Role of lipids and emulsifiers in the formulation of SLN

Table 1 show some examples of lipids and surfactants, which are used in the for-

mulation of SLN.

Lipids

Main features for the selection of lipid are as following:

- Lipids carriers should enhance the gastrointestinal solubility and improve lymphatic uptake of poorly bioavailable drugs[9].

- The chemical and physical behavior of the lipid[10].

- The lipid with long chain fatty acids should be considered as they crystallize slower than short chain fatty acid[11].

- Proper care should be taken while selecting the lipid, as some lipids convert from metastable to stable form and try to form ideal crystalline lattice structures[11].

- The lipid influences the drug loading capacity in SLN. The higher amount of drug in lipid results in the more un-entrapped drug in the formulation[12].

- The size of SLN is also influenced by the hydrophobic part of the lipid and found to be increased when the hydrophobic chain length of lipid increases[13].

- The non-erodible and non-digestible properties of lipid[14].

- The selection of lipid depends upon the solubility of the drug in the lipid. In a study, the anticancer drug wogonin showed the highest solubility in the stearic acid[15].

Glyceryl behenate is an ideal excipient for SLN and has been used by various research groups. The stability and zeta potential of SLN prepared with glyceryl behenate is affected by storage conditions[16]. Jannin et al. reported that SLN prepared with glyceryl dibehenate were not digested by pancreatin during in-vitro lipolysis test[14]. In one of the study, it was found that SLN prepared with glyceryl behenate showed higher drug entrapment than compare to glyceryl stearate, as it contains mono, di and triglycerides and produces less ordered lipid crystals than glyceryl stearate[17]. In a study, SLN prepared using glycerol monostearate, stearic acid and glyceryl behenate resulted in an increase in particle size, polydispersity index and entrapment efficiency after long storage. However, the SLN containing tristearin as lipid content was found to be stable[18]. Citral loaded SLN, using glyceryl monostearate as a lipid showed enhanced stability in acidic enviroment[19]. Chantaburanan et al. prepared ibuprofen SLN to evaluate the combined effect of wax (cetyl palmitate) and triglyceride (Softisan 378) on particle size, zeta potential, entrapment efficiency, crystallinity, and drug release. The SLN were resulted in smaller particle size. The drug release was found to be fast followed by sus-

tained release, depending upon the ratio of lipids used[20]. In a study, ketoprofen loaded SLN were prepared using beeswax and carnauba wax. SLN containing higher amount of beeswax showed faster drug release as compared to SLN with the higher amount of carnauba wax[21].

Table 1. List of Lipids and Surfactants used in the formulation of SLN

Lipids	Surfactants
Fatty acids: Behenic acid, Stearic acid, Myristic acid, Palmitic acid, Decanoic acid.	**Sorbitan ethylene or propylene oxide copolymers:** Polysorbate 60, Polysorbate 20, Polysorbate 80.
Acylglycerols: Glycerol palmitostearate, Glyceryl monostearate, Glyceryl behenate, Glyceryl hydroxy stearate.	**Ethylene oxide or propylene oxide copolymers:** Poloxamer 407, Poloxamine 908, Poloxamer 188, Poloxamer 182.
Triacylglycerides: Tripalmitin, Trimyristin, Tricaprin, Tristearin, Trilaurin.	**Alkylaryl polyether alcohol polymers:** Tyloxapol.
Waxes: Beeswax, Cetyl palmitate, Carnouba wax.	**Triacylglycerides:** Tripalmitin, Trimyristin, Tricaprin, Tristearin, Trilaurin.
Cyclic complexes: Cyclodextrin.	**Bile salts:** Sodium cholate, Sodium oleate, Sodium glycocholate, Sodium taurodeoxycholate, Sodium taurocholate.
Hard fat: Witepsol H 35, Witepsol W 35.	**Alcohol:** Butanol.

Digestibility of Lipids

The main problem associated with SLN is the digestibility of lipids by lipases secreted by stomach or pancreas, which further cause degradation of SLN. Lipids are considered as non-erodible and non-digestible. But the presence of surfactant allows lipases to adsorb at the interface when the interfacial tension is sufficiently lowered. Jannin et al. prepared SLN of glyceryl dibehenate to evaluate the digestibility. SLN of Glyceryl dibehenate were produced by two processes, first high-shear homogenization followed by ultra-sonication and second Spray-Flash Evaporation (SFE) method. SLN prepared by ultra-sonication showed a limited digestion of the lipid excipient when tested in-vitro lipolysis using a pH-stat apparatus, although SLN produced by SFE were not digested by lipases. So, it was concluded that the presence of surfactant allows the adsorption of the lipase and degradation of glyceryl behenate[14].

Surfactants

Surfactants are used for the stability of the SLN dispersion and to prevent aggregation of particles. Various research groups have tried different surfactants like tween 20, tween 60, tween 80, span 20, polyvinyl alcohol, cremophor, lecithin, sodium dodecyl sulphate, sodium glycolate, poloxamer 407, and poloxamer 188.

The smaller particle size can be achieved by using higher surfactant ratio. Many of the Surfactant contains the hydrophobic as well as the hydrophilic moiety. The size of SLN decreases with the shorter chain length of hydrophobic part of surfactant. While the stability of formulated SLN decreases with increase in hydrophobic chain length because of the decrease in zeta potential. The HLB value is generally taken into consideration for the selection of surfactant. Sometimes surfactant blend also used to improve stability. The particle size and entrapment efficiency depend upon the concentration of surfactant used. Sun et al. investigated that by increasing the amount of pluronic F68 in the SLN formulation, particle size decreased, and the entrapment efficiency significantly increased[22]. Poloxamer 407 slow down the enzymatic degradation while cholic acid and sodium salts accelerate degradation, tween 80 showed no pronouncing effect on it. Polyethylene glycol as a surface coating material slow down the clearance and prevent liver uptake as it is less prone to plasma protein and other biological materials. Polysorbates coated SLN can effectively cross blood-brain barrier than compare to poloxamer and cremophor. A study reported that the addition of TPGS (Tocopheryl Polyethylene Glycol Succinate) as an emulsifier may improve the solubility, stability and oral bioavailability of entrapped drug[12].

Other Agents

Generally SLN are insufficient for the oral administration of various phyto bioactive compounds, due to burst release property[23]. To overcome this problem surface modifiers are used to improve the oral delivery of phyto bioactive compounds. The list of some counter-ions and surface modifiers are shown in Table 2[11]. Surface modification using counter-ions and surface modifiers elaborates the new physicochemical properties of SLN[11].The coating of a polymer on the SLN surface improves the stability of SLN in acidic medium and prevents the burst release of drug[24]. The quarternized chitosan derivative can be used for the protection of drug from acidic medium and further to stabilize the SLN. The curcumin-loaded SLN coated with N-carboxymethyl chitosan (NCC) by surface charge interaction prevented the immediate release of curcumin in acidic medium and improved its bioavailability[24]. Ramalingam et al. prepared SLN using N-trimethylchitosan (TMC). The curcumin loaded SLN were successfully delivered to the brain via oral administration[12]. Wang et al. prepared cross-linked polymer coated SLN which showed improvement in the physicochemical properties of SLN[25].

Preparation of solid lipid nanoparticles

The choice of method for the preparation of SLN depends upon the type of lipid and surfactant. Table 3 shows the formulation methods along with their advantages and disadvantages.

High pressure homogenization

In this method, the liquid is driven by homogenizers through a narrow orifice by applying high pressure. It is suitable for the production of SLN with high lipid content[22]. Two approaches work on the concept of high pressure homogenization (HPH) are; hot homogenization and cold homogenization, as shown in (Figure 1). In a study, SLN of efavirenz were prepared using this technique was found to be acceptable in term of particle size, Polydispersity index, and entrapment efficiency[6].
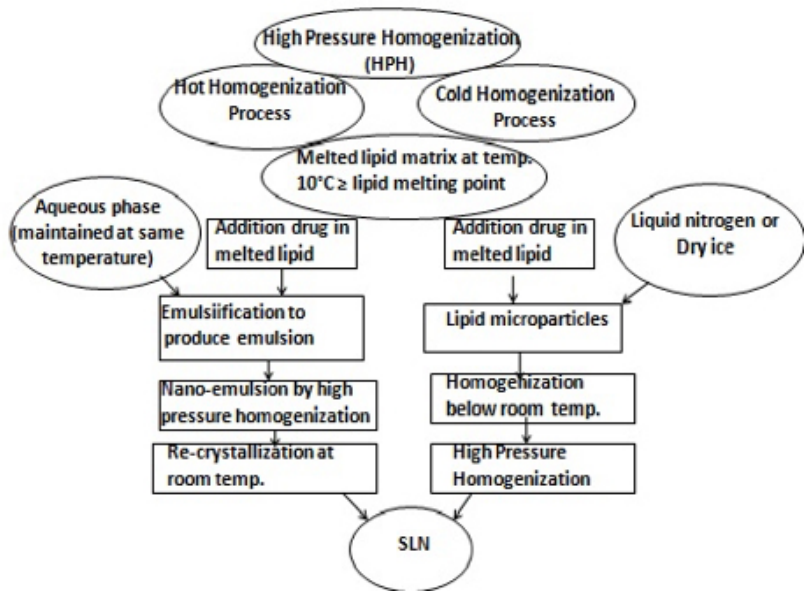
Figure 1. High Pressure Homogenization (HPH)

Table 2. List of some counter-ions and surface modifiers[11]

Counter-ions	Surface modifiers
Mono-hexadecyl phosphate, Sodium hexadecyl phosphate.	α-methoxy- polyethyleneglycol 2000-carboxylic acid-α-lipoamino acids, α-methoxy- polyethyleneglycol 5000-carboxylic acid-α-lipoamino acids.
Dextran sulphate sodium salt.	Stearic acid- polyethyleneglycol 2000.
Mono-decyl phosphate.	Dipalmitoyl-phosphatidyl-ethanolamine-polyethylene glycol 2000.
Mono-octyl phosphate.	Distearoyl-phosphatidyl-ethanolamine-N-polyethyleneglycol 2000.

Ultra-sonication/High speed homogenization

In this method, SLN are prepared by using sonicator or high speed homogenizer. The combination of both techniques can also be used to get smaller particle size [24]. In a study, SLN of non-steroidal anti-inflammatory drugs were prepared using ultra-sonication assisted nano-emulsion method to get the nano-sized emulsion. The author stated that sonication for 15 minutes is necessary to obtained smaller particle size[4]. Ultra-sonication method is preferred over micro emulsion technique to get the smaller particles [26].

Solvent emulsification evaporation

In this method, a water-immiscible organic solvent is used. This technique is generally used for thermo-labile drugs[27].

Solvent emulsification diffusion

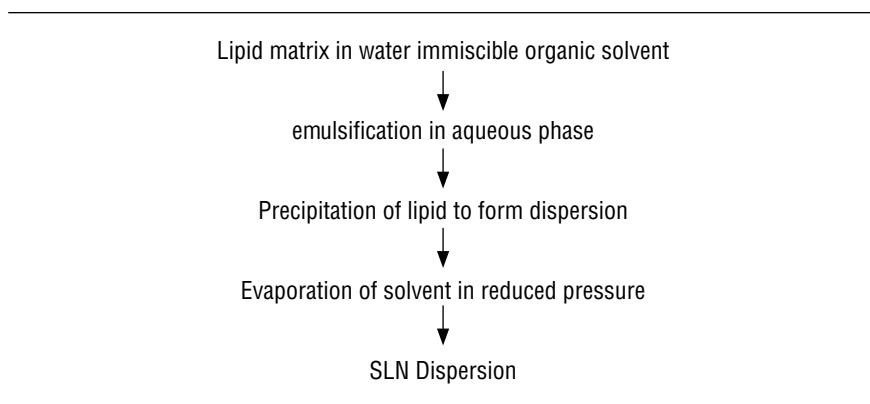In this method, the lipid matrix containing drug is dissolved in a water-immiscible organic solvent and then emulsified in an aqueous phase to get SLN (Figure 2).

Lipid matrix in water immiscible organic solvent

↓

emulsification in aqueous phase

↓

Precipitation of lipid to form dispersion

↓

Evaporation of solvent in reduced pressure

↓

SLN Dispersion

Figure 2. Solvent Emulsification-Diffusion Method

Supercritical Fluid Technology

This technique is used for the production of SLN of water-insoluble drugs. Carbon dioxide solution is the best choice as a solvent. Chattopadhyay et al. developed SLN of ketoprofen and indomethacin using this technique. The SLN with smaller particle size were obtained[28].

Micro Emulsion Method

In this method, hot micro emulsion is prepared which is further dispersed in cold water with continuous stirring as shown in Figure 3. SLN using double emulsion method can also be used to overcome the problems like release of drug during

emulsification process[13]. Behbahani et al. encapsulated curcumin in SLN using micro emulsion method followed by ultra-sonication. The spherical shape SLN with uniform size distribution was obtained[5].
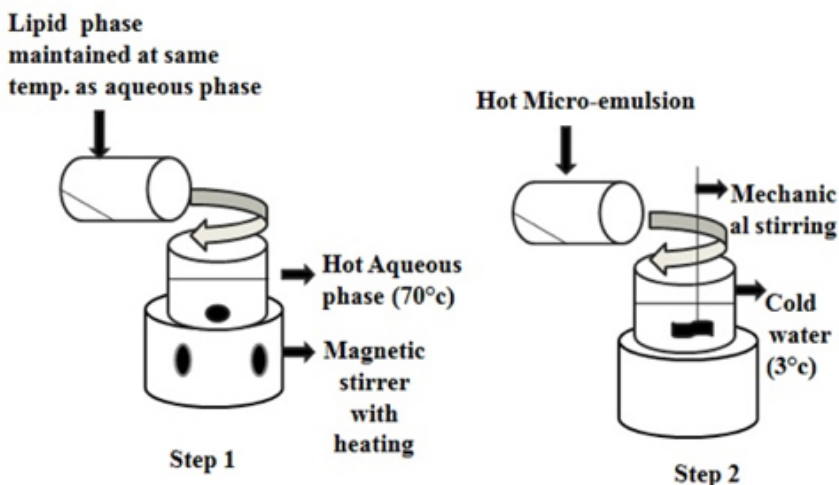
Figure 3. Micro-emulsion method.

Spray Drying Method

In this technique, high melting point lipids are used. The re-dispersion of SLN after drying is the main problem with this method. To overcome this problem, Wang et al. prepared SLN using the layer by layer technique followed by nano spray drying method to get ultra fine powders. Particles obtained were spherical in shape and easily redispersed[29].

Double Emulsion Based Method

The process involves the preparation of w/o micro emulsion which is added to aqueous surfactant solution to obtain a clear w/o/w system. This double emulsion is then dispersed in cold water and further washed with dispersion medium using ultra-filtration system. Severino et al. prepared SLN of polymyxin by w/o/w emulsification method, which showed appropriate particle size (200nm), high entrapment efficiency (90%) and desired zeta potential (-30mV). The method was found to be useful for the preparation of SLN[30].

Solvent Injection Technique

In this method, the organic solvent and lipid mixture is slowly injected into aqueous surfactant solution with continuous stirring27. The resulted dispersion is then sonicated for about 12 minutes to get the SLN dispersion (Figure 4). The solvent injection-lyophilization is a modification of solvent injection method, which overcomes the problems of solvent injection[31].
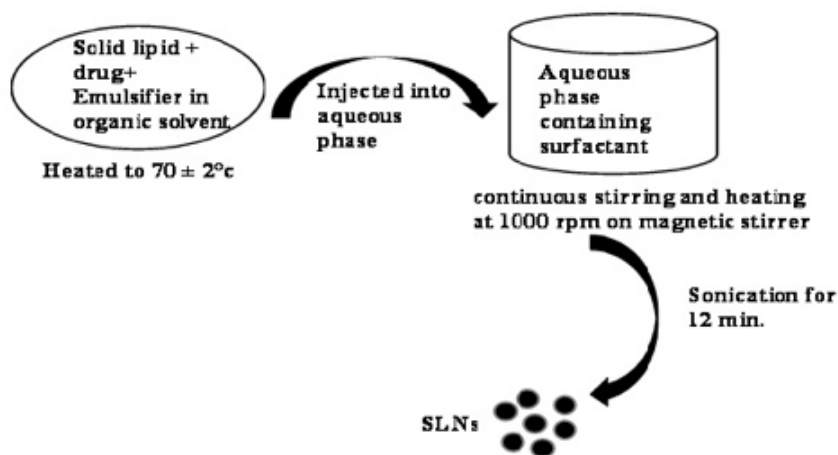
Figure 4. Solvent Injection Method.

Membrane Contractor Method

This process is developed by Charcosset et al.[32]. In this method, the lipid phase is pressed through the membrane pores and allows the formation of small droplets at the pore outlets, which are swept away by the running water. The SLN obtained after cooling the preparation at room temperature.

Models for Incorporation of Active Compounds

For the incorporation of active compound in SLN, three types of models are used (Figure 5). In Type I model, drug is homogenously dispersed in lipid matrix and released through diffusion from the solid lipid matrix. Type II model is achieved when the drug concentration is low and present in the outer shell. In Type III, The concentration of the drug is high in the lipid melt; a drug enriched core is formed. The drug release is governed by the fick's law of diffusion.
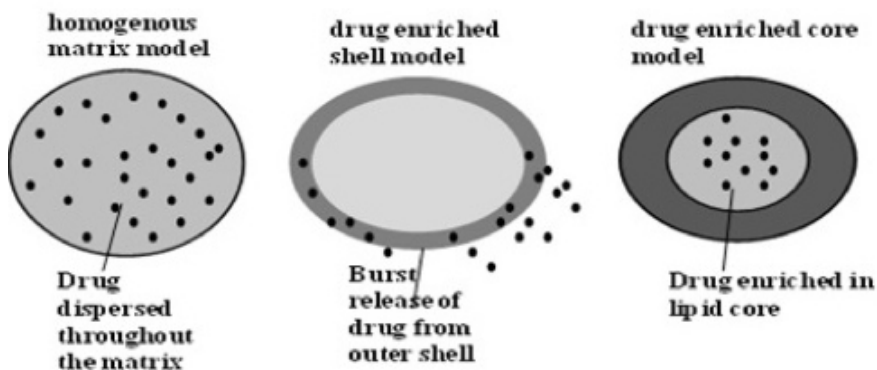
Figure 5. Drug Incorporation Models

Stability of SLN

Any change in particle size, appearance, drug content, zeta potential, and viscosity with time can be used to determine the stability of prepared SLN. For long-term stability, parameters like temperature and light are to be observed. The most acceptable temperature condition for storage of SLN is 4°C. For long term storage 20°C is preferred because at this temperature SLN are stable. While on increasing the temperature up to 50°C, rapid growth in particle size is observed. Gaber et al. developed gelucire-based solid lipid nanoparticles of myricetin for protection of drug from degradation. The author stated that antioxidant should be added in the SLN for the protection at high temperature and buffers should be added along with surfactants for better protection of drug[33].

Table 3. Method of preparation along with their advantages and disadvantages

Sr. No.	Formulation procedure	Advantages	Disadvantages
1.	High pressure homogenization	Economical, possible at laboratory scale	Polydisperse distribution, energy intensive process
2.	Ultra-sonication	Reduced shear stress, avoid temperature induced degradation	Possibility of metal contamination, particle growth upon storage
3.	Solvent emulsification evaporation	Easily scalable, continuous process	Polydisperse distributions, energy intensive process, biomolecule damage
4.	Solvent emulsification diffusion	Avoid heat during preparation	Residual organic solvent, anergy intensive process
5.	Supercritical fluid technology	Particles are obtained in form of dry powder, low pressure and temperature conditions	High cost
6.	Micro emulsion	Low mechanical energy input, theoretical stability	Extremely sensitive to changes, low yield
7.	Solvent injection	Fast production of SLN, process without technically sophisticated equipment	Use of organic solvent
8.	Double emulsion	Sterically stabilized, Suitable for hydrophilic drugs.	High percentage of particles in micro range.

Characterization of SLN

Several parameters like particle size, entrapment efficiency, zeta potential, drug loading capacity, and degree of crystallinity affect the stability and release of drug from SLN. The parameter along with their characterization techniques are given in Table 4.

The particle size of the lipid nanoparticles is strongly affected by the concentration of surfactants and lipids. Generally, the smaller particle size is obtained with the high concentration of surfactant17. Lipid concentration above 5% results in larger particle size. Zeta potential below -25 mV and above + 25mV are required for full electrostatic stabilization of the formulation. The main factor which may not show an exact result in characterization is entrapment efficiency[34]. Entrapment efficiency may affect by the concentration of lipid and surfactant. The loading capacity of the drug in the lipid depends upon the solubility of the drug in the lipid, structure of lipid matrix, and physical state of lipid. The solvent removal process brings some changes in lipids which can be determined using differential scanning calorimetry (DSC) and X-ray scattering. The nuclear magnetic resonance (NMR) and electron spin resonance (ESR) techniques are used for the investigation of structures in nano compartments of the lipid dispersions. The structure of lipids can also be determined using spectroscopic methods like infra-red and raman spectroscopy. Any modification in functional groups can be detected by NMR spectroscopy.

Routes of Administration for SLN

SLN can be designed for all the existing routes enlisted below.

Oral administration

SLN improves absorption of the drug through GI tract and increases oral bioavailability of drugs when used as a carrier in oral route. In one of the study, famotidine loaded SLN showed prolonged release and 2.06-fold increase in oral bioavailability as compared to commercial product7. Aripiprazole is an antipsychotic drug, the oral administration showed a reduction in in-vivo effects due to rapid first-pass metabolism. SLN of aripiprazole was developed by Sinha et al. using tristearin as a lipid and sodium taurocholate, tween 80 as surfactants. The in-vivo efficacy was found to be increased in lace mice using dizocilpine-induced schizophrenic model. The pharmacokinetic studies of SLN formulation showed 1.6 fold higher oral bioavailability of aripiprazole compared to its suspension[35].

Table 4. Parameters for Characterization of Solid lipid nanoparticles

Sr. No.	Parameters	Characterization Methods
1.	Particle size measurement	Scanning electron microscopy, photo correlation spectroscopy, transmission electron microscopy, atomic force microscopy, size exclusion chromatography, laser defractrometer
2.	Charge determination	Zeta potentiometer, laser dopler anemometer
3.	Loading capacity and entrapment efficiency	Spectro fluorophotometry, high-performance liquid chromatography, UV-spectrophotometry
4.	Release profile	In-vitro release studies
5.	Crystallinity and modification of lipid	DSC, X-ray diffraction
6.	Drug excipient Interaction study	DSC
7.	Drug stability	Bioassay of drug extract from nanoparticles, physical and chemical analysis of drug
8.	Co-existence of extra structures	Nuclear magnetic resonance, electron spin resonance

Parenteral administration

The SLN due to their small size can travel through the vascular system and minimize the side effects of the administered drug. SLN contain physiologically well-tolerated lipids which are safe to use for parental administration. They prevent macrophage uptake in the systemic circulation. Targeted delivery of hyaluronic acid coated SLN were reported by Zhou et al. In this study, SLN containing glucocorticoid prednisolone were targeted to affected joint tissues which resulted in reduction in joint swelling and inflammatory cytokines level in blood[36].

Topical administration

Topical treatment with SLN delivers a higher amount of drug at the specific site of action and shows minimum side effects. Topical preparations may be used for surface effects, stratum corneum effect and systemic effects. Auraptene is an anti-inflammatory agent; low aqueous solubility restricts the use for topical administration. The SLN of auraptene for topical delivery were developed by Daneshmand et al., which showed enhanced cutaneous uptake along with desirable anti-inflammatory activity[37]. SLN are the best way for the delivery of antifungal drugs for topical administration. The SLN gel of fluconazole was prepared to treat pityriasis versicolor. The prepared gel showed improved therapeutic activity against pityriasis versicolor compared to candistan® 1% cream[38].

Rectal administration

This route is preferred for pediatric patients for the ease of application. The plasma level and therapeutic effectiveness of rectally administered drugs were reported to be high as compared to oral or intramuscular route in the similar doses. Din et al. developed SLN loaded dual-reverse thermosensitive hydrogel of flurbiprofen. In comparison with the drug and hydrogel, SLN loaded hydrogel showed higher drug release than compare to pure drug and lower drug release than compare to hydrogel; due to its slow initial burst effect[39].

Nasal administration

Nasal route is preferred for the fast absorption and rapid onset of action of the drug. As it avoids the GI tract thus prevent the drug degradation. The SLN of efavirenz, when administered through intra-nasal route, drug concentration in the brain was found to be increased6.

Ophthalmic administration

The main problem with the ophthalmic administration of a drug is poor bioavailability. Only 5% of the drug can pass through the cornea after administration40. In a study, ophthalmic administration of voriconazole SLN showed burst release followed by sustained release. The prolonged residence time of drug on the ocular surface was observed[26].

Pulmonary administration

SLN dispersions in the form of aerosols can be delivered to lungs, which evade the first-pass metabolism of the drug and further increase the drug absorption. The drug showed controlled release behavior when entrapped in SLN. In a comparative study of SLN and liposomes, after pulmonary administration, SLN showed prolong exposure to lung[41]. This may be useful for the delivery of some drugs. The paclitaxel SLN were formulated by Rosiere et al. for the lung tumor. The SLN were coated with chitosan and a folate-grafted copolymer of polyethylene glycol and delivered by pulmonary route. The coated SLN resulted in good pharmacokinetic profile, prolonged release of paclitaxel in lungs, and found to be effective in inhaled therapy of paclitaxel[42].

Recent Work on Solid Lipid Nanoparticles

SLN for genetic materials

SLN have the potential for the delivery of DNA, miRNA, siRNA, nucleic acids and other genetic materials. Special cationic SLN are used for the delivery of genetic materials. Botto et al. prepared cationic SLN. The thermal analysis of cationic SLN showed the interaction with plasmid DNA. The result indicated that the efficient

delivery of gene therapy depends upon the amount and type of surfactant used in the preparation[43]. Kotmakci et al. developed cationic SLN for delivery of RNAi-mediating plasmid DNA to reduce the over expression of STAT3 and to overcome the resistance of cisplatin in lung cancer cells. Cationic SLN of plasmid DNA complexes down-regulated the STAT3 expression in resistant cell lines and decreases the resistance of cisplatin in cells[44]. Sharma et al. developed TRPV1-targeting siRNA loaded SLN without using any cationic agent. The author demonstrated that PEG600 as a surfactant decreases the particle size and also affects the endosomal uptake. After topical administration of TRPV1-targeting siRNA loaded SLN to rat, it was proved that SLN are effective for the silencing of the skin TRPV1[45]. Ekbaba et al. developed SLN of shRNA-encoding plasmid to reduce the level of 5-α reductase enzyme; which is responsible for diseases like benign prostatic hyperplasia, prostate cancer, and androgenic alopecia. The formulation was found to be efficient to reduce the level of 5-α reductase enzyme in the DU-145 cell line in-vitro with minimum cytotoxicity[46].

SLN in tuberculosis disease

In a study, Costa et al. prepared SLN of isoniazid by functionalized with mannose (M-SLN). The M-SLN showed more uptakes on alveolar macrophage cell than the SLN. The M-SLN was found to be more effective for the delivery of anti tubercular drug to alveolar macrophages[47]. In another study, SLN surface were engineered with mannose for the delivery of rifampicin, for treatment of tuberculosis. The Mannosylated SLN found feasible to maintain the drug load before entering the macrophage and cause phagocytosis of alveolar macrophage[48]. Vieira et al. prepared chitosan coated rifampicin SLN. The chitosan coated SLN showed highest mucoadhesive properties in-vitro and higher drug release in alveolar epithelial cells A549 than compare to uncoated SLN[49].

SLN in cancer

SLN have numerous applications in various types of cancer. In a study, solid lipid nanoparticles of curcumin and piperine using TPGS (tocopheryl polyethylene glycol succinate) and Brij 78 as a co-delivery vehicle was prepared. SLN were found to be effective in, in-vitro studies of reversing P-glycoprotein-mediated multidrug resistance in A2780/Taxol cells. Curcumin SLN selectively killed tumor cells with low intrinsic toxicity[50]. The bioavailability of solid lipid nanoparticles can be increased by surface modification with N-carboxymethyl chitosan(NCC). The intestinal delivery, lymphatic uptake, and cytotoxicity were enhanced by surface modification of SLN with NCC. The bioavailability and effect on tumor cells was found to be increased, as the cellular uptake on MCF-7 cells was increased[24]. A study on HCT-116 colon cells by Chirio et al. proved that the SLN can incorporate the higher amount of drug

and can be used for the treatment of cell cultures with low cytotoxicity[51]. Chuang et al. developed pH-sensitive cationic polyoxyethylene SLN of camptothecin (CPT-PEG-SLNs+) to make it tumor targeting. CPT-PEG-SLNs+ showed accumulation for a long time (>120 hours) in several types of tumor, and increase the efficiency of camptothecin against HCC36 or CL1-5 tumors[52]. Badawi et al. prepared SLN of pomegranate extract to increase its anticancer activity. The study was conducted using the normal cell line and several cancer cell lines. It was found that the SLN of pomegranate extract were more selective for the cancer lines especially for MCF-7 breast cancer cell than the normal cell[53]. The SLN of doxorubicin in combination with sclareol prepared by Oliveira et al. found to be useful in the treatment of cancer as they showed activity against 4T1 cells with prolonged drug release[54].

SLN in depression

SLN of curcumin and dexanabinol were prepared by He et al. to investigate the antidepressant effect in corticosterone induced depression model. SLN overcome the problems associated with curcumin like low solubility and low bioavailability with enhancement in antidepressant effect. The SLN showed an increase in curcumin level in the brain of mice and prolong the drug release which facilitates the antidepressant effect of curcumin[55]. Fatouh et al. prepared SLN of agomelatine; which is an antidepressant drug, to increase its bioavailability and target delivery to the brain. SLN were administered by intranasal route, which were found to be more effective than the intravenous route for brain targeting. The pharmacokinetic study proved that absolute bioavailability of agomelatine SLN was higher when compared to the oral suspension of valdoxan[56].

SLN in cosmetics

Generally, UV radiations are extremely harmful to skin. SLN are useful carrier in cosmetics as they show controlled release of the drug, excellent blockage of UV rays, and uniform dispersion on skin without using any greasy oil[57]. Silymarin is a natural sunscreen agent having antioxidant properties. The SLN of silymarin was prepared and further formulated as sunscreen cream. After evaluation of cream, the sun protection factor in-vivo and in-vitro was 14.1 and 13.80 respectively and no changes appeared in accelerated stability studies, which showed that SLN of silymarin can be used for photoprotective action when formulated as sunscreen cream[58].

SLN for antimicrobial activity

SLN can be used for the enhancement of antimicrobial activity of the natural products. In a study conducted by Fazly et al. the effectiveness of SLN against the human pathogen was investigated. For this, SLN of Eugenia caryophyllata essential oil was prepared and tested for antimicrobial activity against Pseudomonas aerug-

inosa, Salmonella typhi, Staphylococcus aureus and Candida albicans. The study revealed that the SLN of Eugenia caryophyllata essential oil was either better or equivalent to the essential oil[59]. Jourghanian et al. conducted the antimicrobial studies to compare SLN of curcumin with the free curcumin via well diffusion test using E.coli, and S. aureus. The increased effect was observed with SLN than compare to free curcumin[60].

SLN for proteins and peptides delivery

SLN have been proved as alternative carriers for the delivery of proteins, peptides, and antigens. They can entrap hydrophobic as well as hydrophilic proteins. SLN protects the peptides from proteolytic degradation and makes them able to cross the epithelial membrane and increase their bioavailability[61]. Xu et al. developed SLN of insulin containing an endoscopy escaping agent, HA2 peptide. During intracellular transport HA2 peptide SLN preserve the insulin and resulted in higher hypoglycemic effect in the diabetic rats[62].

SLN as a carrier for sustain drug delivery

SLN can control the release of drug from its matrix. SLN used for the sustain delivery of hydrophilic and lipophilic drugs. In a study, conducted by Jourghanian et al., sustained release with improved antibacterial efficacy was obtained with curcumin loaded SLN[60]. Shazly et al. developed SLN of domperidone. The prepared SLN showed sustain release of domperidone up to 12 hrs than compare to the conventional tablet, which showed immediate release. The results obtained from pharmacokinetic studies showed enhancement of oral bioavailability of domeperidone[63]. Zhao et al. prepared SLN of yuxingcao essential oil (YEO) for pulmonary administration. The SLN showed prolonged release after intra-tracheal administration to rats. The study revealed that, SLN of YEO resulted in sustain effect after inhalation delivery than compare to YEO solution[64]. The SLN of *Houttuynia cordata* extract were prepared by Kim et al. for control drug delivery and high loading efficiency. The SLN of *Houttuynia cordata* extract showed sustain release of quercitrin from extract[65].

SLN for brain targeted drug delivery

SLN can be targeted to the brain using the extremely small particle size of 50 nm. SLN have the ability to cross the blood-brain barrier and used as a drug delivery system for the treatment of CNS diseases. The functionalization of SLN with ligands makes them appropriate for targeting the brain sites. A study conducted by Ramalingam et al. revealed that TMC (N-trimethyl chitosan) coated SLN improved brain delivery as compared to drug suspension. The surface modification with TMC protects them in the environment of the stomach, so that a large amount

of drug can reach to systemic circulation and can cross the blood-brain barrier after oral administration[12]. Andrographolide is a natural product used in various brain disorders like cerebral ischemia. But the problem associated with its brain delivery is; low bioavailability, instability, and poor solubility. Graverini et al. developed SLN of andrographolide for brain delivery. In in-vivo studies, SLN were delivered to brain parenchyma outside the vascular bed; after crossing the blood-brain barrier[66]. Loureiro et al. proved that SLN when combined with anti-transferrin receptor monoclonal antibody efficiently target the brain cells than compare to normal SLN. SLN-antibody conjugation was used for the delivery of grape extract with resveratrol to the brain to treat Alzhimer disease by inhibiting amyloid-β peptide aggregation. The cellular uptake was found to be higher in SLN-antibody conjugation than the normal SLN[67]. The surface modification of SLN with apolipoprotein E-derived peptide (SLN-mApoE) was efficiently crossed the blood-brain barrier when tested using in-vitro model by Dal et al. The more confinement in the brain was found after pulmonary administration of SLN-mApoE, when compared to intravenous and intraperitoneal administration[68]. In a study, tocopherol succinate loaded SLN were developed for brain delivery of rivastigmine hydrogen tartrate for Alzheimer's disease. The prepared SLN were found with optimum particle size and high loading efficiency along with sustain release in-vitro[69].

Stealth nanoparticles

SLN avoided by the immune system, so specific cells can also be targeted by SLN. Stealth SLN are efficiently used in malaria, lymphatic disease, and lung disease. Recent work on stealth solid lipid nanoparticles is shown in table 5.

Table 5. Recent Work on Stealth Solid-lipid Nanoparticle

Drug	Method	Inference	Reference
Aloe-emodin (AE)	Surface-functionalized polyethylene glycol liquid-crystalline nanoparticles (PEG-LCNPs)	PEGylated LCNPs was found to be promising nanocarrier for delivery of Aloe-emodin to cancer cells.	70
Dimethyl fumarate, Retinyl palmitate, Progesterone, URB597	Modification of the SLN surface with polysorbate 80	The solubility of drugs was improved by 4 to 8 fold.	71
Epigallocatechingallate (EGCG)	Encapsulation of EGCG in solid lipid nanoparticle	Cytotoxicity of EGCG-SLN in MDA-MB 231 human breast cancer and DU-145 human prostate cancer cells was found to be increased.	72
Lipoyl-memantine (LA-MEM),	Emulsification-evaporation- solidifying method	LA-MEM loaded SLN were found to be a potential candidate for in-vivo studies in the brain.	73

In a study, stealth solid lipid nanoparticles (SSLN) were prepared by Wang et al. using polyoxyethylene stearate as stealth agent. The study of evading phagocytic uptake by mouse peritoneal macrophages using *in- situ* model concluded that, some amount of SLN and SSLN was uptake by macrophages. The interactions between cells and nanoparticles were perfectly evaluated using in situ model[74].

CONCLUSIONS

Solid lipid nanoparticle system is a promising drug delivery system for the delivery of low aqueous soluble drugs as well as several natural products. The present review focused on various methods of preparation using various biodegradable polymers along with their applications in different fields. The lipids used in the preparation of lipid nanoparticles are included in the category of GRAS. SLN are considered as a potential and effective technique for controlled and targeted drug delivery of various drugs. Due to small particle size, SLN efficiently crosses blood-brain barrier and hence can efficiently deliver the drug to the brain and used to treat various CNS related disorders. Further, due to its nature, SLN can be used for the delivery of genetic materials, proteins, peptides and various antimicrobial agents. The review also discussed the role of SLN as a carrier in cosmetic formulations. Moreover, with the numerous applications, SLN claims to overcome the shortcomings of other colloidal drug delivery system and further seems to be promising in designing of ligand-target drug delivery in various chronic diseases.

CONFLICT OF INTERESTS

The authors declare that there is no conflict of interest regarding the publication of this paper.

REFERENCES

1. Yun, Y. H.; Lee, B. K.; Park, K. Controlled Drug Delivery: Historical perspective for the next generation. *J Control Release*. **2015,** *219, 2–7.*

2. Teja, V. R. C.; Chowdary, V. H.; Raju, Y. P.; Surendra, N.; Vardhan, R. V.; Reddy B. K. A Glimpse on solid lipid nanoparticles as drug delivery systems. Journal *of Global Trends in Pharmaceutical Sciences*. **2014,** 5(2), 1649-57.

3. Lin, C. H.; Chen, C. H.; Lin, Z. C.; Fang, J. Y. Recent advances in oral delivery of drugs and bioactive natural products using solid lipid nanoparticles as the carriers. *Journal of food and drug analysis*. **2017,** 25(2), 219-234.

4. Kumar, R.; Singh A.; Garg, N.; Siril, P. F. Solid lipid nanoparticles for the controlled delivery of poorly water soluble non-steroidal anti-inflammatory drugs. *Ultrasonics Sonochemistry*. **2018,** 40, 686-696.

5. Behbahani, E. S.; Ghaedi, M.; Abbaspour, M.; Rostamizadeh, K. Optimization and characterization of ultrasound assisted preparation of Curcumin-loaded solid lipid nanoparticles: Application of central composite design, thermal analysis and X-ray diffraction techniques. *Ultrasonics Sonochemistry*. **2017,** 38, 271-280.

6. Gupta, S.; Kesarla, R.; Chotai, N.; Misra, A.; Omri, A. Systematic Approach for the Formulation and Optimization of Solid Lipid Nanoparticles of Efavirenz by High Pressure Homogenization Using Design of Experiments for Brain Targeting and Enhanced Bioavailability. *BioMed Research International*. **2017,** 2017.

7. Shafique, M.; Khan, M. A.; Khan, W. S.; Ahmad, W.; Khan, S. Fabrication, Characterization, and in vivo Evaluation of Famotidine Loaded Solid Lipid Nanoparticles for Boosting Oral Bioavailability. *Journal of Nanomaterials*. **2017,** 2017.

8. Doktorovova, S.; Souto, E. B.; Silva, A. M. Hansen solubility parameters (HSP) for prescreening formulation of solid lipid nanoparticles (SLN): in vitro testing of curcumin-loaded SLN in MCF-7 and BT-474 cell lines. *Pharmaceutical Development and Technology*. **2018,** 23(1), 96-105.

9. Chakraborty, S.; Shukla, D.; Mishra, B.; Singh, S. Lipid – An emerging platform for oral delivery of drugs with poor bioavailability. *European Journal of Pharmaceutics and Biopharmaceutics*. **2009,** 73, 1-15.

10. Pandya, J. B.; Parmar, R. D.; Soniwala, M. M.; Chavda, J. R. Solid Lipid Nanoparticles: Overview on Excipients. *Asian Journal of Pharmaceutical Technology & Innovation*. **2013,** 1(3), 01-09.

11. Shah, R.; Eldridge, D.; Palombo, E.; Harding, I. Lipid nanoparticles: Production, characterization and stability. *New York: Springer International Publishing*. **2015,** 11-22.

12. Ramalingam, P.; Ko, Y. T. Enhanced Oral Delivery of Curcumin from N-trimethyl Chitosan Surface-Modified Solid Lipid Nanoparticles: Pharmacokinetic and Brain Distribution Evaluations. *Pharm Res*. **2015,** 32(2), 389-402.

13. Shi, L.; Li, Z.; Yu, L.; Jia, H.; Zheng, L. Effects of Surfactants and Lipids on the Preparation of Solid Lipid Nanoparticles Using Double Emulsion Method. *Journal of Dispersion Science and Technology*. **2011,** 32(2), 254-259.

14. Jannin, V.; Blas, L.; Chevrier, S.; Miolane, C.; Demarne, F.; Spitzer, D. Evaluation of the digestibility of solid lipid nanoparticles of Glyceryl dibehenate produced by two techniques: Ultrasonication and spray-flash Evaporation. *European Journal of Pharmaceutical Science*. **2017,** 111, 91–95.

15. Baek, J.; Na, Y., Cho, C. Sustained Cytotoxicity of Wogonin on Breast Cancer Cells by Encapsulation in Solid Lipid Nanoparticles. *Nanomaterials*. **2018,** 8(3), 159.

16. Freitas, C.; Muller, R. H. Effect of light and temperature on zeta potential and physical stability in solid lipid nanoparticle (SLN™) dispersions. *International Journal of Pharmaceutics*. **1998,** 168, 221-9.

17. Ghada, A.; Fahmy, R. H. Diazepam-Loaded Solid Lipid Nanoparticles: Design and Characterization. *American Association of Pharmaceutical Scientists*. **2009,** 10 (1), 211-219.

18. Rawat, M. K.; Jain, A.; Mishra, A.; Muthu, M. S.; Singh, S. Effect of lipid matrix on repaglinide loaded solid lipid nanoparticles for oral delivery. *Therapeutic Delivery,* **2010,** 1, 63-73.

19. Tian, H.; Lu, Z.; Li, D.; Hu, J. Preparation and characterization of citral-loaded solid lipid nanoparticles. *Food Chemistry*. **2017,** 248, 78-85.

20. Chantaburanan, T.; Teeranachaideekul, V.; Chantasart, D.; Jintapattanakit, A.; Junyaprasert, V. B.. Effect of binary solid lipid matrix of wax and triglyceride on lipid crystallinity, drug-lipid interaction and drug release of ibuprofen-loaded solid lipid nanoparticles (SLN) for dermal delivery. *Journal of colloid and interface science*. **2017,** 504, 247-256.

21. Kheradmandnia, S.; Farahani, E. V.; Nosrati, M.; Atyabi, F. Preparation and characterization

of ketoprofen-loaded solid lipid nanoparticles made from beeswax and carnauba wax. *Nanomedicine: Nanotechnology, Biology, and Medicine*. **2010,** 6, 753-9.

22. Sun, J.; Bi, C.; Chan, H. M.; Sun, S.; Zhang, Q.; Zheng, Y. Curcumin-loaded solid lipid nanoparticles have prolonged in vitro antitumour activity, cellular uptake and improved in- vivo bioavailability. *Colloids and Surfaces B: Biointerfaces*. **2013,** 111, 367-375.

23. Ganesan, P.; Ramalingam, P.; Karthivashan, G.; Ko, Y. T.; Choi, D. K. Recent developments in solid lipid nanoparticle and surface-modified solid lipid nanoparticle delivery systems for oral delivery of phyto-bioactive compounds in various chronic diseases. *International Journal of Nanomedicine*. **2018,** 13, 1569-1583.

24. Baek, J. S.; Cho, C. W. Surface modification of solid lipid nanoparticles for oral delivery of curcumin: improvement of bioavailability through enhanced cellular uptake, and lymphatic uptake. *European Journal of Pharmaceutics and Biopharmaceutics*. **2017,** 117, 132-140.

25. Wang, T.; Ma, X.; Lei, Y.; Luo, Y. Solid lipid nanoparticles coated with cross-linked polymeric double layer for oral delivery of curcumin. *Colloids and Surfaces B: Biointerfaces*. **2016,** 148, 1–11.

26. Khare, A.; Singh, I.; Pawar, P.; Grover, K. Design and evaluation of voriconazole loaded solid lipid nanoparticles for ophthalmic application. *Journal of drug delivery*. **2016,** 2016.

27. Das, S.; Chaudhury, A. Recent Advances in Lipid Nanoparticle Formulations with Solid Matrix for Oral Drug Delivery. *AAPS Pharm Sci Tech*. **2011,** 12(1), 62-76.

28. Chattopadhyay, P.; Shekunov, B. Y.; Yim, D.; Cipolla, D.; Boyd, B.; Farr, S. Production of solid lipid nanoparticle suspensions using supercritical fluid extraction of emulsions (SFEE) for pulmonary delivery using the AERx system. *Advanced Drug Delivery Reviews*. **2007,** 59, 444-453.

29. Wang, T.; Hu, Q.; Zhou, M.; Xia, Y.; Nieh, M.; Luo, Y. Development of "all natural" layer-by-layer redispersible solid lipid nanoparticles by nano spray drying technology. *European Journal of Pharmaceutics and Biopharmaceutics*. **2016,** 107, 273-285.

30. Severino, P.; Silveira, E. F.; Loureiro, K.; Chaud, M. V.; Antonini, D.; Lancellotti, M.; Sarmento, V. H.; da Silva, C. F.; Santana, M. H. A.; Souto, E. B. Antimicrobial activity of polymyxin-loaded solid lipid nanoparticles (PLX-SLN): Characterization of physicochemical properties and in vitro efficacy. *European Journal of Pharmaceutical Sciences*. **2017,** 106, 177-184.

31. Ting, W.; Ning, W.; Yingying, Z.; Wancui, S.; Xingmei, G.; Tiefu, L. Solvent injection-lyophilization of tert-butyl alcohol/water cosolvent systems for the preparation of drug-loaded solid lipid nanoparticles. *Colloids and Surfaces B: Biointerfaces*. **2010,** 79, 254–261.

32. Charcosset, C.; El-Harati, A.; Fessi, H. Preparation of solid lipid nanoparticles using a membrane contactor. *Journal of Controlled Release*. **2005,** 108, 112–120.

33. Gaber, D. M.; Nafee, N.; Abdallah, O. Y. Myricetin solid lipid nanoparticles: Stability assurance from system preparation to site of action. *European Journal of Pharmaceutical Sciences*. **2017,** 109, 569-580.

34. Daneshmand, S.; Golmohammadzadeh, S.; Jaafari, M. R.; Movaffagh, J.; Rezaee, M.; Sahebkar, A.; Malaekeh-Nikouei, B. Encapsulation challenges, the substantial issue in solid lipid nanoparticles characterization. *Journal of cellular biochemistry*. **2017.** (Article in press)

35. Sinha, V. R.; Silki. Enhancement of In Vivo Efficacy and Oral Bioavailability of Aripiprazole with Solid Lipid Nanoparticles. *AAPS PharmSciTech*. **2018,** 1-10. (Article in press)

36. Zhou, M.; Hou, J.; Zhong, Z.; Hao, N.; Lin, Y.; Li, C. Targeted delivery of hyaluronic acid-coated solid lipid nanoparticles for rheumatoid arthritis therapy. *Drug Deliv*. **2018,** 25(1), 716-

722.

37. Daneshmand, S.; Jaafari, M. R.; Movaffagh, J.; Malaekeh-Nikouei, B.; Iranshahi, M.; Moghaddam, A. S.; Najaran, Z. T.; Golmohammadzadeh, S. Preparation, characterization, and optimization of auraptene-loaded solid lipid nanoparticles as a natural anti-inflammatory agent: In vivo and in vitro evaluations. *Colloids and Surfaces B: Biointerfaces*. **2018,** 164, 332-339.

38. El-Housiny, S.; Shams Eldeen, M. A.; El-Attar, Y. A.; Salem, H. A.; Attia, D.; Bendas, E. R.; El-Nabarawi, M. A. Fluconazole-loaded solid lipid nanoparticles topical gel for treatment of pityriasis versicolor: formulation and clinical study. *Drug delivery*. **2018,** 25(1), 78-90.

39. Ud Din, F.; Mustapha, O.; Kim, D. W.; Rashid, R.; Park, J. H.; Choi, J. Y.; Ku, S. K.; Yong, C. S.; Kim, J. O.; Choi, H. G. Novel dual-reverse thermosensitive solid lipid nanoparticle-loaded hydrogel for rectal administration of flurbiprofen with improved bioavailability and reduced initial burst effect. *European Journal of Pharmaceutics and Biopharmaceutics*. **2015,** 94, 64-72.

40. Sánchez-López, E.; Espina, M.; Doktorovova, S.; Souto, E. B.; García, M. L. Lipid nanoparticles (SLN, NLC): overcoming the anatomical and physiological barriers of the eye–part I–barriers and determining factors in ocular delivery. *European Journal of Pharmaceutics and Biopharmaceutics*. **2017,** 110, 70-75.

41. Haque, S.; Whittaker, M.; McIntosh, M. P.; Pouton, C. W.; Phipps, S.; Kaminskas, L. M. A comparison of the lung clearance kinetics of Solid lipid nanoparticles and Liposomes by following the 3 H-labelled structural lipids after pulmonary delivery in rats. *European Journal of Pharmaceutics and Biopharmaceutics*. **2018,** 125, 1-12.

42. Rosiere, R.; Van Woensel, M.; Gelbcke, M.; Mathieu, V.; Hecq, J.; Mathivet, T.; Vermeersch, M.; Van Antwerpen, P. G.; Amighi, K.; Wauthoz, N. A new folate-grafted chitosan derivative to improve the delivery of paclitaxel-loaded solid lipid nanoparticles for lung tumour therapy by inhalation. *Molecular pharmaceutics*. **2018,** 15(3), 899-910.

43. Botto, C.; Mauro, N.; Amore, E.; Martorana, E.; Giammona, G.; Bondì, M. L. Surfactant effect on the physicochemical characteristics of cationic solid lipid nanoparticles. *International journal of pharmaceutics*. **2017,** 516(1-2), 334-341.

44. Kotmakçi, M.; Çetintaş, V. B.; Kantarci, A. G. Preparation and characterization of lipid nanoparticle/pDNA complexes for STAT3 downregulation and overcoming chemotherapy resistance in lung cancer cells. *International journal of pharmaceutics*. **2017,** 525(1), 101-111.

45. Sharma, G.; Chopra, K.; Puri, S.; Bishnoi, M.; Rishi, P.; Kaur, I. P. Topical delivery of TRP-siRNA-loaded solid lipid nanoparticles confer reduced pain sensation via TRPV1 silencing, in rats. *Journal of drug targeting*. **2018,** 26(2), 135-149.

46. Akbaba, H., Akbaba, G.E. and Kantarci, A.G. Development and evaluation of antisense shRNA-encoding plasmid loaded solid lipid nanoparticles against 5-α reductase activity. *Journal of Drug Delivery Science and Technology*. **2018,** 44, 270-277.

47. Costa, A.; Sarmento, B.; Seabra, V. Mannose-functionalized solid lipid nanoparticles are effective in targeting alveolar macrophages. *European Journal of Pharmaceutical Sciences*. **2018,** 114, 103-113.

48. Maretti, E.; Costantino, L.; Rustichelli, C.; Leo, E.; Croce, M. A.; Buttini, F.; Truzzi, E.; Iannuccelli, V. Surface engineering of Solid Lipid Nanoparticle assemblies by methyl α-d-mannopyranoside for the active targeting to macrophages in anti-tuberculosis inhalation therapy. *International journal of pharmaceutics*. **2017,** 528(1-2), 440-451.

49. Vieira, A. C.; Chaves, L. L.; Pinheiro, S.; Pinto, S.; Pinheiro, M.; Lima, S. C.; Ferreira, D.; Sarmento, B.; Reis, S. Mucoadhesive chitosan-coated solid lipid nanoparticles for better management of tuberculosis. *International journal of pharmaceutics*. **2018,** 536(1), 478-485.

50. Tang, J.; Ji, H.; Ren, J.; Li, M.; Zheng, N.; Wu, L. Solid lipid nanoparticles with TPGS and Brij 78: A co-delivery vehicle of curcumin and piperine for reversing P-glycoprotein-mediated multidrug resistance in vitro. *Oncology Letters*. **2017,** 13, 389-395.

51. Chirio, D.; Gallarate, M.; Peira, E.; Battaglia, L.; Serpe, L.; Trotta, M. Formulation of curcumin-loaded solid lipid nanoparticles produced by fatty acids coacervation technique. *Journal of Microencapsulation*. **2011,** 28(6), 537-548.

52. Chuang, C. H.; Wu, P. C.; Tsai, T. H.; Fang, Y. P.; Tsai, Y. H.; Cheng, T. C.; Huang, C. C.; Huang, M. Y.; Chen, F. M.; Hsieh, Y. C.; Lin, W. W. Development of pH-Sensitive Cationic PE-Gylated Solid Lipid Nanoparticles for Selective Cancer-Targeted Therapy. *Journal of Biomedical Nanotechnology*. **2017,** 13(2), 192-203.

53. Badawi, N. M.; Teaima, M. H.; El-Say, K. M.; Attia, D. A.; El-Nabarawi, M. A.; Elmazar, M. M. Pomegranate extract-loaded solid lipid nanoparticles: design, optimization, and in vitro cytotoxicity study. *Int J Nanomedicine*. **2018,** 13, 1313-1326.

54. Oliveira, M. S.; Lima, B. H. S.; Goulart, G. A. C.; Mussi, S. V.; Borges, G. S. M.; Oréfice, R. L.; Ferreira, L. A. M. Improved Cytotoxic Effect of Doxorubicin by Its Combination with Sclareol in Solid Lipid Nanoparticle Suspension. *Journal of nanoscience and nanotechnology*. **2018,** 18(8), 5609-5616.

55. He, X.; Yang, L.; Wang, M.; Zhuang, X.; Huang, R.; Zhu, R.; Wang, S. Targeting the Endocannabinoid/CB1 Receptor System for Treating Major Depression Through Antidepressant Activities of Curcumin and Dexanabinol-Loaded Solid Lipid Nanoparticles. *Cellular Physiology and Biochemistry*. **2017,** 42, 2281-94.

56. Fatouh, A. M.; Elshafeey, A. H.; Abdelbary, A. Intranasal agomelatine solid lipid nanoparticles to enhance brain delivery: formulation, optimization and in vivo pharmacokinetics. *Drug design, development and therapy*. **2017,** 11, 1815-1825.

57. Jose, J.; Netto, G. Role of solid lipid nanoparticles as photoprotective agents in cosmetics. *Journal of Cosmetic Dermatology*. **2018.** (article in press)

58. Netto MPharm, G.; Jose, J. Development, characterization, and evaluation of sunscreen cream containing solid lipid nanoparticles of silymarin. *Journal of cosmetic dermatology*. **2017.** (Article in press)

59. Fazly, B. B. S.; Khameneh, B.; Namazi. N.; Iranshahi, M.; Davoodi, D.; Golmohammadzadeh, S. Solid Lipid Nanoparticles (SLN) carrying Eugenia caryophyllata essential oil: The novel nanoparticulate systems with broad-spectrum antimicrobial activity. *Lett Appl Microbiol*. **2018,** article in press.

60. Jourghanian, P.; Ghaffari, S.; Ardjmand, M.; Haghighat, S.; Mohammadnejad, M. Sustained release Curcumin loaded Solid Lipid Nanoparticles. *Adv Pharm Bull*. **2016,** 6(1), 17-2.

61. Dumont, C.; Bourgeois, S.; Fessi, H.; Jannin, V. Lipid-based nanosuspensions for oral delivery of peptides, a critical review. *International journal of pharmaceutics*. **2018,** 541(1-2), 117-135.

62. Xu, Y.; Zheng, Y.; Wu, L.; Zhu, X.; Zhang, Z.; Huang, Y. Novel Solid Lipid Nanoparticle with Endosomal Escape Function for Oral Delivery of Insulin. *ACS applied materials & interfaces*. **2018,** 10(11), 9315-9324.

63. Shazly, G. A.; Alshehri, S.; Ibrahim, M. A.; Tawfeek, H. M.; Razik, J. A.; Hassan, Y. A.; Shakeel, F. Development of Domperidone Solid Lipid Nanoparticles: In Vitro and In Vivo Characterization. *AAPS PharmSciTech*. **2018,** Article in press.

64. Zhao, Y.; Chang, Y. X.; Hu, X.; Liu, C. Y.; Quan, L. H.; Liao, Y. H. Solid lipid nanoparticles for sustained pulmonary delivery of Yuxingcao essential oil: preparation, characterization and in

vivo evaluation. *International journal of pharmaceutics*. **2017,** 516(1-2), 364-371.

65. Kim, J. H.; Baek, J. S.; Park, J. K.; Lee, B. J.; Kim, M. S.; Hwang, S. J.; Lee, J. Y.; Cho, C. W. Development of Houttuynia cordata Extract-Loaded Solid Lipid Nanoparticles for Oral Delivery: High Drug Loading Efficiency and Controlled Release. *Molecules*. **2017,** 22(12), 2215.

66. Graverini, G.; Piazzini, V.; Landucci, E.; Pantano, D.; Nardiello, P.; Casamenti, F.; Pellegrini-Giampietro, D. E.; Bilia, A. R.; Bergonzi, M. C. Solid lipid nanoparticles for delivery of andrographolide across the blood-brain barrier: in vitro and in vivo evaluation. *Colloids Surf B Biointerfaces*. **2018,** 161, 302-313.

67. Loureiro, J. A.; Andrade, S.; Duarte, A.; Neves, A. R.; Queiroz, J. F.; Nunes, C.; Sevin, E.; Fenart, L.; Gosselet, F.; Coelho, M. A.; Pereira, M. C. Resveratrol and grape extract-loaded solid lipid nanoparticles for the treatment of Alzheimer's disease. *Molecules*. **2017,** 22(2), 277.

68. Dal Magro, R.; Ornaghi, F.; Cambianica, I.; Beretta, S.; Re, F.; Musicanti, C.; Rigolio, R.; Donzelli, E.; Canta, A.; Ballarini, E.; Cavaletti, G. ApoE-modified solid lipid nanoparticles: A feasible strategy to cross the blood-brain barrier. *Journal of Controlled Release*. **2017,** 249, 103-110.

69. Malekpour-Galogahi, F.; Hatamian-Zarmi, A.; Ganji, F.; Ebrahimi-Hosseinzadeh, B.; Nojoki, F.; Sahraeian, R.; Mokhtari-Hosseini, Z. B. Preparation and optimization of rivastigmine-loaded tocopherol succinate-based solid lipid nanoparticles. *Journal of liposome research*. **2017,** 1-10.

70. Freag, M. S.; Elnaggar, Y. S.; Abdelmonsif, D. A.; Abdallah, O. Y. Stealth, biocompatible monoolein-based lyotropic liquid crystalline nanoparticles for enhanced aloe-emodin delivery to breast cancer cells: in vitro and in vivo studies. *International journal of nanomedicine*. **2016,** 11, 4799.

71. Esposito, E.; Drechsler, M.; Mariani, P.; Carducci, F.; Servadio, M.; Melancia, F.; Ratano, P.; Campolongo, P.; Trezza, V.; Cortesi, R.; Nastruzzi, C. Lipid nanoparticles for administration of poorly water soluble neuroactive drugs. *Biomedical microdevices*. **2017,** 19(3), 44.

72. Radhakrishnan, R.; Kulhari, H.; Pooja, D.; Gudem, S.; Bhargava, S.; Shukla, R.; Sistla, R. Encapsulation of biophenolic phytochemical EGCG within lipid nanoparticles enhances its stability and cytotoxicity against cancer. *Chemistry and physics of lipids*. **2016,** 198, 51-60.

73. Laserra, S.; Basit, A.; Sozio, P.; Marinelli, L.; Fornasari, E.; Cacciatore, I.; Ciulla, M.; Türkez, H.; Geyikoglu, F.; Di Stefano, A. Solid lipid nanoparticles loaded with lipoyl–memantine codrug: preparation and characterization. *International journal of pharmaceutics*. **2015,** 485(1-2), 183-191.

74. Wang, Y.; Wu, W. In situ evading of phagocytic uptake of stealth solid lipid nanoparticles by mouse peritoneal macrophages. *Drug Deliv*. **2006,** 13, 189-92.

In Vitro Antimicrobial and Antioxidant Activity of Some Berry Species

Tuğba İduğ[1]*, Hilal Hızlı[2], Ali Şen[3], Fatma Koç[4]

1 Istanbul Medipol University, School of Pharmacy, Department of Pharmacognosy, Istanbul, Turkey.
2 Istanbul Medipol University, Faculty of Health Sciences, Department of Nutrition and Dietetics, Istanbul, Turkey.
3 Marmara University, Faculty of Pharmacy, Department of Pharmacognosy, Istanbul, Turkey.
4 Istanbul Medipol University, International School of Medicine, Department of Clinical Microbiology, Istanbul, Turkey.

ABSTRACT

The aim of this work was to determine antioxidant and antimicrobial activities of extracts obtained from fresh and dried fruits of *Vaccinium macrocarpon, Morus nigra, Fragaria X ananassa*. Antioxidant and antimicrobial activity of extracts were assayed by DPPH and disc diffussion methods. Antioxidant activity of extracts decreased in the following order: *Fragaria X ananassa* fresh fruit (FAF) > *Vaccinium macrocarpon* fresh fruit (VMF) > *Morus nigra* fresh fruit (MNF) > *Morus nigra* (MND2) > *Morus nigra* (MND1) > *Vaccinium macrocarpon* (VMD1) > *Fragaria X ananassa* (FAD1) > *Vaccinium macrocarpon* (VMD2) > *Fragaria X ananassa* (FAD2). Fresh fruits showed higher antioxidant activity than dried fruits. FAF showed highest antimicrobial activity aganist *E. coli* and MND2 showed higher antimicrobial activity aganist *E. coli* and *S. aureus* in comparison to other extracts. Other extracts showed nearly same antimicrobial activity. All extracts showed no antimicrobial activity aganist *C. albicans*.

Keywords: Mulberry, Strawberry, Cranberry, Antioxidant activity, Antimicrobial activity

INTRODUCTION

Dietary patterns characterized by relatively high intakes of fruits and vegetables are consistently associated with reductions in the incidence of noncommunicable diseases such as coronary heart disease, stroke, cancer, and various chronic disease[1]. Berries provide significant health benefits because of their high levels of polyphenols, antioxidants, vitamins, minerals, and fibers[2]. Most berries are

delicious and powerful disease-fighting foods and make up the largest proportion of fruit that is consumed in the human diet. Berry fruits are popularly consumed not only in fresh and frozen forms but also as processed and derived products, including dried[3].

Oxidative stress plays an important role in the pathogenesis of most chronic diseases[4]. ROS is said to play an important role in many chronic diseases such cardiovascular diseases, diabetes, inflammation, anaemia, degenerative diseases, cancer[5]. Antioxidants molecules had defensive effects against reactive oxygen species (ROS) in the body. The plants have been known since ancient times as a good antioxidant[4]. Fruits rich in antioxidants can prevent or delay oxidative damage[6]. Fresh fruits are rich in acids, also contain anthocyanins and flavonoids[7]. Anthocyanins and flavonoids have been identified as strong antioxidant[8]. Especially, berry fruits worldwide known and consumed have been well studied Berries, including raspberries, blueberries, black currants, red currants, and cranberries are a rich source of dietary antioxidant[1].

Vaccinium macrocarpon known as cranberry naturally grows North America. Fresh fruits are rich in acids, also contain anthocyanins and flavonoids[7]. Anthocyanins and flavonoids have been identified as strong antioxidant[8]. *Morus nigra* known as mulberry is native to southwestern Asia also cultivated so long time and natural origin is unknown. Mulberries contain vitamins, minerals and anthocyanins[9]. *Fragaria X ananassa* is cultivated variety of strawberries[10]. Strawberries contain various phenolic compounds such as hydroxycinnamic acids, ellagic acid, ellagitannins, flavan-3-ols, flavonols, and anthocyanins[11].

Certain berries rich in tannins have been found to increase bacterial infections. Among the berries, cranberries, cloudberries, red raspberries, strawberries, and bilberries possess clear antimicrobial effects against human pathogens. Berry ellagitannins are strong antimicrobial agents acting as possible anti-adherence compounds in preventing the colonization and infection of many pathogens. Several mechanisms of action in the inhibition of bacteria are involved, such as destabilization of cytoplasmic membrane, permeabilization of plasma membrane, inhibition of extracellular microbial enzymes, direct actions on microbial metabolism, and deprivation of the substrates required for microbial growth[12, 13]. However, there is very little information about the antimicrobial capacity of phenolics present in berries, except in cranberry[3].

The aim of this study was to determine antioxidant and antimicrobial activities of extracts obtained from fresh and dried fruits of *Vaccinium macrocarpon, Morus nigra, Fragaria X ananassa.*

METHODOLOGY

Plant Material

Fresh fruits and two different dried fruits of *Vaccinium macrocarpon, Morus nigra and Fragaria* X *ananassa* were purchased from different local markets (Table 1).

Table 1. List of sample and abbreviations used in this study

Botanical name	*Fragaria X ananassa*	*Vaccinium macrocarpon*	*Morus nigra*
Fresh fruits	FAF	VMF	MNF
Dried fruits 1	FAD1	VMD1	MND1
Dried fruits 2	FAD2	VMD2	MND2

Chemicals

Methanol, ethanol, 2,2-diphenyl-1-picrylhydrazyl (DPPH) were provided from Sigma (Steinheim, Germany). Müeller Hinton agar, Saubaroud Dextrose broth were provided from Merck (Darmstadt, Germany).

Extraction of Plant Material

All fruit samples (100 g) were ground in a grinder and macerated with methanol (200 ml) for four days at room temperature and the extracts were filtered. Then methanol was evaporated with rotary evaporator. All extracts were stored in refrigerator at 4 C° until use.

DPPH Radical Scavenging Activity

The ability to scavenge DPPH radical of extracts was determined according to the method of Yanping Zou[14]. Briefly stock extracts were prepared at 10 mg/mL concentration and diluted to 2,5 mg/mL, 0,625 mg/mL, 0,156 mg/mL with methanol. 10 µL of all dilutions were added 190 µL DPPH solution in a well of 96 well-plate. The mixture was shaken quietly and left in room temperature and dark for 30 minutes. After then the absorbance was measured aganist methanol using a microplate reader at 517 nm.

DPPH radical scavenging activity were calculated according to following:

Antioxidant activity (%) = $[(A_0 - A_1) / A_0] \times 100$

Where A_0 is the absorbance of control, A1 is the absorbance of extracts/standard. Extract concentration providing 50% inhibition (IC_{50}) was calculated from the graph plotting inhibition percentage aganist extract concentration. Test were carried out in dublicated. Ascorbic acid was used as positive control.

In vitro Antimicrobial Activity Assay

In this study, disk diffusion method was used to determine of antimicrobial activity of the berries. This method is used for detection whether the samples have inhibition effect on microorganisms[15]. Also used for determination effects of drug and comparison of standards[16].

Microbial Strains And Growth Conditions

The assessment of antimicrobial activity was performed on gram positive bacteria *Staphylococcus aureus* ATCC 25923, gram negative bacteria *Echerichia coli* ATCC 25922 and yeast *Candida albicans* ATCC 10231 was determined by the disc diffusion method. Bacterial cultures were grown at 37oC for 24 hours in Brain Heart Inhibition broth or agar (BHB, BHA, Merck, Darmstadt, Germany), yeast strain was grown at 30 oC for 48 hours in Saubaroud Dextrose broth or agar (SDB, SDA, Merck, Darmstadt, Germany). Microbial cultures for antimicrobial testing were prepared by picking colony from 24 or 48-h-old BHA/SDA plates and it was suspended in saline solution to dilute 10^5-10^6 CFU/mL (%0,89 NaCl). The disk diffusion method was performed on Müeller Hinton agar (MHA, Merck, Darmstadt, Germany) for bacterial strains and SDA for yeast strain.

Disk Diffusion Method

Each of extracts were diluted in sterile distilled water (0,1 w/v). For the disk diffussion assay 0,1 mL of each microbial suspension was spread on a solid growth medium in a Petri dish. Three sterile paper disk (6 mm diameter) were impregnated with 15 uL each plant extract solution and were placed on the surface of agar plate. Plates were incubated for appropriate conditions for microbial strains. Antimicrobial activity was determined with inhibition zone around the disk following incubation. Impregnated discs with ethanol used as positive control[17].

Minimum Inhibitory Concentration (MIC) Assay

Minimum inhibitory concentration (MIC) is described as the lowest concentration of antimicrobial agent is needed to kill the bacteria[18]. MIC of all extracts were determined by microdilution techniques in Mueller-Hinton broth (MHB) for bacteria. Inoculates prepared in the MHB at a density adjusted to 0,5 McFarland turbidity standard and diluted 1/10 for the broth microdilution procedure[15]. The data were given as means±standard deviations and analysed by one-way analysis of variance (ANOVA) followed by the Tukey's multiple comparison tests using GraphPad Prism.

RESULTS AND DISCUSSION

Our focus in this study was to complement the previous knowledge of antioxi-

dant and antimicrobial activities of fresh and dry samples of berries.

The antioxidant power of fruit is closely correlated to the presence of efficient oxygen radical scavengers, such as vitamin C and phenolic compounds[19]. Berries are consistently ranked among the top sources of total phenolics and TAC, with levels up to 4 times greater than other fruits, 10 times greater than vegetables[20]. In a study by Tulipani et al. individual contribution was investigated in different strawberry cultivars, where vitamin C was found to be one of the most important components responsible for more than 30% of the TAC of strawberry extracts, followed by anthocyanins contributing 25% to 40%[21]. Viskelis and others reported that significantly larger amounts of anthocyanins were determined in the overripe cranberries of the cultivars[22]. Similarly, antioxidant activity in fresh strawberry was found to be highest in our study, followed by fresh cranberry and mulberry extracts.

A low IC_{50} value (the concentration of extract, which is required to scavenge 50% of DPPH free radical) means strong antioxidant activity. FAF showed the highest antioxidant activity with IC_{50} value of 0,327 mg/mL, while FAD2 showed the lowest antioxidant activity with IC_{50} value of 3,331 mg/mL in DPPH assay. All extracts showed low antioxidant activity compared to standard. It was determined that fresh extracts showed higher antioxidant activity. Antioxidant activities of extracts decreased in the following order: FAF>VMF>MNF>MND2>MND1>VMD1>FAD1>VMD2>FAD2 (Table 2).

It was thought that, drying and storage conditions may have affected the antioxidant capacity of dry extracts. In the phytochemical studies on these plants, it have been reported that this species contained phenolic compounds such as flavonoids and anthocyanins intensively. Therefore, the antioxidant activity of these fruits might be resulting from the phenolic contents of them.

Table 2. Antioxidant activities of extracts

Extracts / Standards	DPPH activity IC$_{50}$ (mgmL^{-1})
FAF	0,327±0,002c
FAD2	3,331±0,024j
FAD1	2,189±0,005h
VMF	0,408±0,007cd
VMD2	2,332±0,054i
VMD1	1,640±0,021g
MNF	0,454±0,005d
MND2	1,145±0,045e
MND1	1,318±0,004f
Ascorbic acid	0,002±0,000a
Butylated hydroxyanisole	0,057±0,000b

Low IC$_{50}$ value indicates high antioxidant activity.

Each value in the table is represented as mean ± SD (n = 3)

Different letter superscripts in the same column indicate significant differences (P < 0.05)

In this study, disc diffusion method was used to determination of antimicrobial activity of strawberries, blueberries and black mulberies on *E. coli* ATCC 25922, *S. aureus* ATCC 25923 and *C. albicans* ATCC 10231. Inhibition zones were measured and shown in Table 3.

This study showed that, dry strawberry (FAD2) has the highest level of antimicrobial activity was observed against *E. coli*. There was no inhibition zone against *C. albicans*. The dry blueberry (VMD2) has inhibition zone of 7 mm diameter against *S. aureus*.

In addition to disk diffusion method, broth dilution method was also performed to observe effect against on *E. coli* and *S. aureus*. Fresh strawberry (FAF), fresh blueberry (VMF) and dry black mulberry (MND1) were found that most effective on *S. aureus*. Dry black mulberry (MND1) was also found that most effective extract against to *E. coli* (Table 4).

One of the study showed that the highest antimicrobial activity of blueberry against *E. coli* and it has 18,67±1,15 mm inhibition zone also the lowest antimicrobial activity was found that against *S. aureus* and has 11,00±2,00 mm diameter[23]. Howell reported that high-molecular weight proanthocyanidins (condensed tannins)

from cranberry juice inhibit the adherence of uro-pathogenic fimbriated *E. coli* and thus offer protection against urinary tract infections[24]. Compared with our study, it was observed that blueberries did not produce any antimicrobial product against *S. aureus* and *C. albicans,* which showed that higher antimicrobial activity against *E. coli.* Another study showed that blueberry inhibited the growth of *E. coli* and *S. aureus,* but did not inhibit the *C. albicans*[25]. It was shown that, Black mulberry has more effectively inhibition against to Gram positive bacteria than Gram negative bacteria[26]. All of the extracts did not have any effect on the growth of the yeast species *(C. albicans)* studied.

Table 3. Inhibition zone around disks

Extracts / Control	*E. coli*	*S. aureus*	*C. albicans*
Ethanol	9 mm	9 mm	10 mm
FAF	6 mm	-	-
FAD2	10 mm	-	-
FAD1	11 mm	-	-
VMF	10 mm	-	-
VMD2	9 mm	-	-
VMD1	9 mm	-	-
MNF	-	-	-
MND2	8 mm	7 mm	-
MND1	9 mm	-	-

Table 4. MIC results

Extracts/Control	MIC (mg/mL)	
	S. aureus	*E. coli*
Ethanol	0,1	0,1
MNF	0,003125	0,05
FAF	0,0015625	0,05
VMF	0,0015625	-
MND2	0,00625	0,0125
FAD2	0,0125	0,1
VMD2	0,0125	0,05
MND1	0,0015625	0,00625
FAD1	0,003125	0,1
VMD1	0,05	-

In conclusion, fresh samples of fruits showed higher antioxidant and antimicrobial capacity than dried samples. Strawberries also showed higher effects than other berry samples. The antioxidative and antimicrobial activity depends on the cultivar, growth conditions, storage of raw material, and the method of isolation of active substances. Drying can affect the amount and activity of antioxidant ingredients. Further studies are needed to verify the antioxidant and antimicrobial activity of the compounds of berries.

ACKNOWLEDGMENTS

REFERENCES

1. Borges, G.; Degeneve, A.; Mullen, W.; Crozier, A. Identification of flavonoid and phenolic antioxidants in black currants, blueberries, raspberries, red currants, and cranberries. *J. Agric. Food. Chem.* **2010,** 58, 3901-3909.

2. Zhao, Y.; Berry fruit value-added products for health promotion. CRC press, New York, **2007,** pp: 154-166.

3. Nile, S. H.; Park, S. W. Edible berries: Review on bioactive components and their effect on human health. *Nutrition.* **2013,** 1-11.

4. Mahdi-Pour, B.; Jothy, S. L; Latha L.Y; Chen, Y; and Sasidharan S. Antioxidant activity of methanol extracts of different parts of *Lantana camara,* Asian. Pac. *J. Trop. Biomed,* **2012,** 2(12), 960-965.

5. Kalın, P.; Gülçin, İ.; Gören, A. C. Antioxidant activity and polyphenol content of cranberries *(Vaccinium macrocarpon) Rec. Nat. Prod.* **2015,** 9(4), 496-502.

6. Silva, K. D. R. R.; Sirasa M. S. F. Antioxidant properties of selected fruit cultivar grown in Sri Lanka. *Food Chem.* **2018,** 238, 203-208.

7. Bruneton, J. Pharmacognosy Phytochemistry Medicinal Plants, 2nd ed. Lavoisier Publishing: Paris, **1999,** pp: 363-364.

8. Yan, X.; Murphy, B. T.; Hammond, G. B.; Vınson, J. A.; Neto, C. C. Antioxidant activities and antitumor screening of extracts from cranberry fruit (*Vaccinium macrocarpon*). *J. Agric. Food Chem.* **2002,** 50, 5844-5849.

9. Yiğit, D.; Mavi, A.; Aktaş, M. Antioxidant activities of black mulberry (*Morus nigra*). *EUF-BED.* **2008,** 1-2, 223-232

10. Aharoni, A.; Giri, A. P.; Verstappen, F. W. A.; Bertea, C. M.; Sevenier, R.; Sun, Z.; Jongsma, M. A.; Schwaab, W.; Bouwmeester, H. J. Gain and Loss of fruit flavor compounds prodused by wild and cultivated strawberry species. *Plant Cell.* **2004,** 16, 3110-3131.

11. Oszmianski, J.; Wojdyto, A. Comparative study of phenolic content and antioxidant activity of strawberry puree, clear, and cloudy juices. *Eur. Food. Res. Technol.* **2009,** 228, 623-631

12. Puupponen, P. R.; Nohynek, L.; Alakomi, H. L.; Aksman-Caldentey, K. M. Bioactive berry compounds novel tools aganist human pathogens. *Appl. Microbiol. Biotechnol.* **2005,** 67, 8-18.

13. Puupponen, P. R.; Nohynek, L.; Hartmann-Schmidlin, S.; Kahkonen, M.; Heinonen, M.;

Maastta-Riihinen, K. et all. Berry phenolics selectively inhibit the growth of intestinal pathogens. *J. Appl. Microbiol.* **2005,** 98, 991-1000.

14. Zou, Y.; Chang, S. K. C.; Gu, Y.; Qian, S. Y. Antioxidant activity and phenolic compositions of lentil (*Lens culinaris var.* Morton) extract and its fractions. *J. Agric. Food Chem,* **2011,** 23; 59(6), 2268-2276.

15. Pessini, G. L.; Filho, B. P. D.; Nakamura, C. S.; Cortez, D. A. G. Antibacterial activity of extracts and neolignans from *Piper regnellii* (Miq.) C. DC. var. *pallescens* (C. DC.) Yunck. *Mems. Inst. Oswaldo Cruz.* **2003,** 98(8), 1115-1120.

16. Alzoreky, N. S.; Nakahara, K. Antibacterial activity of extracts from some edible plants commonly consumed in Asia. *Int. J. Food Microbiol.* **2003,** 80(3), 223-230.

17. Klancnik, A.; Piskernik, S.; Jersek, B.; Mozina, S. S. Evaluation of diffusion and dilution methods to determine the antibacterial activity of plant extracts. *J. Microbiol. Methods.* **2010,** 81(2), 121-126.

18. Balouiri, M.; Sadiki, M.; Ibnsouda, S. K. Methods for in vitro evaluating antimicrobial activity: A review, *J. Pharm. Anal.* **2016,** 6, 71–79.

19. Giamperi, F.; Tulipani, S.; Alvares-Suarez, J. M.; Quiles, J.L.; Mezzetti, B.; Battino, M. The strawberry: Composition, nutritional quality, and impact on human health. *Nutrition.* **2012,** 28, 9-19.

20. Halvorsen, B. L.; Holte, K.; Myhrstad, M. C. W.; Barikmo, I, Hvattum, E.; Remberg, S. F; et al. A systematic screening of total antioxidants in dietary plants. *J. Nutr.* **2002,** 132, 461-471.

21. Tulipani, S.; Mezzetti, B.; Capocasa, F.; Bompadre, S.; Beekwilder, J.; Ric de Vos C. H.; et al. Antioxidants, phenolic compounds, and nutritional quality of different strawberry genotypes. *J. Agric. Food Chem.* **2008,** 56, 696-704.

22. Viskelis, P.; Rubinskiene, M.; Jasutiene, I.; Sarkinas, A.; Daubaras, R.; Cesoniene, L. Anthocyanins, antioxidative, and antimicrobial properties of Amerikan cranberry *(Vaccinium macrocarpon Ait.)* and their press cakes. *J. Food Sci.* **2009,** 74(2), 157-161.

23. Bekki, S. Investigation of the antibacterial and cytotoxic effects of thyme oil, bilberry juice, cabbage juice and broccoli juice an ın vitro conditions. **2010,** Cumhuriyet University, Master of sicience thesis. Department of Microbiology, Sivas, Advisor: Zeynep Sümer (In Turkish).

24. Howell, A. B. Cranberry proanthocyanidins and maintenance of urinary tract health. *Crit. Rev. Food Sci. Nutr.* **2002,** 42, 273-278.

25. Nohynek, L. J.; Alakomi, H.; Kähkönen, M. P.; Heinonen, M.; Ilkka, M.; R. H. Puupponen-pimiä, R. H.; Helander, I. M. Berry Phenolics : Antimicrobial Properties and Mechanisms of Action Against Severe Human Pathogens. *Nutr Cancer.* **2006,** 54(1), 18-32.

26. Khalid, N.; Fawad, S. A.; Ahmed, I. Antimicrobial activity, phytochemical profile and trace minerals of black mulberry *(Morus Nigra L.)* fresh juice. *Pak. J. Bot.* **2011,** 43, 91-96.

MEDIPOL MEGA UNIVERSITY HOSPITAL
ORGAN TRANSPLANT CENTER

Donate an organ and give a second life.

MEDIPOL CALL CENTER

+90 **444 70 44**

International WhatsApp Line:
+90 549 794 13 45
www.internationalmedipol.com

MEDİPOL MEGA
MEDİPOL MEGA HOSPITAL COMPLEX

UNIVERSITY HOSPITAL

medipolsaglik   edipolsaglik   edipolsaglik   MedipolSaglik

Beta Hematin Inhibition: Evaluating the Mechanism of Action of Some Selected Antimalarial Plants

Oyindamola O. Abiodun[1]*, Olayide M. Oladepo[1]

1 University of Ibadan, Department of Pharmacology & Therapeutics, Ibadan, Nigeria.

ABSTRACT

There is paucity of information regarding the mechanism of action of medicinal plants with antimalarial activity. Thus, the mechanism of action of twenty antimalarial plants using the β-hematin inhibition assay was evaluated. Beta-hematin synthesis from bovine hemin in the presence of saturated acetate solution at a temperature of 60°C and pH 7.5 was initiated with a fixed concentration of 0.69 mg/mL of chloroquine or methanol extracts of the selected plants. The fifty percent inhibitory concentration (IC_{50}) of the six most active plant extracts/standard drug was determined using linear regression. Two of the plant extracts *A. boonei* and *M. charantia* (IC_{50} = 0.09 ± 0.03 and 0.11 ± 0.02 mg/mL), showed significant activity than chloroquine (0.36 ± 0.16 mg/ml. P<0.05) a potent β-hematin inhibitor. The β-haematin colorimetric assay is a reliable assay for determining the mechanism of action of medicinal plants that utilize the pathway.

Keywords: Beta haematin, antimalarial plants, Nigerian ethnomedicine

INTRODUCTION

Malaria is a major public health problem in sub-Sahara Africa with high rate of morbidity and mortality common in children less than 5 years of age and pregnant women [1]. In the last five years, malaria incidence rates (new malaria cases) fell by 37% globally and by 42% in Africa. During this same period, malaria mortality rates fell by 60% globally and by 66% in the African Region[2]. The recent worldwide gain achieved in reducing malaria burden is threatened by emergence and spread of drug resistance to artemisinins the most effective antimalarial available today[3-5]. Thus, there is need to enrich the antimalarial drug discovery pipeline with new effective agents and explore the mechanism of action of promising antimalarial agents at the early stage of drug discovery. Fortunately, several unique

*Corresponding author: Oyindamola O. Abiodun, e-mail: oyindamolaabiodun1@gmail.com

pathways have been identified such as; inhibition of DNA synthesis, de novo haem biosynthesis, glycolysis and hemozoin formation that can serve as drug targets[6-9]. Inhibition of hemozoin formation was explored in this study. Hemozoin is an insoluble, nontoxic disposal product formed from the digestion of haemoglobin by some blood-feeding parasites. These hematophagous organisms such as *Plasmodium sp., Rhodnius sp. and Schistosoma* sp. digest haemoglobin and release high quantities of free haem, which rapidly oxidizes to toxic Fe(III) hematin and is further sequestered as a nontoxic crystalline hemozoin also known as β-hematin[10-12]. The formation of hemozoin is essential to the survival of these parasites and can be considered as an attractive target for developing drugs for the related diseases. Quinine, and its synthetic homologs chloroquine, mefloquine, and others[13-15] putatively work by blocking conversion of hematin to a non-toxic crystalline hemozoin[16]. Similarly, artemisinin, another antimalarial drug of plant origin has been shown to bind to haem[17-18]. Effort in this report was directed towards the determination of the mechanism of action of twenty medicinal plants selected from Nigerian antimalarial compendium through the β-hematin inhibition assay.

METHODOLOGY

Plants Selection, Collection and Authentication

Twenty plants were selected through an extensive literature search of plants used for the treatment of malaria. Twenty plant species from 16 different families were collected, and identified by a plant taxonomist at Forestry Research Institute of Nigeria (FRIN), Ibadan in March 2013.

Extraction of Plant Materials

Powdered plant material (200 g) were percolated in 70% methanol for 72 h. Methanol extracts were filtered and concentrated under vacuum at 40°C using a rotary evaporator. Thereafter, the marc was further percolated in 70% methanol and processed as described above. The extraction process was repeated 2 times for exhaustive extraction of all plant materials. The yields of the methanol extracts were determined and extracts stored at -20°C until needed for study.

Reagents

Bovine hemin, pyridine anhydrous 99.8%, hydroxyethylpiperazine-N-[2-ethanesulfonic acid] (HEPES), sodium acetate, acetic acid, sodium hydroxide (NaOH) and chloroquine diphosphate were obtained from Sigma Aldrich Co. St. Louis, U.S.A. Hydrogen chloride (HCl), methanol and dimethyl sulfoxide (DMSO).

Qualitative Determination of Inhibition of ß-Haematin Synthesis of Twenty Selected Medicinal Plants

The assay was performed based on the method of Vargas and co-workers[19]. A stock concentration (25 mg/mL) of the plant extract/standard antimalarial drug (chloroquine) was prepared in aliquot of DMSO and subsequently diluted in solution containing 0.1M HCl, methanol and DMSO in the following ratio 5:3:1 to give 12.5 mg/mL working solution. The final concentration after addition of various reagents in the test plate (24-well plate) resulted in 0.69 mg/mL. Briefly, 10 µL of plant extract 1, 2 and chloroquine were dispensed into different wells in column 1 - 6 in duplicates. In this format two extracts and a standard drug (chloroquine) were tested in the 24-well plates. In addition, 10 µL of 1M HCl was added to all plant extracts or chloroquine in the 24-well plates. Into the wells in row A and B (the first two rows) 100 µL of freshly prepared hematin solution was added while wells in row C and D received 100 µL of 0.1M NaOH. The test plate was shaken at 450 rpm for 10 min. This was followed by addition of 60 µL of saturated acetate solution, pre-warmed at 60°C into all the wells. The test plate was further incubated at 60°C for 90 min. Thereafter, 750 µL of 15% pyridine was added to wells in the first and the third rows (row A and C) while 750 µL HEPES (pH 7.5) was added to wells in the second and the fourth rows (row B and D). Furthermore, the test plate was shaken at 450 rpm for 10 min and allowed to settle for 15 min. An aliquot of 100 µL was transferred in duplicates to a new 96-well plate and absorbance read at 405 nm with a spectrophotometer (SPECTRAmax GEMINI XS, Molecular Devices, USA).

Following the initial screening, methanol extract of 6 most active medicinal plants were quantitatively tested on the β-hematin assay at concentrations ranging from 0.04 to 1.38 mg/mL.The plant extract/drug concentrations were plotted against $I_{Analysis}$. The IC_{50} of the plant extract/standard drug was determined using a linear regression in a commercially available statistical package Microcal Origin®.

Data Analysis

For each plant extract/drug tested, (the absorbance, represented as $A_{Analysis}$) there was a control analysis ($A_{Analysis; \ Blank}$), which differed from the plant extract/drug submitted for the analysis ($A_{Analysis}$) by the addition of 750 µL of 20 mM HEPES instead of pyridine, after incubation. In addition, for each plant extract/drug, a blank control ($A_{CLT; \ Blank}$) as well as its blank ($A_{CLTBlank; \ Blank}$) were prepared in the absence of hematin but with 750 µL of 15% pyridine or 750 µL of HEPES.

1. Absorbance of the complex due to the remaining hematin in wells was calculated using the following formula:

Change in absorbance $(\Delta A_{Analysis}) = A_{Analysis} - A_{Analysis;\ Blank}$

2. The residual absorbance $(\Delta A_{CLT;\ Blank})$ of the plant extract/drug independent from the inhibition of the β-hematin complex was calculated using the following formula:

$$\Delta_{ACLT;\ Blank} = A_{CLTBlank} - A_{CLTBlank;\ Blank}$$

3. The resulting inhibition of the β-hematin synthesis induced by the plant extract/drug was calculated using the following formula:

$$I_{Analysis} = \Delta A_{Analysis} - \Delta_{ACLT;\ Blank}$$

A positive $I_{Analysis}$ is considered as positive (active sample) whereas a negative value indicated a negative result[47]. The IC$_{50}$ values were means ± standard deviation of three independent experiments. Mann-Whitney U test was used to compare the mean IC50 of the plant extracts with that of chloroquine. P-value < 0.05 was considered significant.

RESULTS

The $I_{Analysis}$ values of methanol extracts of the 20 medicinal plants at a fixed concentration of 0.69 mg/mL varied and ranged from -0.002 to 0.39 (Table 1). At this fixed concentration, nineteen (19) out of the 20 methanol extracts showed positive $I_{Analysis}$ values. Only methanol extract of leaf of *Ocimum gratissimum* showed negative $I_{Analysis}$ value (-0.002) signifying inability to inhibit the formation of β-hematin). Methanol extract of *Alstonia boonei* stem bark displayed the highest $I_{Analysis}$ value of 0.39 while methanol extract of Sida acuta displayed the lowest $_{IAnalysis}$ value of 0.06 at a fixed concentration of 0.69 mg/mL. In addition, the $I_{Analysis}$ value of the standard drug chloroquine was 0.17 (Table 1).

Table 1. Percentage Yield and Beta-Hematin Inhibition of Twenty Selected Medicinal Plant Extracts

S/N	Plants/Drug	Family	Percentage Yield (%)	$I_{analysis}$ (0.69 mg/mL)
1.	*Morinda lucida*	Rubiaceae	23.0	0.11
2.	*Terminalia catappa*	Combretaceae	9.2	0.18
3.	*Ocimum gratissimum*	Lamiaceae	7.0	-0.002
4.	*Cajanus cajan*	Fabaceae	9.6	0.15
5.	*Vitex doniana*	Lamiaceae	6.4	0.13
6.	*Gossypium barbandense*	Malvaceae	7.3	0.17
7.	*Azadirachta indica*	Meliaceae	12.2	0.12
8.	*Mangifera indica*	Anacardiaceae	13.1	0.21
9.	*Phyllantus amarus*	Phyllanthaceae	6.3	0.24
10.	*Senna siamea*	Fabaceae	10.1	0.09
11.	*Lawsonia inermis*	Lythraceae	22.2	0.26
12.	*Nicotiana tabacum*	Solanaceae	18.6	0.21
13.	*Xylopia aethiopica*	Annonaceae	28.7	0.10
14.	*Allium sativum*	Amaryllidaceae	3.0	0.10
15.	*Euphorbia hirta*	Euphorbiaceae	11.7	0.07
16.	*Vernonia amygdalina*	Asteraceae	15.9	0.12
17.	*Momordica charantia*	Cucurbitaceae	9.2	0.26
18.	*Cymbopogon citratus*	Poaceae	3.2	0.19
19.	*Sida acuta*	Malvaceae	9.8	0.06
20.	*Alstonia boonei**	Apocynaceae	5.2	0.39
21.	Chloroquine+	NA	NA	0.17

* With the exception of *Alstonia boonei* where the stem bark extract was tested, the methanol extract of leaves of the other medicinal plants were evaluated, +Standard antimalarial drug, NA – not applicable.

In addition, the 50% inhibitory concentration (IC_{50}) of the 6 most active medicinal plants from the initial screening was ($I_{Analysis} \geq 0.21$) quantitatively tested on the β-hematin assay at concentrations ranging from 0.04 to 1.38 mg/mL. Of the six methanol extracts tested, five possessed higher inhibitory activity greater than the standard drug chloroquine. Methanol extract of *Alstonia boonei* was the most ac-

tive with IC_{50} value of 0.09 ± 0.03 mg/mL while the extract of *Nicotiana tabacum* was the least active with IC_{50} value of 0.49 ± 0.05 mg/mL (Table 2). The mean IC_{50} value of chloroquine a potent β-hematin inhibitor was 0.36 ± 0.16 mg/mL (Table 2).

Table 2. Fifty Percent Inhibitory Concentration (IC_{50}) of Ten Medicinal Plants in a Beta-Haematin Inhibition Assay

S/N	Plant Extracts/Drug	IC_{50} (Mean ± S.D) (mg/mL)
1	*Alstonia boonei*	0.09 ± 0.03*
2	*Momordica charantia*	0.11 ± 0.02*
3	*Phyllantus amarus*	0.19 ± 0.03
4	*Lawsonia inermis*	0.24 ± 0.05
5	*Mangifera indica*	0.25 ± 0.07
6	*Nicotiana tabacum*	0.49 ± 0.05
	Chloroquine	0.36 ± 0.16

N = 3, *Chloroquine vs *Alstonia boonei* and *Momordica charantia* P<0.05

DISCUSSION

Host haemoglobin is an essential source of amino acids for parasite growth[20,21] for intraerthrocytic stages of malaria parasite i.e. rings, trophozoites and schizonts[20-22]. The food vacuole of the parasites contains specialised aspartic and cysteine proteases. These enzymes degrade the protein component of haemoglobin to amino acids, which are utilised by the parasite for protein synthesis[23-24]. The remaining part of the degraded haemoglobin is the haem (ferriprotoporphyrin IX), which is released intact. The haem produced along with amino acids after degradation of host haemoglobin is toxic to the parasites. Haem is membrane toxic, capable of lysing both the parasites and the red blood cells[25]. The parasites detoxified haem by converting it to an insoluble, unreactive crystalline material called haemozoin (malaria pigment) or β-haematin[26].Inhibition of conversion of toxic haem to β-haematin by 4–aminoquinolines or the complex formed by toxic haem and some antimalarial drugs would effectively allow the build-up of haem to a level that become irreversibly toxic to the parasite. Thus, the haemozoin formation pathway has been widely studied and explored as the mechanistic pathway for the 4-aminoquinolines antimalarial drugs such as chloroquine, mefloquine and amodiaquine13-15. This pathway is also considered a suitable target for antimalarial drug discovery[27-29].

The β-haematin formation pathway was explored in this study to evaluate the mechanism of antimalarial activity of twenty medicinal plant species from six-

teen different families reputed to be of importance in ethnomedicine for the treatment of malaria. Nineteen out of the twenty plant extracts showed positive $I_{Analysis}$ values which signified activity against β-hematin synthesis. Two of the plant extracts *(A. boonei and M. charantia)*, showed significant activity than chloroquine (P<0.05). Others active plant extracts were *P. amarus, L. inermis, M. indica* and *N. tabacum*. These plants showed higher inhibition of β-hematin synthesis than chloroquine a known β-hematin synthesis inhibitor. The previously reported antimalarial activity of *A. boonei*[30], *M. charantia*[31-33] *P. amarus*[34], *L. inermis*[30], and *M. indica*[35] in a parasite based assay using *in vitro P. falciparum* might due to inhibition of β-hematin synthesis in the parasites. It appears there is no information on antimalarial activity of *N. tabacum*. However, larvicidal, mosquitocidal and antioxidant activities of *N. tabacom* were previously reported [36-37] The mechanism of antimalarial activity of these plant species from sixteen different families vis-a-vis inhibition of β-hematin synthesis is being reported for the first time.

CONCLUSION

The β-hematin colorimetric assay is a reliable assay for determining the mechanism of action of antimalarial agents that utilize the pathway.

Both authors reviewed and approved of the final manuscript.

ACKNOWLEDGEMENT

CONFLICT OF INTEREST

We declare no conflict of interest.

REFERENCES

1. WHO.. Fact Sheet: Malaria. **2016.** http://www.who.int/mediacentre/factsheets/fs094/en/

2. WHO. Fact Sheet: World Malaria Report. 2015. http://www.who.int/malaria/media/world-malaria-report-2015/en/

3. Noedl, H.; Se, Y.; Schaecher, K.; Smith, B.L.; Socheat, D.; Fukuda, M.M. Evidence of artemisinin-resistant malaria in western Cambodia. Artemisinin Resistance in Cambodia 1 (ARC1) Study Consortium. N Engl J Med. **2008,** 359(24), 2619-20.

4. Dondorp, A.; Nosten, F.; Yi, P.; Das, D.; Phyo, A.P.; Tarning, J.; Lwin, K.M.; Ariey, F. Hanpithakpong, W.; Lee, S.J.; Ringwald, P.; Silamut, K.; Imwong, M.; Chotivanich, K.; Lim, P.; Herdman, T.; An, S.S.; Yeung, S.; Singhasivanon, P.; Day, N. P.; Lindegardh, N.; Socheat. D.; White, N. J. . Artemisinin resistance in Plasmodium falciparum malaria. N Engl J Med. **2009,** 361(5), 455-67.

5. Dondorp, A.M.; Fairhurst, R.M.; Slutsker, L.; Macarthur, J.R.; Breman, J.G.; Guerin, P.J.;

Wellems, T.E.; Ringwald, P.; Newman, D.; Plowe, C.V. The threat of artemisinin-resistant malaria. N Engl J Med. **2011,** 365(12), 1073-5.

6. Surolia, N.; Padmanaban, G.G. de novo biosynthesis of heme offers a new chemotherapeutic target in the human malarial parasite. Biochem Biophys Res Commun. **1992,** 187(2),744-50.

7. Subbayya, I.N.; Ray, S.S.; Balaram, P.; Balaram, H. Metabolic enzymes as potential drug targets in Plasmodium falciparum. Indian J Med Res. **1997,** 106, 79-94.

8. Egan, T.J.; Haemozoin (malaria pigment): a unique crystalline drug target. Targets. **2003,** 115–124.

9. Mitra, P.; Deshmukh, A.S.; Dhar, S.K. DNA replication during intra-erythrocytic stages of human malarial parasite Plasmodium falciparum. Curr Sci. **2012,** 102, 725-740.

10. Ridley, R.G. Medical need, scientific opportunity and the drive for antimalarial drugs. Nature. **2002,** 415(6872), 686–693.

11. Pagola, S.; Stephens, P.W.; Bohle, D.S.; Kosar, A.D.; Madsen, S.K. The structure of malaria pigment β-haematin. Nature. **2000,** 404(6775), 307–310.

12. Soares, J.B.C.; Menezes, D.; Vannier-Santos, M.A.; Ferreira-Pereira, A.; Almeida, G.T.; Venancio, T.M.; Verjovski-Almeida, S.; Zishiri, V. K.; Kuter, D.; Hunter, R.; Egan, T.J. Interference with hemozoin formation represents an important mechanism of schistosomicidal action of antimalarial quinoline methanols. PLoS Negl Trop. Dis. **2009,** 3(7), e477.

13. Egan, T.J.; Ross, D.C.; Adams, P.A. Quinoline anti-malarial drugs inhibit spontaneous formation of beta-haematin (malaria pigment). FEBS. Lett. **1994,** 352(1), 54–57.

14. Egan, T.J. Haemozoin formation. Mol Biochem Parasitol. **2008,** 157, 127–136.

15. de Villiers, K.A.; Egan, T.J. Recent advances in the discovery of haem-targeting drugs for malaria and schistosomiasis. Molecules **2009,** 14(8), 2868–2887.

16. Sullivan, D.J. Theories on malarial pigment formation and quinoline action. Int. J. Parasitol. **2002,** 32(13), 1645–1653.

17. Eastman, R.T.; Fidock, D.A. Artemisinin-based combination therapies: A vital tool in efforts to eliminate malaria. Nat Rev Microbiol. **2009,** 7(12), 864–874.

18. Haynes, R.K.; Cheu, K.W.; Li, K.Y.; Tang, M.M.K.; Wong, H.N.; Chen, M.J.; Guo, Z.F.; Guo, Z.H.; Coghi, P., and Monti, D. 2A partial convergence in action of methylene blue and artemisinins: antagonism with chloroquine, a reversal with verapamil, and an insight into the antimalarial activity of chloroquine. Chem Med Chem. **2001,** 6(9), 1603-1615.

19. Vargas, S.; Ioset, K.N.; Hay, A.E.; Ioset, J.R.; Wittlin, S.; Hostettmann, K. Screening medicinal plants for the detection of novel antimalarial products applying the inhibition of β-hematin formation. J Pharm Biomed Anal. **2011,** 56(5), 880-886.

20. Rosenthal, P.J.; Meshnick, S.R. Hemoglobin processing and the metabolism of amino acids, heme & iron. In: Malaria; Parasite Biology, Pathogenesis & Protection. I.W. Sherman ed. ASM press, Washington D.C.P. **1998,** 145-158.

21. Banerjee, R.; Goldberg, D.E. The Plasmodium food vacuole. In: Antimalarial chemotherapy. P.J. Rosenthal, ed. Human Press, Totowa, NJ.P. **2001,** 43-63.

22. Egan, T.J; Ross, D.C.; Adams, P.A. The mechanism of action of quinolines and related antimalarial drugs. S Afr J Sci. **1996,** 92, 11-14.

23. Banerjee, R.; Lin, J.; Beatty, W.; Pelosof, L.; Klembe, M.; Goldberg, D.E. Four plasmepsins areactive in the Plasmodium falciparum food vacuole, including a protease in an active site histidine. Proc Natl Acad Sci. **2002,** 99, 995.

24. Goldberg, D.E.; Slater, A.F.G.; Beavis, R.; Chait, B.; Cerami, A. Hemoglobin degradation in human malaria pathogen Plasmodium falciparum: a catabolic pathway initiated by a specific aspartic protease. J Exp Med. **1991,** 173(4), 961-9.

25. Fitch, C.D.; Chevli, R.; Bayal, A.S.; Philips, G.; Pfaller, M.A.; Krogstad, D.J. Lysis P. falciparum by ferriprotoporphyrin IX & a CQ - ferriprotoporphyrin IX complex. Antimicrob Agents Chemother. **1982,** 21, 819-82.

26. Slater, A.F.G.; Cerami, A. Inhibition of chloroquine of a novel haem polymerase enzyme activity in malaria trophozoites. Nature, **1992,** 355, 167-169

27. Dorn, A.; Vippagunta, S.R.; Matile, H.; Jaquet, C.; Vennerstrom, J. L.; Ridley, R.G. An assessment of drug-haematin binding as a mechanism for inhibition of haematin polymerisation by quinoline antimalarial. Biochem Pharm. **1998,** 55, s727–736.

28. Egan, T.J. Haemozoin (malaria pigment): a unique crystalline drug target. Targets. **2003,** 115–124.

29. Sullivan, D.; Gluzman, I.Y.; Russell, D.G.; Goldberg, D.E. On the molecular mechanism of chloroquine's antimalarial action. Proc Natl Acad Sci. **1996,** 93, 11865–11870.

30. Okpekon, T.; Yolou, S.; Gleye, C.; Roblot, F.; Loiseau, P.; Bories, C.; Grellier, P.; Frappier, F.; Laurens, A.; Hocquemiller, R. Antiparasitic activities of medicinal plants used in Ivory Coast. J Ethnopharmacol. **2004,** 90(1), 91-7.

31. Kamaraj, C.; Kaushik, N.K.; Rahuman, A.A.; Mohanakrishnan, D.; Bagavan, A.; Elango, G.; Zahir, A.A.; Santhoshkumar, T.; Marimuthu, S.; Jayaseelan, C.; Kirthi, A.V.; Rajakumar, G.; Velayutham, K.; Sahal, D. Antimalarial activities of medicinal plants traditionally used in the villages of Dharmapuri regions of South India. J Ethnopharmacol. **2012,** 141(3),796-802.

32. Olasehinde, G.I.; Ojurongbe, O.; Adeyeba, A.O.; Fagade, O.E.; Valecha, N.; Ayanda, I.O.; Ajayi, A.A.; Egwari, L.O. In vitro studies on the sensitivity pattern of Plasmodium falciparum to anti-malarial drugs and local herbal extracts. Malar J. **2014,** 20, 13, 63.

33. Amorim, C.Z.; Marques, A.D.; Cordeiro, R.S. Screening of the antimalarial activity of plants of the Cucurbitaceae family. Mem Inst Oswaldo Cruz. **1991,** 86, Suppl 2, 177-80.

34. Abiodun, O.; Gbotosho, G.; Ajaiyeoba, E.; Happi, T.; Falade, M.; Wittlin, S.; Sowunmi, A.; Brun, R.; Oduola, A. In vitro antiplasmodial activity and toxicity assessment of some plants from Nigerian ethnomedicine. Pharm Biol. **2011,** 49(1), 9-14.

35. Arrey, T. P.; Franzoi, K. D.; Lee, S.; Lee, E.; Vivarelli, D.; Freitas-Junior, L.; Liuzzi, M.; Nolé, T.; Ayong, L.S.; Agbor, G.A.; Okalebo, F.A.; Guantai, A.N. In vitro antiplasmodial activities and synergistic combinations of differential solvent extracts of the polyherbal product, Nefang. Biomed Res Int. **2014,** 2014(835013).

36. Ileke, K.D.; Oyeniyi, E.A.; Ogungbite, O.C.; Adesina, J. M. Nicotianatabacum a prospective mosquitocide in the management of Anopheles gambiae (Giles). International J Mosquito Res. **2015,** 2(4), 19-23.

37. Gratão, P. L.; Pompeu, G.B.; Capaldi, F.R.; Vitorello, V.A.; Lea, P.J. Azevedo RA. Antioxidant response of Nicotiana tabacum cv. Bright Yellow 2 cells to cadmium and nickel stress. Plant Cell Tiss Organ Cult **2008,** 94(1), 73-83.

Synthesis, Antimicrobial, Antioxidant and Docking Study of Novel Isoxazoline Derivatives

Ghosoun Laftaa Mohsen[1], Ahmed Mutanabbi Abdula[1]*,
Abdulkadir Mohammed Noori Jassim[1]

1 Mustansiriyah University, Department of Chemistry, Baghdad, Iraq.

ABSTRACT

A novel series of isoxazoline derivatives (3-10) was synthesized and characterized by using spectral analysis. The synthesized derivatives were *in vitro* screened against several bacterial species as well as *Candida albicans* and exhibit moderate to potent activity. All the synthesized products were screened qualitatively for their antioxidant property by using *TLC* technique and the percent DPPH radical scavenging activity of the potent derivatives (4-6,8) were evaluated. Docking study of isoxazoline derivatives 7 and 8 against L-Glutamine: D-fructose-6-phosphate amidotransferase (glucosamine-6-phosphate synthase), the target enzyme in antimicrobial chemotherapy, was evaluated to explore the interactions of the synthesized hits inside the amino acid residues of the enzyme active site. The docking outcomes strongly supported the *in vitro* assay of new derivatives against several microbial species.

Keywords: Isoxazoline, antimicrobial, antioxidant, docking study.

INTRODUCTION

Synthesis and evaluation of efficacious antimicrobial, due to limited number of effective drugs[1] and antioxidant agents to protect human body from free radicals[2] represent the main goal for the several research groups worldwide. Recently, considerable attention has been given to isoxazoline derivatives due to their varied pharmacological activities like antimicrobial[3], anti-inflammatory[4], anti-tubercular[5], antidepressant[6], antioxidant[7], antitumor and DNA Methyltransferase 1 Inhibitors[8]. Therefore, our attempts to find novel antimicrobial and antioxidant agents focus on the isoxazoline derivative. A novel series of isoxazolines (3-10) were synthesized and characterized by spectral data. Isoxazoline derivatives (3-

10) were *In vitro* screened against several bacterial species *(gram positive and garm negative)* as well as *Candida albicans* and found to exhibit moderate to potent activity. The synthesized derivatives screened for their reducing properties with 2, 2-diphenyl-l-picrylhydrazyl (DPPH) radical by the TLC autographic. The percent of DPPH scavenging by using spectrophotometric assay for isoxazoline derivatives (4-6, 8) which exhibited strong yellow or blue fluorescence under UV light in TLC autographic was evaluated. Docking study of the potent antimicrobial derivatives (7, 8) against L-Glutamine: D-fructose-6-phosphate amidotransferase[9], the specific target for antibacterial and antifungal agents, was achieved to explore and explain the interactions of the discovered hits within the amino acid residues of the enzyme active pocket. The docking results enhanced the activity of new derivatives as promising antimicrobial agents. Autodock 4.2, the efficacious tool for examining the binding alliance of small ligand to enzyme binding pocket[10] was applied to explore the interactions between the isoxazoline derivatives and the glucosamine-6-phosphate synthase active site.

METHODOLOGY

General Synthesis

All starting materials and solvents were obtained from Sigma-Aldrich and used without any additional purification. Melting points were measured on a electrothermal capillary apparatus and are uncorrected; FT-IR spectrum were recorded on a Shimadzu model FTIR-8400S. Mass spectra were obtained on a Shimadzu GCMS-QP2010 Ultra apparatus. 1H NMR spectra were achieved with a Bruker spectrophotometer model ultra-shield at 300 MHz in CDCl3 or DMSO-d6 solution with the TMS as internal standard.

Synthesis of *(E)-1-(4-aminophenyl)-3-(3,4-dimethoxyphenyl)prop-2-en-1-one (1)*

This compound was synthesized according to the procedure described in the published work[11]. Sodium hydroxide (1ml, 40%) was added to a solution of p-aminoacetophenone (1 mmol) in ethanol (10 mL), and the reaction mixture was stirred for half hour. After that 3,4-dimethoxybenzaldehyde (1 mmol) was added and the reaction crude was stirred for 24 h. The reaction crude was stand at the room temperature. The collected product was dried and purified from ethanol as recrystallizing solvent.

Yellow powder, yield 90%, m.p 124-126∘C; IR (cm^{-1}): 3445, 3347 *(NH$_2$)*, 3150 (aromatic *C-H*), 2963 (aliphatic *C-H*), 1642 *(C=O)*, 1598 *(CH=CH)*, 1579 *(C=C)*. ^{1}H-NMR (300MHz, DMSO-d$_6$) δ (ppm): 3.81 (s, 3H, *OCH$_3$*), 3.86 (s,3H, *OCH$_3$*), 6.11 (s, 2H, *NH$_2$*), 6.61-7.95 (m, 9H, *Ar-H, CH=CH*). *Mass (NCI)* m/e: 283 M$^+$ *For*

C17H17NO3. Rf =0.72 (5:5, Hexane:Ethyl acetate).

Synthesis of *4-(5-(3,4-dimethoxyphenyl)-4,5-dihydroisoxazol-3-yl) aniline (2)*

This compound was prepared as described in reference[12]. To the starting material 1 (1mmol) in ethanol (10ml), a mixture of sodium hydroxide (40%, ml) and NH2OH.HCl (1.5 mmol) was added and the crude reaction was refluxed for 15 h. The completion of reaction was monitored by a thin layer chromatography using ethyl actate: hexane system (1:1). The starting material was precipitate by adding crush ice then it was filtered, washing with water, dried and purified using ethanol as recrystallized solvent.

Orange powder, yield 90%, m.p 110-113 °C; IR (cm-1): 3365 (NH_2), 3001 (aromatic *C-H*), 2950 (aliphatic *C-H*), 1604 (*C=N*), 1510 (*C=C*). ^{1}HNMR (300 MHz, $CDCl_3$) δ (ppm): 3.24-3.33 (*dd*, 1H, j= 8.7, 16.5 Hz, CH- isoxazoline), 3.64-3.70 (dd, 1H, j= 10.7, 16.5 Hz, *CH-isoxazoline*),3.88 (s, 2H, NH_2), 3.94 (s, 3H, OCH_3), 3.96 (s, 3H, OCH_3), 5.64 (m, 1H, *CH- isoxazoline*), 6.70 (*d*, j = 8.5 Hz, 2H, Ar-H), 6.85-6.96 (m, 3H, *Ar-H*), 7.52 (d, j= 8.56, 2H, A*r-H*). Mass (NCI) m/e: 298 M+ *For C17H18N2O3, Rf =0.72 (1:1, Hexane: Ethyl acetate).*

Synthesis of Schiff bases (3-7)

These compounds were prepared according to the procedure described in the published reference[13]. To solution of substituted benzaldehyde (1mmol) in methanol (10ml) with few drops of glacial acetic acid, isoxazoline compound 2 (1mmol) was added. The reaction crude was refluxed for 10-12 h and the reaction was checked by a thin layer chromatography (ethyl acetate:hexane ,1:1 and 3:7). The precipitate was filtered and washed with methanol, dried and recrystallized from ethanol.

1-(4-(dimethoxymethyl)phenyl)-N-(4-(5-(3,4-dimethoxyphenyl)-4,5-dihydroisoxazol-3-yl)phenyl)methanimine (3)

Yellow off-white powder, yield 50%, m.p 132-134 ◦C; IR (cm-1): 3059 (aromatic *C-H*), 3001 (aliphatic *C-H*), 1626 (*CH=N*), 1610 (*C=N*), 1521 (*C=C*). 1H-NMR (300MHz, CDCl3) δ (ppm): 3.32-3.41 (dd, j = 8.9, 16.5 Hz, 1H, CH-isoxazoline), 3.72-3.81 (dd, j = 10.7, 16.4 Hz,1H, CH-isoxazoline), 3.89 (s, 3H, OCH3), 3.90 (s, 3H, OCH3), 5.71 (m, 1H, CH-isoxazoline), 6.85-7.93 (m, 11H, Ar-H), 8.48 (s, 1H, CH=N). Rf =0.78 (1:1, Hexane: Ethylacetate)

N-(4-(5-(3,4-dimethoxyphenyl)-4,5-dihydroisoxazol-3-yl)phenyl)-1-(1H-pyrrol-2-yl)methanimine (4)

Yellow powder, yield 75%, m.p 173-175 ◦C; IR (cm⁻¹): (*N-H*), 3055 (aromatic *C-H*), (aliphatic *C-H*), 1670 (*CH=N*), 1593 (*C*=N), 1512 (*C=C*). ^{1}H-NMR (300MHz,

CDCl$_3$) δ (ppm): 3.38-3.48 (m, 1H, *CH- isoxazoline*), 3.73 (s, 3H, *OCH$_3$*), 3.81-3.86 (m, 1H, *CH- isoxazoline*), 3.85 (s, 3H, *OCH$_3$*), 5.56 (m, 1H, *CH- isoxazoline*), 6.13-7.99 (m, 10H, *Ar-H*), 6.28 (s, 1H, *CH=N*), 9.46 (s, 1H, *N-H*). Mass (NCI) m/e: 375 M$^+$ for C$_{22}$H$_{21}$N$_3$O$_3$. R$_f$ =0.48 (1:1, Hexane:Ethylacetate).

N-(4-(5-(3,4-dimethoxyphenyl)-4,5-dihydroisoxazol-3-yl)phenyl)-1-(4-nitrophenyl)methanimine (5)

Yellow powder, yield 79%, m.p 149-151 °C; IR (cm^{-1}): 3090 (aromatic *C-H*), 2997 (aliphatic *C-H*), 1627 *(CH=N)*, 1599 *(C=N)*, 1521 -1346 Two band (*N-O*). ¹H-NMR (300MHz, *CDCl$_3$*) δ (ppm): 3.40-3.49 (m, 1H, *CH-isoxazoline*), 3.76 (s, 3H, *OCH$_3$*), 3.79-3.88 (m, 1H, *CH-isoxazoline*), 3.84 (s, 3H, *OCH$_3$*), 5.67 (m, 1H, *CH-isoxazoline*), 6.68 (s, 1H, *CH=N*), 6.96-8.91 (m, 11H, *Ar-H*),. Mass (NCI) m/e: 429 M$^+$ for C$_{24}$H$_{21}$N$_3$O$_5$, R$_f$ =0.79 (1:1, Hexane: Ethyl acetate).

4-(((4-(5-(3,4-dimethoxyphenyl)-4,5-dihydroisoxazol-3-yl)phenyl)imino)methyl)-N,N-dimethylaniline (6)

Orange powder, yield 50%, m.p 159-161 °C; IR (cm^{-1}): 3080 (aromatic *C-H*), 2968 (aliphatic *C-H*), 1618 (*CH=N*), 1606 *(C=N)*, 1521 (*C=C*). ¹H-NMR (300MHz, *CDCl$_3$*) δ (ppm): 3.07 (s,*6H, N(CH$_3$)*2, 3.29-3.37 (dd, *1H, CH-isoxazoline, j = 16.7, 8.8 Hz*), 3.70-3.81 (dd, 1H, CH-isoxazoline, j = 16.5, 10.6 Hz), 3.89 (s, *3H, OCH$_3$*), 3.95 (s, *3H, OCH$_3$*), 5.69 (m, *1H, CH-isoxazoline*), 6.69-8.36 (m, *12H, CH=N, 11 Ar-H*). Mass (NCI) m/e: 428 M$^+$ for C$_{26}$H$_{26}$N$_3$O$_3$. R$_f$ =0.48 (1:1, Hexane:Ethylacetate).

N-(4-(5-(3,4-dimethoxyphenyl)-4,5-dihydroisoxazol-3-yl)phenyl)-1-(2,4-dinitrophenyl)methanimine (7)

Yellow powder, yield 70%, m.p 172-174 °C; IR (cm^{-1}): 3047 (aromatic *C-H*), 2997(aliphatic *C-H*), 1631 (*CH=N*), 1597(*C=N*), 1512-1340 Two band N-O. Rf = 0.60 (1:1, Hexane: Ethylacetate).

Synthesis of methyl (4-(5-(3,4-dimethoxyphenyl)-4,5-dihydroisoxazole-3-yl)phenyl)carbamate (8)

This compound was prepared according to the modified procedure described in reported work[14]. A mixture of isoxazoline derivatives 8 (1mmol) and excess of methyl chloroformate (0.2 ml) in acetone (10ml) were strrired for 2hrs. The precipitate formed was filtered, washed with acetone and recrystilized from ethanol

Yellow powder, yield 50%, m.p 119-120 °C; IR (cm^{-1}): 3329 broad peak (*NH*), 3003 (aromatic *C-H*), 2937 (aliphatic *C-H*), 1718 (*C=O*), 1604 *(C=N)*, 1516 (*C=C*). *¹HNMR (300 MHz, CDCl$_3$*) δ (ppm): 3.37-3.44 (m, 1H, *CH-isoxazoline*), 3.68 (s, 3H, CH$_3$), 3.75 (s, 3H, *OCH$_3$*), 3.83 (s, 3H, *OCH$_3$*), 3.85-3.87 (m, 1H, *CH-isoxazoline*), 5.64 (m, 1H, *CH-isoxazoline*), 6.94-7.84 (m, 7H, *Ar-H*), 9.96 (s, 1H, *NH*).

Mass (NCI) m/e: 356 M$^+$ *For C$_{19}$H$_{20}$N$_2$O$_5$, R$_f$ =0.56 (7:3, Hexane: Ethyl acetate).*

Synthesis 3-(N-substituted-4-aminophenyl)-5-substitutedarylisoxazoline derivatives [9,10]

These compounds were synthesized according to the modified procedure described in the published work[15]. Anhydrous sodium acetate (1.2 mmol) was added to a mixture of isoxazoline derivative 2 (1mmol) and the corresponding anhydrides (1mmol) (phthalic or maleic anhydride) in glacial acetic acid (3ml) then the mixture was refluxed for 1 h. After completion of the reaction (monitored by *TLC*), the reaction crude was added to crushed ice and stirred. The separated product was filtered and washed with water, dried and recrystallized from ethanol.

2-(4-(5-(3,4-dimethoxyphenyl)-4,5-dihydroisoxazol-3-yl)phenyl) isoindoline-1,3-dione (9)

Gray powder, yield 68 %, m.p 220-222 °C; IR (cm^{-1}): 3009 (aromatic *C-H*), 2939 (aliphatic *C-H*), 1741, 1712 *(C=O)*, 1604 *(C=N)*, 1518*(C=C)*. Mass (NCI) m/e: 428 M$^+$ *For C$_{25}$H$_{20}$N$_2$O$_5$.* R$_f$ =0.48 (3:7, Hexane:Ethylacetate).

1-(4-(5-(3,4-dimethoxyphenyl)-4,5-dihydroisoxazol-3-yl)phenyl)-1H-pyrrole-2,5-dione (10)

Brown powder, yield 76 %, m.p 139-141 °C; IR (cm^{-1}): 3005 (aromatic *C-H*), 2949 (aliphatic *C-H*), 1716, 1668 (*C=O*), 1606 (*C*=N), 1518 (*C=C*). Mass (NCI) m/e: 378 M$^+$ *For C$_{21}$H$_{18}$N$_2$O$_5$, R$_f$ = 0.13 (3:7, Hexane:Ethylacetate).*

Antimicrobial Studies

The synthesized isoxazoline derivatives (3-10) were screened for their antimicrobial activity against *Escherichia coli, Pseudomonas aeruginosa* (*Gram negative*), *Staphylococcus aureus, Streptococcus Spp (Gram positive)* as well as *Candida albicans* by using the well diffusion method (Table 1)[16]. DMSO was used as a control and the test was performed at 2 mg/mL concentration by using DMSO solvent. Amoxicillin was used as standard drugs. An experiment for each compound was made in triplicate and the average reading was recorded.

Antioxidant study (DPPH. radical scavenging assay)

TLC autographic assay: Few milligrams of isoxazoline derivatives (3-10) dissolved in methanol were added to the *TLC* plate by extremely small capillary. After drying, *TLC* plates were sprayed with methanolic solution of 0.2 % DPPH. The plates were examined half hour after spraying. Potent derivative appears as yellow or blue spots against a purple background[17].

Spectrophotometric (DPPH) assay: At first 1.0 mL of the samples at concen-

tration of 100, 300 and 500 μg/ mL was mixed with 0.5 mL of DPPH solution (1.3 mg DPPH / mL methanol) and the volume was complete to 3 mL with methanol. The reaction mixture was left to stand for 30 min in dark place. The control contained all reagents without the sample while gallic acid was used as standard. The DPPH radical scavenging activity was determined by reading the absorbance at 517 nm against the blank. The capability to scavenge the DPPH radical was calculated by using the following equation: DPPH scavenging effect (%) = (A_o-A_1/A_o) X100, where A_o is the absorbance of the control reaction, and A_1 is the absorbance in the presence of compounds or standards[18].

Docking study

AutoDock 4.2 tool was used to specify the affinity of the potent isoxazoline derivatives (7, 8) to the binding site of GlcN-6-P synthase as described by the reported reference[19]. The pdb enzyme file of receptor was downloaded from the RCSB Protein Data Bank (PDB code 1MOQ) and used as a fixed molecule. All the water molecules were eliminated and hydrogens were added to the amino acid residues. ChemDraw ultra 7.0 software was used to construct the chemical structure of examined derivatives as mol format, while the open Babel 2.3.1 software was used to build the pdb file. The docking study was achieved by using grid dimensions 30.5, 17.5 and -2.2, respectively. Docking algorithm using Lamarckian Genetic was employed with 150 population size, 10 runs and 2,500,000 maximum number of energy evaluations, while the maximum number of generations was 27,000.

RESULTS AND DISCUSSION

Organic Synthesis

Chalcone derivative 1 and the isoxazoline compound 2 were prepared and characterized as described by our previous work[20]. Shiff bases (3-7) were synthesized from the reaction of isoxazoline derivative 2 with different aromatic aldehydes in acidic methanolic solution (Scheme 1).
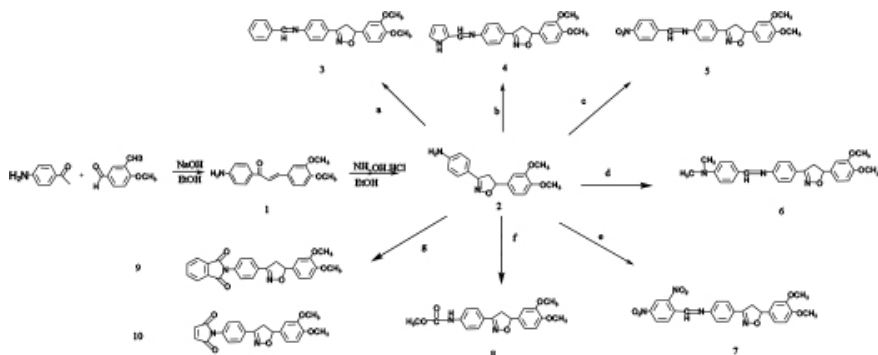
Scheme 1. (a) benzyaldehyde-dimethylacetal, MeOH (b) pyrrole-2-carboxalde-hyde, EtOH (c) p-nitrobenzyaldehyde, EtOH (d) 4-N,N-dimethylbenzylaldehyde, EtOH (e) 2,4-dinitrobenzylaldehyde, MeOH (f) methyl chloroformate , acetone(g) phthalic anhydride or maleic anhydride, glacial acetic acid

The structures of the obtained compounds were confirmed by spectral analysis (see experimental section). The *FT-IR* spectra of compounds (3-7) showed the absorption bands at 1670-1618 cm^{-1}, 1606-1593 cm^{-1} regions due to the stretching vibrations of the *CH=N* and *C=N* groups. The disappearance of the NH$_2$ stretching frequencies strongly enhances the elucidation of prepared compounds. The mass spectra are consistent with the molecular ion peak values of the prepared compounds. The ^{1}HNMR spectra of compound 4 and 5 showed singlet within the 8.89, 8.91 ppm regions due to *CH=N* protons with the absent of the singlet signal at 3.88 related to NH$_2$ group in compound 2. The amide derivative 8 was obtained by the reaction of isoxazoline compound (2) with methyl chloroformate in glacial acetic acid. *IR* spectrum showed broad peak at 3329 cm^{-1} of NH stretching and characteristic peak at 1718 cm-1 due to C=O group. ^{1}HNMR spectra showed two singlet signals at 3.68 and 9.96 ppm related to CH$_3$OCO and NH protons. The reaction between the isoxazoline derivative 2 with phthalic and maleic anhydride was carried out (Scheme1) and purified by recrystallization from ethanol to yield *N*-substitutedphthalimide 9 and *N*-substitutedmaleimide 10 in high yiled. The structures of the N-substituteimide derivatives were confirmed by using IR spectroscopy. The stretching of two carbonyl groups appeared at 1741, 1712 and 1716, 1668 cm^{-1} for compound 9 and 10, respectively. Further elucidation of molecular ion was confirmed via Mass spectroscopy.

Antimicrobial Activity

The *in vitro* assay of the isoxazoline derivatives (3-10) against several microbial species was achieved by using 2 mg /mL concentration as illustrated in Table 1. The tested compounds displayed auspicious activity against different species. Compound 7 and 8 were the potent agents against *gram positive, gram negative* as well as *Candida Albicans.*

Table 1. In vitro antimicrobial inhibition zone (mm) of the synthesized compounds

Isoxazoline derivatives	Gram positive		Gram negative		Fungi
	E.coli	*P.aeruginosa*	*S.aureus*	*Streptococcus Spp*	*C. albicans*
3	15	10	-	11	9
4	-	11	14	11	15
5	10	10	-	12	14
6	13	-	-	10	14
7	11	14	18	13	-
8	10	14	15	12	14
9	11	12	-	-	13
10	11	-	13	-	16
Amoxicillin	20	15	33	21	28

(-) exhibit no activity at specific concentration

Antioxidant Activity

The scavenging properties of all the synthesized derivatives (3-10) were evaluated against DPPH radical by using *TLC* autographic assay. The isoxazoline derivatives dissolved in methanol were transferred to the one end of a *TLC* plate by using spotting capillary. After drying and spraying the DPPH solution, the active compounds (4-6,8) appeared as yellow or blue spots with purple background. The scavenging activity of the lead derivatives (4-6,8) was determined by using spectroscopic method as described in the indicated reference[18]. The relationships between the *in vitro* percentage inhibition and the concentration of the potent hits (100, 200 and 300 µg/mL) are summarized in Figure 1.

a   b
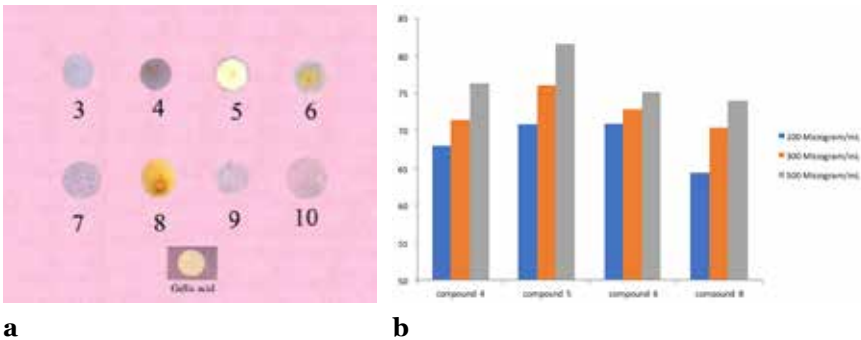
Figure 1. a- TLC autographic assay of the isoxazoline derivatives (3-10), b- Comparison of DPPH scavenging assay of potent compounds (4-6, 8)

Docking Study

The docking study of the potent active isoxazoline derivatives (7, 8) toward antimicrobial species inside the active pocket of L-Glutamine: D-fructose-6-phosphate amidotransferase, the active target for antimicrobial agents was explored. As described by the X-ray study, the binding pocket of target enzyme including the following subsequent residues, cysteine 300, glycine 301, threonine 302, serine 303, serine 347, glutamine 348, serine 349, threonine 352, valine 399, serine 401, alanine 602 and lysine 603 as shown in Figure 2[21].
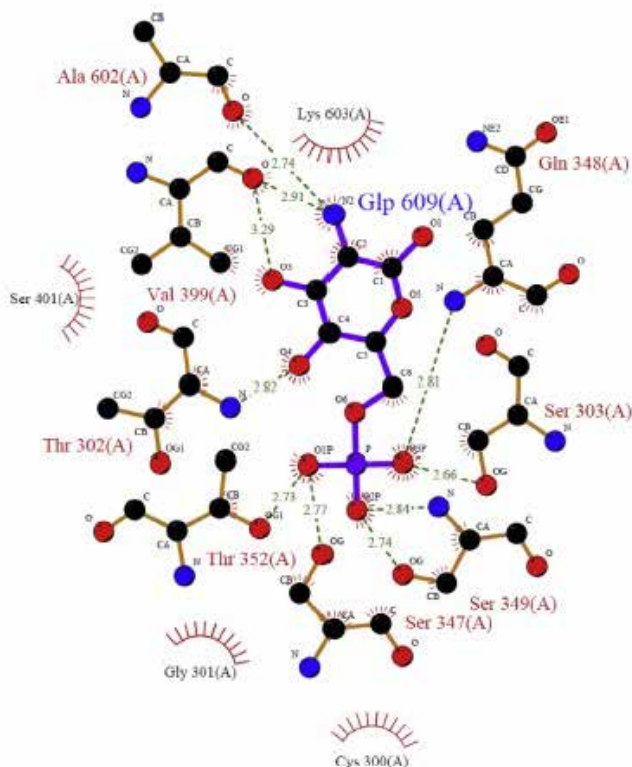
Figure 2. The binding of glucosamine-6-phosphate inside the active site of target enzyme.

The binding energy of active compounds inside the known three-dimensional structure of the specific enzyme was explored by using Autodock 4.2. The binding of the best building conformers for compounds 7 and 8 inside the binding pocket of L-Glutamine: D-fructose-6-phosphate amidotransferase is illustrated in Figure 3.
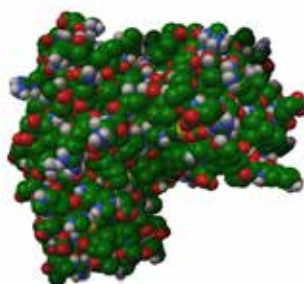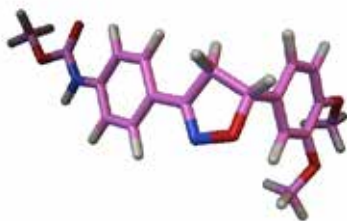
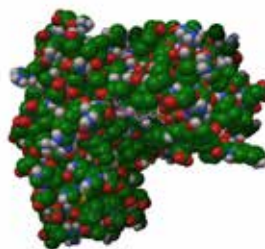3D structure of glucoseamine-6-phosphate synthase (GlcN-6-p)

Compound 7
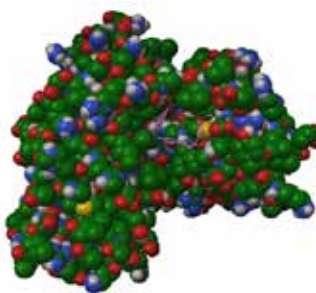
The best conformer of compoud 7 inside binding pocket of GlcN-6-P

Compound 8

The best conformer of compoud 8 inside binding pocket of GlcN-6-P

Figure 3. The docking of the best generated conformers of the potent discovered hits (7 and 8) inside the binding pocket of L-Glutamine: D-fructose-6-phosphate amidotransferase (GlcN-6-P).

As indicated by molecular docking parameters (Table 1), the high-ranking binding energies of the generated conformer was - 5.31and - 5.68 kcal mol^{-1} for compound 7 and 8, respectively. The docking results of all generated conformers of compounds within the binding pocket are strongly enhancing antibacterial and antifungal activities as depicted in Table 1. Furthermore, the inhibition constant

Ki, intermolecular energy and hydrogen bonds were also determined and recorded in Table 2.

Table 2. Docking parameters of isoxazoline compounds (7 and 8)

Compounds		Binding Energy (Kcal mol-1)	Inhibition constant (µM)	Intermolecular energy (kcalmol^{-1})	H-bonds	Bonding
		-5.31	128.24	-7.7	1	GLN348: HE22: LIG:O
	2	-5.24	144.17	-7.63	1	SER604:HN: LIG:O
	3	-5.00	214.77	-7.39	1	GLY301:HN: LIG: N
	4	-4.85	280.90	-7.23	2	GLY301:HN: LIG: N
	5	-4.77	317.38	-7.16	2	ALA602:HN: LIG: O
	6	-4.58	440.84	-6.96	-	GLY301:HN: LIG: N
	7	-4.39	602.48	-6.87	3	ALA602:HN: LIG: O
	8	-4.28	723.19	-6.67	1	-
	9	-3.87	1460.00	-6.26	1	GLN348: HE22: LIG:O
	10	-3.55	2490.00	-5.94	-	LIG:O: SER604:O
8	1	-5.68	68.83	-7.47	1	LYS603:HN: LIG:N
	2	-5.68	68.30	-7.47	2	GLY301:HN: LIG: O
	3	-5.63	75.14	-7.42	1	GLY301:HN: LIG: O
	4	-5.53	88.24	-7.23	1	-
	5	-5.19	157.24	-6.98	-	ASP354:HN: LIG:O
	6	-5.13	173.35	-6.92	-	LIG:H: ASN305:OD1
	7	-5.11	180.95	-6.90	-	ASN305:HD22 LIG:O
	8	-5.09	187.11	-6.88	1	ASN305:HD22: LIG: O
	9	-4.95	233.34	-6.74	1	GLY301:HN: LIG: N
	10	-4.67	380.49	-6.46	1	-
						-
						-
						ASN600:HD22: LIG: O
						ASN600:HD22: LIG: O
						ASN600:HD22: LIG: O

CONCLUSION

The present work summarized the synthesis of novel isoxazoline derivatives as promising antimicrobial agents. The scavenging activity of the potent antioxidant derivatives was estimated by using DPPH radical. On the other hand, docking study using Autodock 4.2 was achieved to illustrate the bound state of ligand enzyme complex for the potent discovered hits.

ACKNOWLEDGMENT

REFERENCES

1. World Health Organization. The evolving threat of antimicrobial resistance: Options for action, **2012.**

2. Swedish Council on Health Technology Assessment in Health Care (SBU). Preventing disease with antioxidants, **1997.** SBU report no 135/1-135/3 (Stockholm, in Swedish).

3. Jadhav, S.B.; Shastri, R.A.; Gaikwad, K.V.; Gaikwad S.V. Synthesis and Antimicrobial Studies of Some Novel Pyrazoline and Isoxazoline Derivatives. *E-Journal of Chemistry.* **2009,** 6*(S1)*, S183-S188.

4. Filali, I.; Bouajila, J.; Znati, M.; Bousejra-El Garah, F.; Jannet H.B. Synthesis of new isoxazoline derivatives from harmine and evaluation of their anti-Alzheimer, anti-cancer and anti-inflammatory activities. *J Enzyme Inhib Med Chem.* **2014,** 1475-6366 (print), 1475-6374.

5. Al Houari, G.; Kerbal, A.; Bennani, B.; Baba, M.F.; Daoudi, M.; Hadda, T.B. Drug design of new antitubercular agents: 1,3-dipolar cycloaddition reaction of para-substituted-benzadoximes and 3-para-methoxybenzyliden-isochroman-4-ones. *General Papers,* **2008,** 1551-7012, 42-50.

6. Pravin O. P.; Sanjay B. B. Synthesis and Antidepressant Activity of Some New 5-(1H-Indol-3-yl)-3-(substituted aryl)-4,5-dihydroisoxazoline Derivatives. *Journal of Chemistry,* **2013.** Article ID 637205, 7 pages.

7. Zeng, Y.; Zhang, H.; Wang, B.; Zhang, L.; Xue, A.; Zhao, X.. Synthesis and biological evaluation of various new bis-isoxazoline derivatives as potential antioxidant additives. *Journal of Chemical Research.* **2016,** 40, 558–563.

8. Castellano S.; Kuck D.; Viviano, M.; Yoo, Jakyung.; Lopez-Vallejo, F.; Conti, P.' Pinto, L. T.; Medina-Franco, A.J.L.; Sbardella, G. Synthesis and Biochemical Evaluation of Δ2 -Isoxazoline Derivatives as DNA Methyltransferase 1 Inhibitors. *J. Med. Chem.* **2011,** 54, 7663–7677.

9. Bearne, S.L.; Blouin, C. Inhibition of Escherichia coli glucosamine-6-phosphate synthase by reactive intermediate analogues. *J. Biol. Chem.* **2000,** 275(1), 135–140.

10. Morris, G.M.; Goodsell, D.S.; Halliday, R.S.; Huey, R.; Hart, W.E.; Belew, K.R.; Olson, A.J. Automated docking using a Lamarckian genetic algorithm and an empirical binding free energy function. *J. Comput. Chem.* **1998,** 19 (1), 639–1662.

11. Mohammed, O.J.; Radi, M.F.; Abdula, A.M.; AL-ahdami, B.W.; Rodhan, W.F.; Sha'aban, H.G. Synthesis of four chalcone derivatives bearing heterocyclic moieties as new Ache inhibitors by docking simulation. *Int. J. Chem. Sci.* **2015,** 13(1), 157-166.

12. Abdel-Rahman, A.A.H.; Abdel-Megied, A.E.S.; Hawata, M.A. M.; Kasem, E.R.; Shabaan, M.T. Synthesis and Antimicrobial Evaluation of Some Chalcones and Their Derived Pyrazoles, Pyrazolines, Isoxazolines, and 5,6-Dihydropyrimidine-2-(1H)-thiones. *Chemical monthly,* **2007.** 138, 889–897.

13. Seelam, N.; Shrivastava, S.P. Synthesis and in vitro study of [1,3,4]thiadiazol-2yl- 3,3a,5,6-tetrahydro-2H-pyrazolo[3,4-d]thiazoles as antimicrobial agents. *J. Saudi. Chem. Soc.* **2012,** 20, 33–39.

14. Velikorodov, A.V.; Imasheva, N.M. Synthesis of Carbamate Derivatives of 2,3-Dihydro-4H-1,4-benzoxazine. *Russ J Org Chem.* **2008,** 44(3), pp. 369–372.

15. Kavitha, K.; Vangala R.R.; Khagga M.; Sarbani P. Lewis acid free high-speed synthesis of Nimedesulide-based novel N-substituted cyclic imides. J. Braz. Chem. Soc. **2010,** 21, 1060-1064.

16. Kavitha K., Vangala R. Reddy, Khagga M., Sarbani P. Lewis acid free high-speed synthesis of Nimedesulide-based novel N-substituted cyclic imides. *J. Braz. Chem. Soc.* **2010,** 21, 1060-1064.

17. Cuendet, M.; Hostettmann, K.; Potterat, O.; Dyatmiko, W. Iridoid Glucosides with Free Radical Scavenging Properties from Fagvaea blumei. *Helv. Chim. Acta.* **1997,** 80(4), 1144-1152.

18. Sapnakumari, M.; Narayana, B.; Sarojini, B.K.; Madhu, L.N. Synthesis of new indazole derivatives as potential antioxidant agents. *Med Chem Res.* **2014,** 23, 2368–2376.

19. Shia J.S.; Al-bayati, R.I.H.; Abdula. A.M.; Saorb, K.Y. docking study of some n-[4-(4-arylidene)-2-(4-substituted-phenyl)-5-oxo-4,5-dihydro-imidazol-1-yl]-benzenesulfonamide derivatives against glucosamine-6-phosphate synthase. *Int. J. Chem. Sci.* **2015,** 13(4), 1982-1990.

20. Ismail A. H.; Abdula, A. M.; Hama, Y. N. Synthesis, characterization and biological evaluation of new heterocyclic compounds from chalcone derivatives. **2017,** Thesis, department of Chemistry, College of Science, Al-Mustansiriyah University.

21. Teplyakov, A.; Obmolova, G.; Badet-Denisot, M-A.; Badet, B.; Polikarpov, I. Involvement of the C terminus in intramolecular nitrogen channeling in glucosamine 6-phosphate synthase: evidence from a 16 A ° crystal structure of the isomerase domain. Structure. **1998,** 6(8), 1047–1055.

Would you like to be healthy again like over 600 of our DBS patients?

Regain the days you have lost because of Parkinson's disease.

A deep brain stimulator (DBS) is a device that delivers electrical current to the specific regions of the brain which modifies electrical activity of the brain cells. This treatment method, called "neuromodulation", makes it possible to treat many movement disorder diseases, especially Parkinson's disease.

Patients with Parkinson's disease may return to their early period of the disease and resume normal life after the deep brain stimulation surgery.

Phyto-fabrication, characteristics and anti-candidal effects of silver nanoparticles from leaves of Ziziphus mauritiana Lam

Rusol M. Al-Bahrani[1], Sura Muayad Abdel Majeed[1], Mustafa Nadhim Owaid[2,3,*], Abdullah B. Mohammed[1], Duha A. Rheem[1]

1 Department of Biology, College of Science, University of Baghdad, Jadriya, Baghdad 10071, Iraq
2 Department of Heet Education, General Directorate of Education in Anbar, Ministry of Education, Hit, Anbar 31007, Iraq.
3 Department of Ecology, College of Applied Sciences, University of Anbar, Hit, Anbar 31007, Iraq.

ABSTRACT

In this work, silver nanoparticles (AgNPs) were biosynthesized from leaves of *Ziziphus mauritiana* Lam. jujube plant in Iraq and tested against fungal pathogens. Extract of leaves of *Z. mauritiana* mixed with 10^{-3} M AgNO$_3$ exposed to slight sunlight for 3 days. Characterization of AgNPs was done using UV-visible spectroscopy, SPM (scanning probe microscopy) and atomic force microscopy (AFM). The change of solution color from pale brown to dark brown and the exhibited maximum peak at 445 nm accepted as an indicator to biosynthesized AgNPs. Aqueous extract of *Ziziphus mauritiana* is considered as biological reduced and stabilized agent for Ag$^+$ to Ag^0. AFM showed the formation of irregular shapes of AgNPs. The biosynthesized silver nanoparticles have an average of diameter of 67.19. The biosynthesized AgNPs from *Z. mauritiana* leaves were tested as nano-drugs against four human pathogenic fungi. The highest concentration 100% of AgNPs has 25 mm inhibition zone against *Candida krusei*. These nanoparticles were found to be useful to reduce Candidiasis.

Keywords: Pharmaceutical, AgNPs, *Candida* sp., green nanotechnology, Jujube, biosynthesis.

INTRODUCTION

Nanoparticles are the most fundamental component in the fabrication of nanostructures. A nanoparticle is bigger than an atom or a simple molecule that is governed by quantum mechanics[1]. Currently, most of applications of silver nanoparticles are antibacterial and antifungal agents, anticancer nano-drugs[2] and in the drug delivery[3]. The biosynthesis is considered of the best ways to reduce

metal ions to atoms and produce nanoparticles which are prepared by the safe and eco-friendly way using microorganisms and extracts of the plant[4]. Recently, many plants were used to synthesize potent AgNPs from *Cassia fistula fruit[5], Bryophyllum pinnatum leaf extract[6]* and *Limonia acidissima* L. leaf [7] against various fungal and bacterial species.

Few recent studies, started in 2014, were achieved to synthesize silver and gold nanoparticles using barks, and fruits of *Ziziphus* spp. and tested against some human pathogenic bacteria[8-10]. While Divband *et al.[11]* used the produced nanoparticles from *Z. spina christi* fly ash to remove Lead (Pb[+2]) from aqueous solutions. In contrast, many studies were achieved in vitro to test bioactivity of crude extracts of this plant against bacteria, molds, and yeasts. Also, Alcoholic and aqueous extracts of the leaves showed the highest inhibition activity toward *Candida albicans[12]* compared with bacterial strains[13] because Ziziphus plant leaves have many biologically active compounds like phenols, saponins, and alkaloids[14]. Furthermore, saponin extract of *Z. spina-christi* has clear antibacterial activity[15]. Leaves of *Ziziphus* sp. has an antimicrobial effect[12,13,15], thus it was used in the treatment of wounds, diarrhea, and gonorrhea[16].

Jujube, *Ziziphus mauritiana*, is distributing in western and southern Iraq under dry conditions[17]. The genus *Ziziphus* sp. belongs to the evergreen herbal plants and to Rhamnaceae family[18]. Generally, many recent studies investigated antifungal activity of Ag-NPs against *Candida* sp., dermatophytic and plant pathogenic fungi[19]. From literatures, no tests against yeast infections were applied or studied by silver or gold nanoparticles of *Ziziphus* spp. This work is considering the first achievement for using the biosynthesis eco-friendly silver nanoparticles from *Ziziphus mauritiana* Jujube plant in the treatment of Candidiasis (yeasts infections) *in vitro*.

METHODOLOGY

Fungal Isolates

Four *Candida species, C. krusei, C. zeylanoides, C. albicans* and *C. guillermondii,* were obtained from Central Public Health Laboratory, Medical City Hospital, Baghdad, Iraq, which were isolated from mouths of patients. These isolates were maintained using Sabroud Dextrose Agar and used to detect bioactivity test of silver nanoparticles synthesized from *Ziziphus mauritiana* Lam. Leaves toward the fungal pathogens.

Preparing aqueous extract of Ziziphus mauritiana Lam. leaves

Leaves of *Z. mauritiana* Lam. were collected from its tree in Baghdad, washed with distilled water, dried at room temperature at 25±2 °C, and grinded by the

blender. About 200 g of the powder was put in a clean glass bottle, added 2 liters of distilled water 1:10 (w/v), and heated for 1 hour at 60 °C. After the cooling, the aqueous extract was filtered using Whatman No. 1 filter paper. This solution was considered as a crude extract solution and stored at 2 °C until use.

Green synthesis and Characteristics of Ag nanoparticles

The required weight of $AgNO_3$ was dissolved in D.W. and then 5 ml of 10^{-3} M $AgNO_3$ solution was mixed with 45 ml of aqueous extract of *Z. mauritiana* leaves and put in 250 ml-volumetric flask. In another flask 5 ml D.W. was added to 45 ml of the aqueous extract as control. The two flasks exposed to slight sunlight at 26±2 °C for 3 days. When putting $AgNO_3$ solution with aqueous extract of Z. mauritiana leaves, the changing in color was observed that indicated formation of AgNPs. Characterization of AgNPs was done using UV-visible spectroscopy, SPM (scanning probe microscopy) and AFM (atomic force electron microscopy).

Anti-candidal activity of AgNPs

Silver Nanoparticles were applied against fungi by determination zone of inhibition *in vitro*. Anti-fungal activity of the biosynthesized AgNPs was investigated against some *Candida species (C. krusei, C. zeylanoides, C. albicans and C. guillermondii)* by well diffusion method using Sabouraud Dextrose Agar (SDA). The density of the yeast inoculum was adjusted to 105 cfu/ml. One hundred microliters (100 µl) of the yeast inoculum was added on SDA medium and spread using a sterile cotton swab even distribution of the inoculum. A sterile cork was used to make 9 mm wells into the plate, added AgNPs solution and left at cooling place for 30 min to allow absorption of excess fluid. Of AgNPs concentrations 25, 50, 75 and 100%, only 50 µl per well were poured into the wells of the plate. The control well was studied with 50 µl/well crude sample in each concentration (25, 50, 75 and 100%) for comparison purpose. These Petri dishes were then incubated at 35 °C for 18 hours and examined for measuring zone of inhibition.

RESULTS AND DISCUSSION

## Characterization of silver nanoparticles

The changing color of the mix (aqueous extract plus $AgNO_3$ solution) takes place from pale brown to dark brown color, while no color change is observed in the aqueous extract without $AgNO_3$ solution because of the role of Z. mauritiana Lam. leaves extract in the mix as a reductant and stabilizer agent. The change in color from pale brown to dark brown indicates biosynthesis of AgNPs as mentioned by Kredy[15]. The formation of AgNPs by using *Z. mauritiana* Lam. leaves extract is confirmed by UV-Vis spectroscopy after 27 hr under slight sunlight at 26±2 °C. The highest UV-visible peak is 445 nm at absorption 0.925 that confirms the for-

mation of silver nanoparticles due to excitation of surface plasmon vibrations in silver nanoparticles. These results of color and UV-Vis spectrum agree with many recent studies for biosynthesis of AgNPs from plants and fungi extracts[9,20].

Surface topography and size of the sample film were investigated using Granularity Cumulation distribution chart by scanning probe microscopy (SPM) and atomic force electron microscopy (AFM) images. Also, AFM images exhibited the histogram of the percentage of AgNPs as a function of the grain size as in Figure 1. The average particle size determined from SPM is approx. 67.19 nm, and the diameters of 50 nm (≤10%), 65 nm (≤50%), 85 nm (≤90%) and 105 nm (≤2.3) as shown in Table 1 and Figure 1. The range of diameters is from 55 to 105 nm and this is an evidence for silver nanoparticles biosynthesis from *Z. mauritiana* leaf extract. AFM of the surface morphology of the film gives a good indicator for the formation of AgNPs. Of SPM imager surface roughness analysis (Figure 2), average of roughness is 51 nm, core roughness depth is 176 nm and the reduced valley depth is 34 nm. The surface topography of the AgNPs exhibited in Figures 2A (lateral view) and 2B (3D view) and it is clear that Ag nanoparticles are irregular in shape, having a cover of the organic shell[21] and are aggregated as in table1. These results agree with preparations of gold nanoparticles (AuNPs) from extract of *Z. mauritiana* leaves with range from 20 to 40 nm[22].
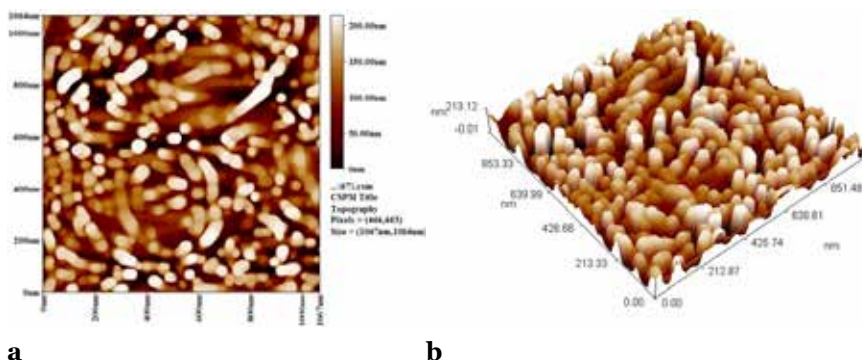
Table 1. Granularity Cumulation distribution, volume and average of diameters of AgNPs

Diameter (nm)<	55	60	65	70	75	80	85	90	95	100	105
Volume (%)	2.3	29.41	27.06	14.12	11.76	1.18	2.35	3.53	3.53	2.35	2.35
Cumulation (%)	2.35	31.76	58.82	72.94	84.71	85.88	88.24	91.76	95.29	97.65	100
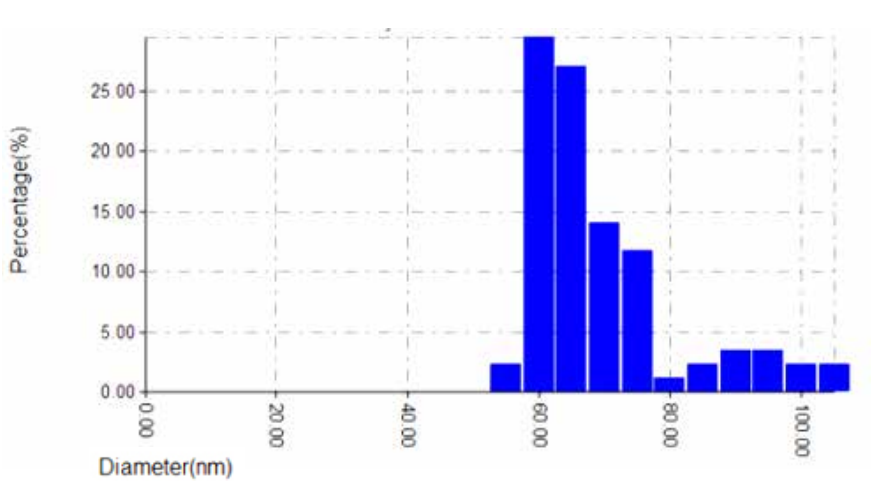
Figure 1. Histogram of particle size distribution of the biosynthesized silver nanoparticles

a   b

**Figure 2.** AFM of the biosynthesized silver nanoparticles

Antifungal activity of the synthesized silver nanoparticles

The biosynthesized AgNPs from *Ziziphus mauritiana* leaves were tested as a nano-drug against human pathogenic fungi which were isolated from patients' mouth in the Medical City Hospital in Baghdad. The possible anti-fungal activities of the biosynthesized AgNPs and the aqueous extract were examined toward four pathogenic fungi, *Candida sp., (C. krusei, C. zeylanoides, C. albicans and C. guillermondii)* on SDA medium by well diffusion method (Figures 3 and 4). The aqueous extract of *Z. mauritian*a at concentration of 100% showed a slight inhibitory effect toward some *Candida species,* while concentrations of 25%, 50%, 75% were not exhibited any inhibitory effects except with the final two concentrations (57% and 50%) as shown in Figure 3. However, this figure showed the bioactivity of silver nanoparticles against *Candida species* is increasing with the increase of AgNPs concentrations. The higher inhibitory effect (zone of inhibition) is 25 mm against *Candida krusei* by the concentration 100% of AgNPs compared with 20 mm by the plant extract alone (100%), followed 24 and 18 mm by the same pathogen in case the concentrations 75% and 50% respectively. Furthermore, the lower concentration of AgNO$_3$ (25%) was inhibited *C. krusei* (12 mm) while the concentration of extract 25% did not have any inhibitory effect as shown in Figures 3B and 4. Generally, the concentrations of extract 25%-75% did not inhibit other species *C. zeylanoides, C. albicans and C. guillermondii* (Figure 3A). The zone of inhibition of AgNPs is 18 mm when using the concentrations 50% and 100% in case *C. krusei and C. zeylanoides,* respectively. From another hand, the zone of inhibition of *C. albicans* and *C. guillermondii* is 16 mm when using the dose 100% (AgNPs). While the lower inhibitory effect is reached 12 mm by the concentration 25% for all *Candida* species (Figure 3B). The results of the zone of inhibition in this study agree with biomedical applications of the biosynthesized AgNPs from this plant against pathogenic bacteria.

Some researchers have reported that the positive charge on the silver ion is critical for its antibacterial and antifungal activities through the electrostatic attractions between the negative charge of the cell membrane of microbes and the positive charge of AgNPs[23,24]. Generally, AgNPs have a moderate inhibitory effect against *Candida* infections that agrees with results of zone of inhibition of AgNPs against *Candida* spp. by Owaid et al.[25]. The bioactivity of *Ziziphus* sp. leaves may be return to their antibacterial and antifungal effects in the crude form as mentioned by many studies[12,13,15] especially toward *Candida* yeasts[12] because *Ziziphus* plant leaves have phenols, saponins, and alkaloids[14]. Also, the role of these AgNPs are considered as antifungal agents, maybe return to the presence of plant bioorganic capping material upon the AgNPs which enables them to observe enhanced anti-candidal activity[26]. All these results are agreeing with the recent works[8,9,16,22] but this study is considered the first test to investigate activity of the biosynthesis AgNPs from leaves of *Ziziphus mauritiana* Lam. against native *Candida* spp.
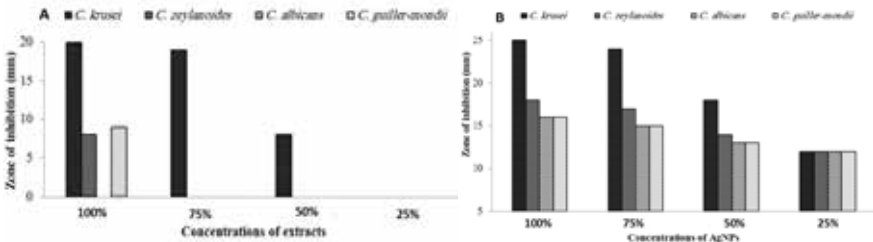
Figure 3. Zone of inhibition of aqueous extract of Jujube leaves (A) and its silver nanoparticles (B) against *Candida* species.
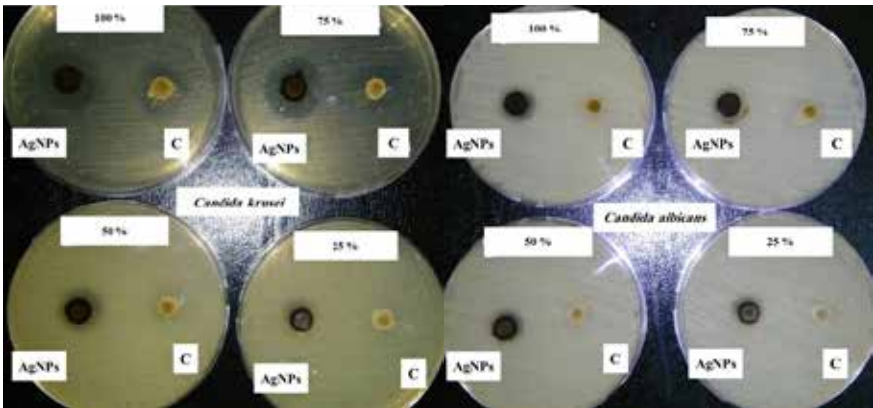
Figure 4. Zone of inhibition of Ag nanoparticles and aqueous extracts of Jujube (C) against *Candida* spp.

CONCLUSION

In this investigation, silver nanoparticles were synthesized in irregular shapes from leaves of *Ziziphus mauritiana* jujube tree in Iraq. The best absorption peak was located at 445 nm which established by using UV-Visible spectrum after change of color of the mix from pale brown to dark brown. The silver nanoparticles of *Z. mauritiana* leaves have average of diameter 67.19 nm with ranging from 55 nm to 105 nm. The biosynthesized AgNPs were used as a nano-drug against human pathogenic fungi (Candida sp.) which were isolated from patients' mouth in the Medical City Hospital in Baghdad. The higher anticandidal activity showed against *Candida krusei* with zone of inhibition 25 mm in case AgNPs concentration 100 % compared with zone of inhibition 20 mm by the plant extract alone (100%), followed 24 and 18 mm by the same pathogen in case the concentrations of AgNPs 75% and 50% respectively. The lower sensitivity of AgNPs was 12 mm recorded for all *Candida* species at the concentration 25%.

ACKNOWLEDGEMENT

REFERENCES

1. W Al-Taa'y, MA Nabi, RM Yusop, E Yousif, BM Abdullah, J Salimon, N Salih and SI Zubairi. Effect of Nano ZnO on the Optical Properties of Poly(vinyl chloride) Films. *Int. J. Polymer Sci.* **2014,** 697809.

2. T Muhsin and A Hachim. Antitumor and Antibacterial Efficacy of Mycofabricated Silver Nanoparticles by the Endophytic Fungus *Papulaspora pallidula. American J. Bioeng. Biotech.* **2016,** 2(1), 24–38.

3. WH De Jong and PJA Borm. Drug delivery and nanoparticles: Applications and hazards. *Int. J. Nanomed.* **2008,** 3, 133–149.

4. A Kusior, J Klich-Kafel, A Trenczek-Zajac, K Swierczek, M Radecka and K Zakrzewska. TiO$_2$-SnO$_2$ Nanomaterials for Gas Sensing and Photocatalysis. *J. Eur. Ceramic Soc.* **2013,** 33, 2285–2290.

5. MI Rashid, LH Mujawa, MI Mujallid, M Shahid, ZA Rehan, MKI Khan and IMI Ismail. Potent bactericidal activity of silver nanoparticles synthesized from Cassia fistula fruit. *Microbial Pathogenesis* **2017,** 107, 354–360.

6. FK Tareq, Mst Fayzunnesa and Md S Kabir. Antimicrobial activity of plant-median synthesized silver nanoparticles against food and agricultural pathogens. *Microbial Pathogenesis* **2017,** 109, 228–232.

7. BN Patil and TC Taranath. *Limonia acidissima* L. leaf mediated synthesis of silver and zinc oxide nanoparticles and their antibacterial activities. *Microbial Pathogenesis* **2018,** 115, 227–232.

8. R Kirubha and G Alagumuthu. Production of biogenic silver nanoparticles using *Ziziphus jujuba* fruit extract. *Int. J. Pharm. Res. Bio-Sc.* **2014,** 3(5), 287–297.

9. BS Maria, A Devadiga, VS Kodialbail and MB Saidutta. Synthesis of silver nanoparticles using medicinal *Zizyphus xylopyrus* bark extract. *Appl. Nanosci.* **2015,** 5, 755–762.

10. MA Abdel-Fatah, NH Hussein, SI Hawash and HH Shaarawy. Investigation of using Sidr leave extracts in nano-silver preparation. *ARPN J. Eng. Appl. Sci.* **2016,** 11(19), 11649–11654.

11. L Divband, M Behzad, SB Nasab and S Divband. Investigation of nano particles efficiency prepared from Cedar fly ash *(Zizyphus spinachristi) f*or lead (Pb^{+2}) removal from aqueous solution. *Iranian J. Health Environ.* **2012,** 5(2), 65.

12. JD Neama, NMJ Abu-Mejdad and AM Jaber. Evaluation the antimicrobial activity of aqueous and alcoholic extracts of leaves *Ziziphus spina-christi* (L) Desf. *Basrah J. Sci B* **2007,** 25(1), 1–16.

13. HI Abd Al-Wahab and TA Hussien. Study the effect of aqueous cold water and alcoholic extracts of *Ziziphus spina christi* against bacteria isolated from conjunctivitis *in vitro and in vivo. Baghdad Sci. J.* **2015,** 12(1), 14–19.

14. RA-M Saqur, WJ Atia and YK Abbas. The study of some chemical components of vegetative parts of Jujube Ziziphus spina-christi L. Wild. var. spina-christi and Banber Cordia myxa L. plants. *J. Thi-Qar Sci.* **2014,** 4(2), 112–120.

15. HM Kredy. Antibacterial activity of saponins extract from Sider *(Ziziphus spina_christi). J. Thi-Qar Univ.* **2010,** 6(1), 16.

16. A Michel. Tree, Shrub and Liana of West African Zone, Margraf Publishers GMBH, Paris. **2002,** p. 440.

17. JA Duke and ES Ayensu. Medicinal plants of China, Reference Publication Inc., **1985,** 20, p.4.

18. DK Cherry, E Hing and DA Woodwell. National Ambulatory Medical Care Survey: 2006 Summary Number 3. August 6, 2008.

19. MN Owaid and IJ Ibraheem. Mycosynthesis of nanoparticles using edible and medicinal mushrooms. *Eur. J. Nanomed.* **2017,** 9(1), 5–23.

20. MN Owaid, SSS Al Saeedi and IA Abed. Study on UV-visible for detection of biosynthesis of silver nanoparticles by oyster mushroom's extracts. *J. Water Environ. Nanotech.* **2017,** 2(1), 66–70.

21. R Bhat, VG Sharanabasava, R Deshpande, U Shetti, G Sanjeev and A Venkataraman. Photobio-synthesis of irregular shaped functionalized gold nanoparticles using edible mushroom *Pleurotus florida* and its anticancer evaluation. *J. Photochem. Photobio. B: Bio.* **2013,** 125, 63–69.

22. B Sadeghi. *Zizyphus mauritiana* extract-mediated green and rapid synthesis of gold nanoparticles and its antibacterial activity. *J. Nanostruct. Chem.* **2015,** 5, 265–273.

23. T Hamouda, A Myc, B Donovan, A Shih, JD Reuter and JR Baker. A novel surfactant nanoemulsion with a unique non-irritant topical antimicrobial activity against bacteria, enveloped viruses and fungi. *Microbiol Res.* **2000,** 156, 1–7.

24. P Dibrov, J Dzioba and KK Gosink. Chemiosmotic mechanism of antimicrobial activity of Ag(+) in *Vibrio cholerae. Antimicrob Agents Chemother* **2002,** 46, 2668–2670.

25. MN Owaid, J Raman, H Lakshmanan, SSS Al-Saeedi, V Sabaratnam and IAA Al-Assaffii. Mycosynthesis of silver nanoparticles from *Pleurotus cornucopiae var.* citrinopileatus and its inhibitory effects against *Candida sp. Mater. Lett.* **2015,** 153, 186–190.

26. S Prabhu and EK Poulose. Silver nanoparticles: mechanism of antimicrobial action, synthesis, medical applications, and toxicity effects. *Int. Nano Lett.* **2012,** 2, 1–10.

A new spectrophotometric method for the determination of gabapentin using chromotropic acid

Olayemi M. Adegbolagun[1], Olusegun E. Thomas[1], Elizabeth O. Aiyenale[1], Olajire A. Adegoke[1]*

1 University of Ibadan, Faculty of Pharmacy, Department of Pharmaceutical Chemistry, Ibadan, Nigeria.

ABSTRACT

The purpose was to develop a colorimetric method for determining gabapentin.

The method was based on the diazo coupling reaction between diazotized gabapentin and chromotropic acid. The method was validated using ICH guidelines before its application to generic brands of gabapentin.

Coupling reaction generated an orange azo adduct whose absorbance was linearly correlated with concentration in the range of 1-6 μg/mL at 470 nm. The method was accurate and precise with recovery range of 97.6-103.1%; intra- and inter-day precisions (%RSD) were less than 0.65% and showed no statistical difference when compared with reference method in the analysis of the dosage forms. The 3D optimization of the adduct revealed an E-type configuration around the azo linkage which would contribute to its stability.

The new method can serve as a reliable alternative to the official method for the routine analysis of gabapentin in bulk and dosage forms.

Keywords: Gabapentin, colorimetric analysis, chromotropic acid, diazo coupling reaction.

INTRODUCTION

Epilepsy is a neurological disorder that is associated with a deficiency in gamma-aminobutyric acid (GABA) receptors in the microgyric cortex of the brain[1]. With an estimated 4 to 10 persons per 1000 people in the general population with active epilepsy i.e. continuing seizures or need for treatment, epilepsy is the fourth most common neurological disorder after migraine, stroke and Alzheimer's disease [2, 3]. Of this world-wide incidence, 80% of those with the disorder live in low- and middle-income countries where the incidence is prob-

ably closer to 7 to 14 per 1000 persons[3]. Epilepsy is characterised by recurrent unprovoked seizures which are either generalized or partial. The latter type can occur with or without alteration of consciousness also known as complete or simple partial seizures respectively[4]. While brain surgery and nervus vagus stimulation and, strict ketogenic diet are useful management options, drug therapy remains the mainstay of epilepsy treatment[5-6]. Unfortunately, adequate seizure control might not be achievable in 20-25% of patients being managed on conventional medicinal agents which include carbamazepine, ethosuximide, phenobarbital, phenytoin, and valproate[7]. Consequently, management of these patients with uncontrolled seizures often involves the inclusion of the newer atypical antiepileptics including gabapentin, lamotrigine, topiramate, levetiracetam[4]. Gabapentin which chemically is 1- (amino methyl) cyclohexane acetic acid and a derivative of endogenous GABA is licensed for use in both adult and paediatric populations and has since emerged as the most frequently included medication in the adjunct treatment of epilepsy. Gabapentin is soluble in water, acidic and alkaline media as the molecule in solution can exist in the cationic, zwitterionic or anionic form at low, physiological and high pH respectively[8-9].

A review of the existing methods of analysis of gabapentin reveal a number of procedures that involve derivatization, a step which is necessitated by the minimal presence of chromophores in the analyte. These methods include derivatization prior to colorimetry[10-12], fluorimetry[13,14], planar chromatographic quantification[15] as well as post column derivatization in chromatographic analysis[16]. In a study comparing the direct spectroscopic methods of analysis of gabapentin with those involving derivatization, the latter consistently yielded the highest sensitivity, lowest limits of detection and quantification[17]. Other previously reported methods are non-aqueous titration[18] and capillary electrophoresis[19]. Due to the lack of extensive chromophores in gabapentin molecule, several chromatographic and electrophoretic methods have been developed and reported for the analysis of the drug in bulk samples, dosage forms and particularly in biological samples. These methods include HPLC[20-25], LC-MS[26] and GC-MS[27-28]. However, a few drawbacks are noticeable in a number of these methods. Majority of the previously reported assay procedures that are based on ion pair complexation and liquid chromatography involve an additional step of solvent extraction and strict control of pH respectively. Some of the UV methods also allow determination only at the UV region which is often fraught with interference leading to decreased selectivity. The objective of this study was therefore to develop a visible spectrophotometric method which offers comparative advantage over the previously reported methods and is sufficiently accurate to serve as an alternative to reference methods.

METHODOLOGY

Chemicals and reagents

Methanol (BDH UK), ethanol, ethyl acetate, sulphuric acid, hydrochloric acid, sodium nitrite (BDH-Poole, England), lactose, magnesium stearate, talc, starch, gelatin, distilled water, Chromotropic acid (Sigma Aldrich USA), gabapentin chemical reference substance.

Instrumentation

Lambda 25 digital UV/VIS spectrometer (Perkin Elmer Inc., Singapore) with 1 cm path length and matched quartz cells, thermostatic water bath (Langford UK), vortex mixer, analytical balance (Mettler PC 400).

Preparation of solutions

Preparation of 0.3%w/v chromotropic acid solution

A 0.075g quantity of chromotropic acid (CTA) was dissolved in about 15.0 mL of water in a 25.0 mL volumetric flask and then made up to volume with distilled water.

Preparation of diazonium solution

A 0.01604 g quantity of gabapentin was transferred into a mixture of 2.0 mL distilled water and 0.12 mL of 2.0 M HCl contained in a beaker with a means of agitation and maintained at 0°C using an ice bath. An aliquot (5.0 mL) of 0.3 M sodium nitrite solution was then added to the mixture and stirred for an additional 20 mins. Thereafter the volume of the diazonium solution was made up to 10.0 mL in a volumetric flask with ice-cold distilled water.

Evidence of coupling reaction

Coupling reaction between the diazotized drug and chromotropic acid was established using spot test and thin layer chromatographic analysis.

Spot test

A 0.5 mL aliquot of the diazonium was added to an equal volume of the chromotropic acid solution in a test tube and vortex-mixed. The colour of the resultant azo adducts after 5 mins and 20 mins following incubation at 30 °C were noted. The procedure was repeated at 70 °C.

Thin layer chromatography

TLC analysis of the diazonium, chromotropic and adduct solutions were carried out by spotting freshly prepared solutions on pre-coated TLC (GF254 0.2 mm, Merck Germany) and then developed using the several mobile phases.

Effect of dilution solvents

The suitability of methanol, ethanol, 1-propanol, ethyl acetate and water to serve as the dilution solvent for UV absorbance measurements was investigated by using each of the solvent in turn to make up the volume of the adduct.

Selection of analytical wavelength

An aliquot (0.5 mL) of the diazonium solution was added to an equal volume of chromotropic acid solution in a test tube. The reaction mixture was vortex mixed and then incubated at 30 °C for 10 mins after which the solution was made up to 5.0 mL with methanol. The UV-vis spectrum, between 190 - 900 nm, of the azo adduct was then acquired using methanol as blank. The UV-vis spectra of 0.5 mL aliquots of chromotropic acid and gabapentin stock solutions in methanol were also acquired.

Optimization of critical response parameters

For the optimization steps, the concentration of diazotized gabapentin utilized was 1.604 µg/mL of gabapentin

Optimization of sodium nitrite concentration for diazotization

Different batches of the diazonium solution were prepared using 5 mL of 0.05, 0.1, 0.2, 0.3, 0.4 and 0.5 M solutions of sodium nitrite as described in 2.3.2. A 0.5 mL aliquot of each of the diazonium solutions was used in turn to generate the adduct with 0.5 mL chromotropic solution. Following incubation at 30 °C for 10 mins, the reaction mixture was made up to 5 mL volume with methanol and the absorbance determined at 470 nm. Each determination was done in duplicates.

Optimization of hydrochloric acid concentration for diazotization

The effect of varying the concentration of the HCl used in the diazotization was investigated by using equal volumes of 0.5, 1.0, 2.0, 2.5 and 3.0 M HCl solutions in turn to prepare different batches of the diazonium solutions. Each diazonium solution was then used to generate the azo adduct and the absorbance determined at 470 nm. Each determination was done in duplicates.

Optimization of volume of hydrochloric acid for diazotization

The effect of varying the volume of the optimized concentration of HCl obtained from section on the optimization of hydrochloric acid concentration for diazotization was investigated by using 0.12, 0.25, 0.5, 1.0 and 2.0 mL of the acid solution in the diazotization procedure. Each diazonium solution was then used to generate the azo adduct and the absorbance determined at 470 nm. Each

determination was done in duplicates.

Effect of chromotropic acid concentration on coupling reaction

The effect of varying the concentration of the coupling agent was investigated by using different CTA solutions corresponding to 0.1, 0.2, 0.3, 0.4, 0.5, 1.0, 2.0 and 3.0% w/v to obtain the adduct with the diazonium. The absorbance at 470 nm of each methanolic solution of the adduct was determined.

Optimization of coupling temperature

Optimization of temperature and time was done using the method of steepest ascent[29]. Equal volumes (0.5 mL) of the diazonium and CTA solutions were vortex mixed in test tubes and then incubated at 30°C for 5 and 20 mins. The entire procedure was repeated at 50, 60 and 70°C. After each time interval, the reaction was terminated by cooling in an ice-bath and the volume of each reaction mixture made up to 5 mL with methanol. The absorbance was determined at 470 nm using methanol as blank. Each determination was carried out in duplicates.

Optimization of coupling time

The effect of coupling time was investigated by varying the incubation times 0, 2, 5, 10, 15, 20, 25 and 30 mins of the azo adduct at the optimized temperature. After each time interval, the reaction was terminated by cooling in an ice-bath and the volume of each reaction mixture made up to 5.0 mL with methanol. The absorbance was determined at 470 nm using methanol as blank. Each determination was carried out in duplicates.

Determination of stoichiometric ratio

The Job's method of continuous variation was employed to determine the stoichiometric ratio that was optimal for colour development[30]. Into nine test tubes containing 0, 0.2, 0.25, 0.33, 0.5, 0.67, 0.75, 0.8 and 1.0 mL of the diazonium, appropriate quantities of CTA were added to make the volume 1.0 mL. Each reaction mixture was then incubated at 30 °C for 10 mins after which the reaction was terminated by cooling in ice and diluting to 5.0 mL with methanol. The absorbance of each of the solutions was determined at 470 nm using methanol as blank. Each determination was done in duplicates.

Validation studies

The calibration line was obtained from the 3-day average curves using volumes of the diazonium solution equivalent to 0.0, 1.0, 2.0, 3.0, 4.0, 5.0 and 6.0 µg/mL of the drug. To each of the test tube, 0.5 mL CTA solution was added, mixed and then incubated at 30 °C for 10 mins. After this, the reaction was terminated

by cooling in ice and dilution to 5.0 mL with methanol before the absorbance was determined at 470 nm using methanol as blank. Each determination was done in triplicates. Model recoveries and repeatability of the new method was carried out on three successive days as stipulated by USP[31]. The percent recoveries of the method as well as the intra- and inter-day precision were determined at three different concentrations equivalent to 2.0, 3.4 and 5.0 μg/mL of the diazotized drug. The current ICH guidelines were employed to determine the limits of detection and quantification as the ratio of the 3.3 and 10 standard deviation of the blank signal (n=6) respectively, divided by the slope of the calibration line.

Method selectivity

The interference liabilities of the new method were demonstrated by the determination of the recoveries of spiked amounts of the analyte in the presence of commonly pharmaceutical aids including starch, lactose, talc, magnesium stearate, gelatin and a mixture of all. Four replicate analyses were carried out with each excipient.

Analytical signal stability

Methanolic solutions of the azo adduct equivalent to 3.4 μg/mL gabapentin were divided into one of either two groups: those exposed to diffuse light or those protected with aluminum foil coverings. The absorbance of the solutions was determined at 30-minute intervals for 3 hours, and after these at twenty-four and seventy hours.

Dosage form analysis

The new method was applied to the active pharmaceutical ingredient content of three brands of gabapentin. The weight uniformity test was determined on twenty capsules and the amount of the powder equivalent to 50 mg of gabapentin transferred to a 10.0 mL volumetric flask. Enough water was added to make up the volume and the mixture filtered after adequate equilibration. A portion of the filtrate (2.0 mL) was then employed for the diazotization procedure as described in section 2.3.2. An aliquot of 0.017 mL of the diazonium (equivalent to 3.4 μg/mL gabapentin) was added to 0.5 mL CTA and then mixed for 10 seconds. The reaction mixture was incubated at 30 °C for 10 mins after which the reaction was terminated by cooling in an ice-bath and dilution with methanol. The absorbance was determined at 470 nm with methanol as the blank.

Non-aqueous titrimetric assay of gabapentin using 0.01 M perchloric acid with 0.2% crystal violet as indicator was used as the reference method. Six replicate analyses of each of the brand were carried out using both methods.

Infra-Red analysis of the isolated adduct

Spectroscopic characterisation of the isolated azo adduct was carried out by the acquisition of the infra-red data of the KBr disc.

2.13 Statistical analysis

The data obtained from the analysis of gabapentin in dosage forms using the new method described in this work and the reference method were compared statistically using Student t-test and F-ratio test. A p value of less than 0.05 was considered to show a statistically significant result.

RESULTS AND DISCUSSION

Evidence of coupling reaction

Diazotised gabapentin reacted instantly with chromotropic acid solution to give an intense orange adduct that was quite distinct from the colourless diazonium and pale-yellow CTA solutions. Similar results were obtained following incubation at higher temperature and prolonged time. The colour was stable for more than forty-eight hours as monitored by the absorbance. The TLC analysis also revealed that the R_f values of the adduct using the mobile phases were different from those of the diazonium and CTA solutions. TLC examination also confirmed the formation of a mono product as only a single spot was observed in the chromatogram.

Selection of analytical wavelength

The overlaid spectra of the drug, the diazonium, CTA and adduct solutions are presented in figure 1. The increase in the conjugation associated with the conversion of the free amino group of the drug to the diazonium functional group was evident in the bathochromic shift of the diazonium which absorbed at 235 and 360 nm when compared with the almost insignificant absorption of the drug at 225 nm. On coupling with CTA, the spectra of the azo adduct also showed extensive bathochromic shift with absorption peaks at 435 nm. The analytical wavelength was therefore selected at 470 nm at which both the diazonium and CTA showed minimal absorptivities.
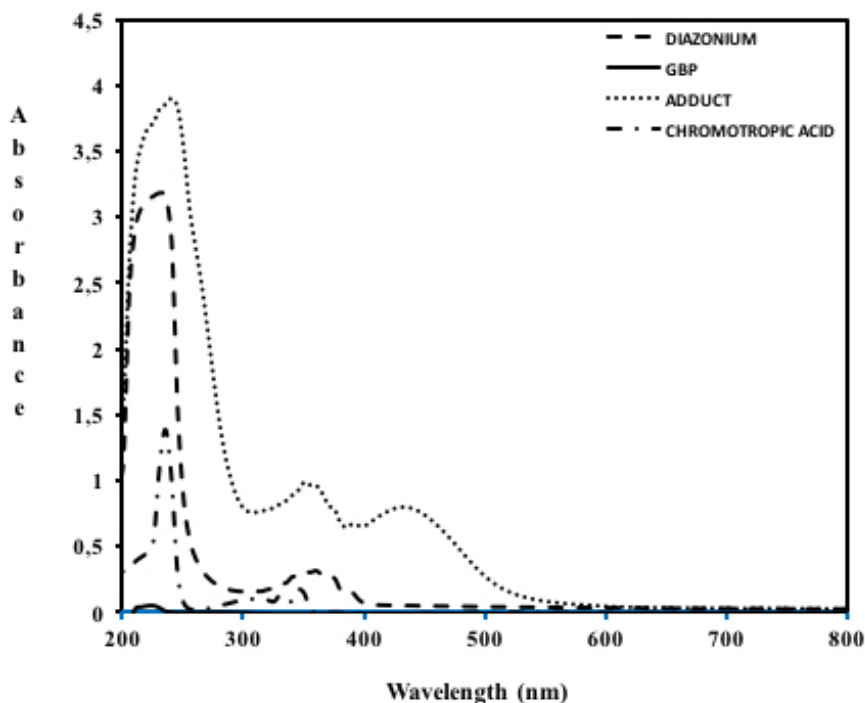
**Figure 1.** Overlaid spectra of gabapentin, the diazonium, CTA and adduct solutions

Optimization of critical response parameters

The optimization of diazotization conditions for gabapentin is necessitated by the fact that being an aliphatic amine, gabapentin lacks aromatic π electrons that can stabilize, via delocalisation, the resultant positive charge on its diazonium. The conversion of the free amino group in the drug to the diazonium was therefore monitored by absorbance changes with increasing concentrations of sodium nitrite as shown in figure 2. The plateau in the absorbance observable at 0.3 M and beyond of sodium nitrite concentration as well as the presence of free nitrous acid after the optimal diazotization time of 20 mins is indicative of the completion of the diazotization process. The results of the variation of acidity on the diazotization process also revealed optimal volume and concentration of 0.1 mL and 2.0 M HCl respectively. Further increase in the volume of the acid solution resulted in a decrease in absorbance as shown in figure 3. Increasing acidity beyond a critical point will be expected to impair diazotization because of the decreased solubility of the amino carboxylic acid drug as well as the permanent ionization of the amino functional group. The effect of CTA concentrations on the colour intensity of the azo adduct is depicted in figure 4. The results show that the optimal concentration is 0.3%w/v and this was adopted for subsequent work. Further increase in the
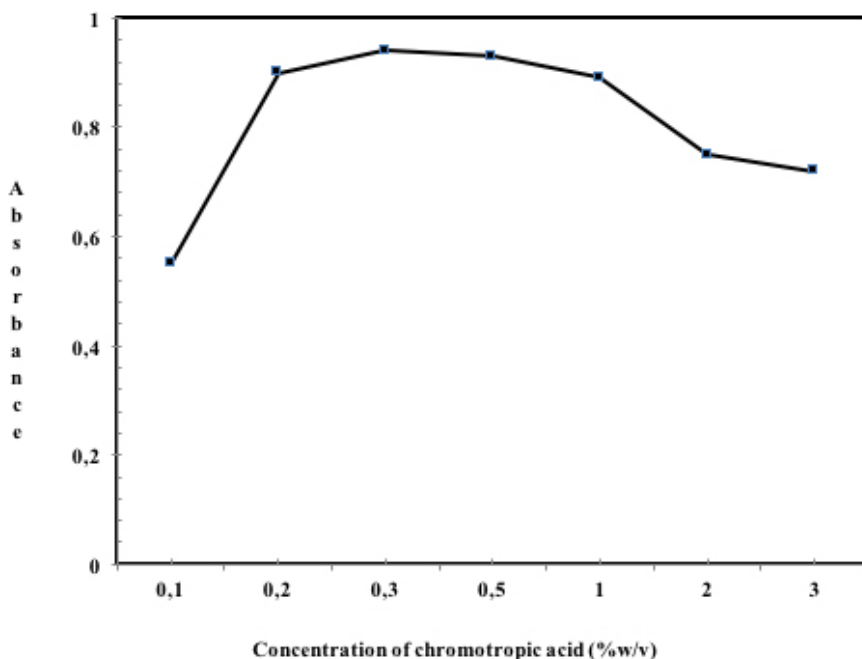
concentration led to a decline in absorptivity.
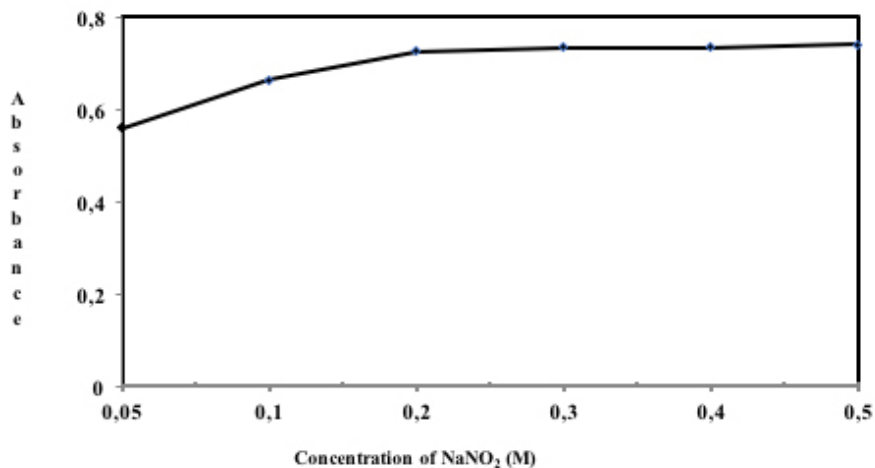
Figure 2. Variation in absorbance with concentration of sodium nitrite solution (1.604 μg/mL of gabapentin)
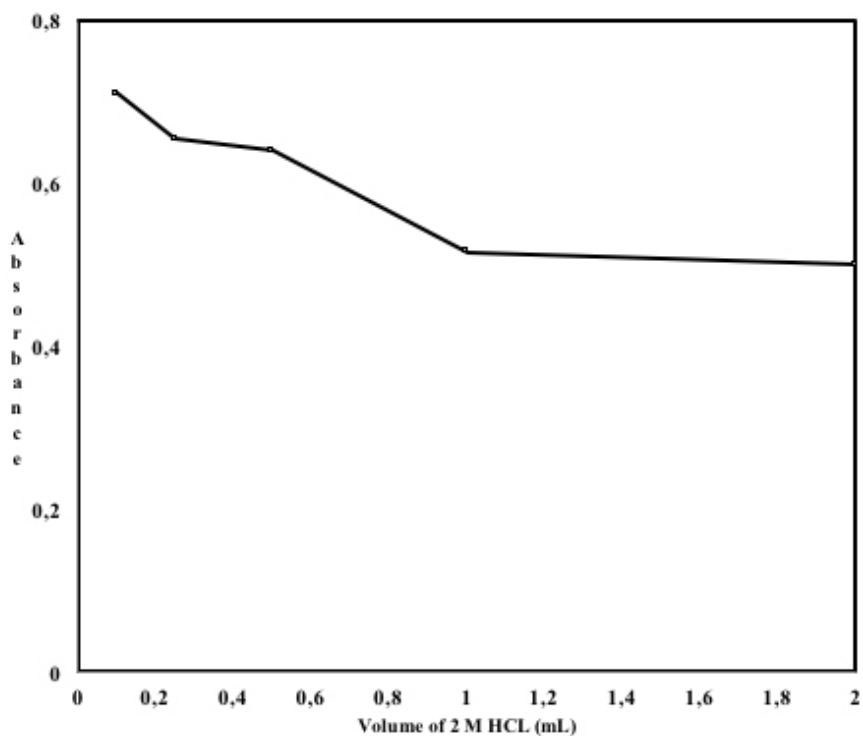

 Figure 3. Optimisation of HCl concentration in the diazotization process (1.604 μg/mL of gabapentin)

Figure 4. Effect of CTA concentration on the absorbance of adduct (1.604 µg/mL of gabapentin)

The method of steepest ascent was employed in establishing the optimal coupling temperature and time. The effect of temperature allowed for coupling reaction to take place as a function of time was carried out at temperature levels of 30, 50, 60 and 70°C. The results as depicted in figure 5 reveal that at 5 min reaction times, there is a gradual increase in the absorbance values as the temperature increased but, at 20 mins a decrease in absorbance was observed with temperature rise. This is most likely due to the thermal decomposition of the azo adduct. While an increase in temperature usually increases the rate of diazo coupling, it will also hasten the spontaneous breakdown of the less stable aliphatic diazonium leading to the formation of the azotate form which lack electrophilic character and therefore cannot couple. A decrease in the thermal stability of the adduct formed by an aliphatic diazonium, as is the case with gabapentin, is also expected. An optimal temperature of 30 °C was therefore selected for subsequent work. The optimal reaction time for the adduct formation was found to be 10 mins as no higher absorbance values were obtained with longer coupling times as shown in figure 6. The completion of the coupling reaction within 10 mins and at 30 °C also attests to the avidity of the reaction between the diazonium and the strongly activated CTA which contains two hydroxyl groups.

Amongst the compounds investigated for their suitability as dilution solvents, methanol gave the highest absorbance values and best correlation at the selected analytical wavelength as shown in figure 7. The suitability of methanol may be due to its ability to mop up excess water in the medium which may otherwise promote hydrolytic degradation of the azo adduct.
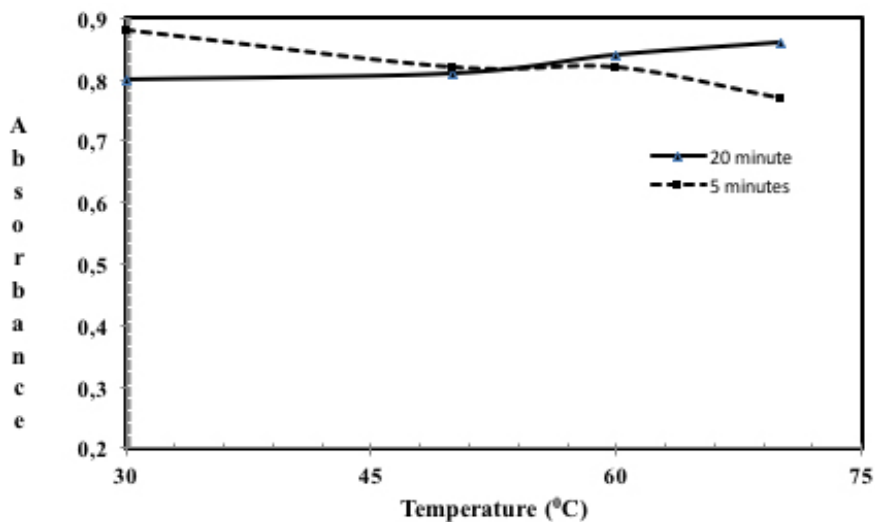
**Figure 5.** Optimisation of coupling temperature (1.604 µg/mL of gabapentin)
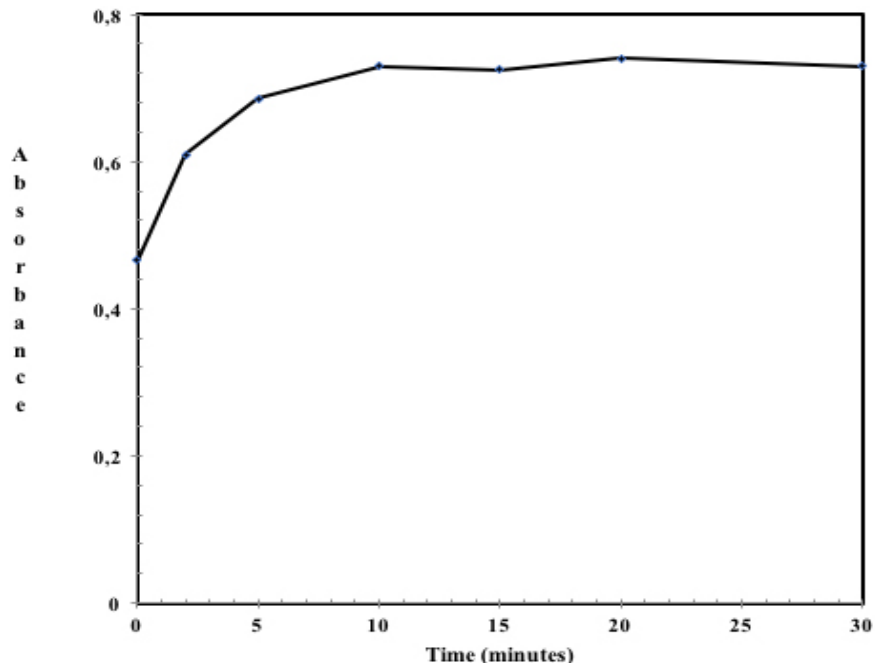
Figure 6. Optimisation of coupling time (1.604 µg/mL of gabapentin)
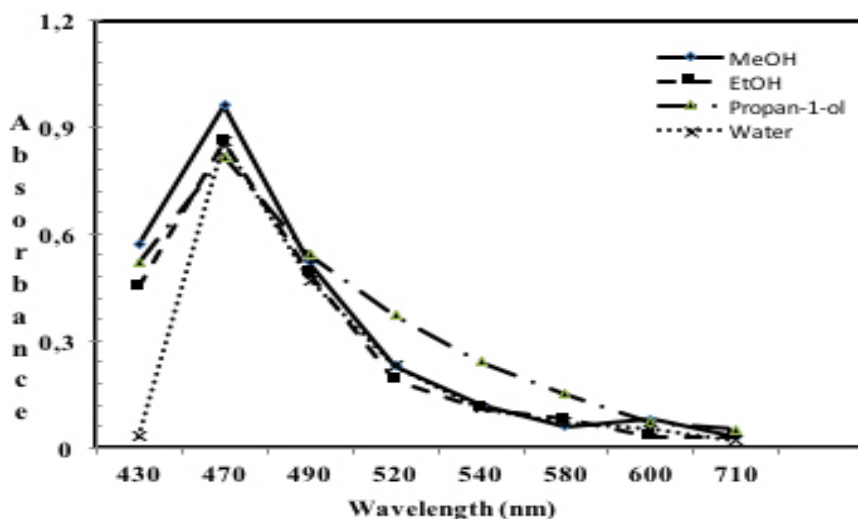
Figure 7. Optimisation of diluting solvents

## Stoichiometric ratio and mechanism of reaction

The variation of the absorbance values with the mole ratio of the coupling agent is depicted in figure 8. Maximum absorbance value was obtained when the diazonium and CTA combined in 1:1 ratio indicating the presence of only one diazotizable group in gabapentin as well as one accessible point of electrophilic attack on the coupling agent. This was also consistent with the observation that only one spot was obtained in the TLC analysis of the azo adduct. Similar 1:1 ratios and mono azo products were reported in a number of studies in which chromotropic acid was employed as coupling agent with diazotizable drugs[32-33].
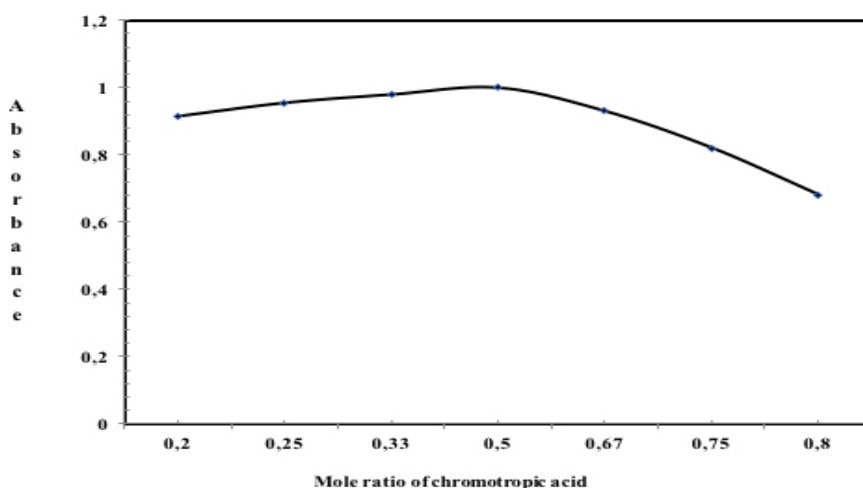
Figure 8. Variation of absorbance of adduct with mole fraction of chromotropic acid

However, unlike these reports that suggest that the point of electrophilic attack of the diazonium on CTA is on the carbon sandwiched between the sulphonic and the hydroxyl groups (in which case the stoichiometric ratio should be 2:1 as there are two of such chemically equivalent positions with little or no possibility of steric interference from each other), we propose that the electrophilic attack will be driven by the strongly activating effect of the hydroxyl group present on chromotropic acid and thus occur at its *para* position as depicted in scheme 1. The new azo substituent will sterically hinder the approach and attack of another diazonium ion on the *para* position of the *peri* (second) hydroxyl group. This mechanism is also in conformity with the well-documented observation that hydroxyl group on naphthyl rings are *ortho* and *para* directing when present at position 1 and 2 respectively and that substitution in between groups that are *meta* to each other (as is the case with the sulphonic and hydroxyl groups in CTA) is less probable due to steric effects[34]. Thus, a 1:1 ratio is observed.
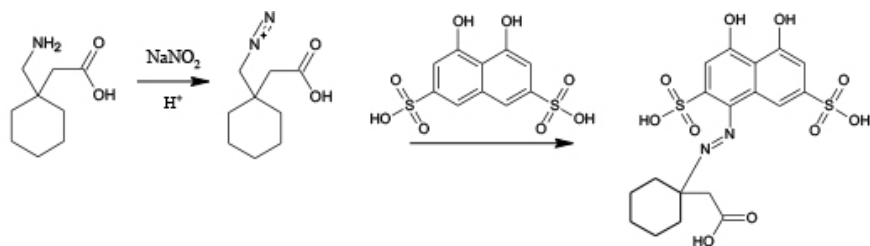
Scheme 1: Proposed coupling reaction pattern between diazotised gabapentin and chromotropic acid

The 3D optimization of the azo adduct is presented in figure 9 and it shows that the highly staggered arrangement of the chair conformational isomer of the alicyclic residue which would contribute to the stability of the azo adduct. The configurational arrangement of substituents around the azo linkage is also of the E-type which precludes steric interference between the t
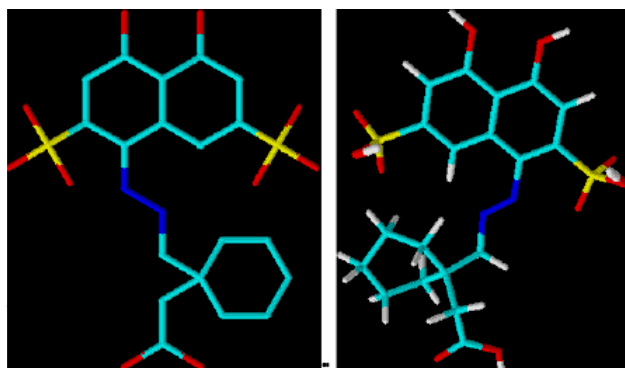

Figure 9. 3D optimization of the proposed azo adduct

Spectroscopic characterization of the azo adduct

A comparison of the IR spectra of gabapentin and the coupling product reveal the formation of a new chemical entity. IR data of gabapentin revealed the presence of twin absorption bands at 2857.14 and 2925.36 cm^{-1} which is characteristic of a primary amino functional group as well as well-defined bands at 3298.33 and 1662.91 cm^{-1} due to the stretching vibrations of the hydroxyl group and the carbonyl functional groups respectively. The most diagnostic feature of the formation of a new chemical entity is the disappearance of the bands of the amino group and the appearance of a new strong absorption band at 1600.00 cm^{-1} that can be attributed to the azo linkage. The broadening of the band previously at 3298.33 cm^{-1} which can now be observed at 3355.0 cm^{-1} in the new azo adduct confirms that the carboxylic acid group is now present in the azo adduct bringing about the OH$_{str}$.

Validation studies

The 3-day calibration revealed that absorbance increased linearly with concentration over the ranges 1.0 – 6.0 µg/mL at 470 nm with a correlation coefficient of 0.997. Other analytical and validation parameters are presented in Table 1.

Table 1. Analytical and validation parameters for the proposed method

Performance parameter	Value
Beer's law limit (µg/mL)	1.0-6.0
Limit of detection (µg/mL)	0.2864
Limit of quantification (µg/mL)	0.8679
Molar absorptivity (L mol^{-1} cm^{-1})	6.232x10^3
Sandell's sensitivity (µg cm-2)	27.48
Slope ± 95% CI	0.0595±0.0312
Intercept ± SD	0.0386±0.0038
Coefficient of determination	0.9982
Standard deviation of slope	1.42x10$^{(-3)}$
Standard deviation of intercept	3.42x10$^{(-3)}$
Interference liabilities (% gabapentin)	95.9±0.01 – 100.0±0.03

Accuracy, which is a measure of the closeness of the test results obtained by the method to the true value, was determined as the difference between the estimated and the reference values and expressed as percent recovery. The mean recoveries of the new method with replicate sample matrices spiked with the analyte are therefore indicated in table 2. The intra-day and inter-day variations at three different concentrations of the analyte were also determined using percentage relative standard deviation.

Table 2. Accuracy and repeatability assessment of the new method

Concentration (µg/mL)	Day 1a		Day 2 a		Day 3 a		Inter-day statistics b	
	Mean recovery (%)	RSD	Mean recovery	RSD	Mean recovery	RSD	Mean recovery	RSD
2	97.6±0.005	(%)	(%)	(%)	(%)	(%)	(%)	(%)
3.4	103.1±0.00	0.25	97.6±0.013	0.65	99.5±0.00	0	98.26±0.007	0.35
5	100.6±0.005	0.00	99.4±0.005	0.15	100.8±0.01	0.29	99.4±0.008	0.24
		0.10	100.4±0.01	0	102.1±0.01	0.12	102.5±0.007	0.14

[a] n=4; [b] n=12

The proposed method competes favourably with previously reported visible spectrophotometric methods for the assay of gabapentin in bulk and dosage forms.

As shown in table 2, the intra-day mean recovery of the method is 98.26–102.5% indicating good accuracy while the percentage relative standard deviation for the intra-day precision did not exceed 0.35% indicating excellent repeatability. For inter-day accuracy, the mean recovery was determined as 96.0–101.47% while the percentage relative standard deviation was 0.14–0.35%, indicating good reproducibility. The new method therefore showed greater accuracy and reproducibility when compared with the intra-day percent recovery values of 102.13-102.8% and the inter-day percent RSD values of 1.42-2.11% obtained using picric acid in the derivatization of gabapentin[10]. The new method also allowed determination at a wavelength longer than those obtained with the use of vanillin[12], 2,3-dichloro-5,6-dicyano-1,4-benzoquinone[35] or 7,7,8,8-tetracyanoquinodimethane[36] as chromogenic agents.

Method selectivity

The mean recoveries of the analyte in the presence of excipients varied from 95.9±0.01 to 100±0.03% showing the selectivity of the method (table 1), except with gelatin for which it returned abnormally high absorbance and recovery values. This is probably due to the acid and/or thermal catalysed degradation of the polypeptide into amino acids which causes dispersion in the reaction mixture.

Analytical signal stability

Over the entire test period of seventy hours, the responses obtained from the two groups of samples were relatively constant corroborating the sufficient stability of the azo adduct to permit accurate and convenient quantification of the analyte.

Application to dosage form analysis

The mean recoveries of the analyte from three commercial brands of gabapentin using the new method and a reference titrimetric method were carried out and are depicted in table 3. A statistical comparison between the mean recoveries using the Student t test did not reveal any significant difference in the mean recoveries obtained with the two methods. Similarly, there was no statistical difference in their variances as estimated by the F test. This establishes that the new method can therefore serve as a suitable alternative as there are no statistical differences in their accuracy and precision. In addition, the new method in comparison to majority of previously reported methods is simple, fast and employs readily available non-toxic reagents. The LOD and LOQ are low and would permit the determination of the analyte when present in minute amounts in sample matrices. The derivatization and signal acquisition did not require prior solvent extraction or the strict control of pH with the use of buffers.

Table 3. Comparative mean recoveries of analyte using the new and reference methods

Drug Formulation	New Method[a]		Reference Method[a]		Statistics (p-values)[c]	
	%Recovery ± SD [b]	RSD (%)	%Recovery ± SD	RSD (%)	F-test	T-test
TEVA	100.7 ± 0.01	0.24	102.0 ± 2.83	2.77	0.61	0.76
Biopentin	100.8 ± 1.08	0.24	102.0 ± 2.83	2.77	0.62	0.69
Akobal-G	99.5 ± 0.001	0.18	98.83 ± 0.41	0.41	0.53	0.75

[a] *Mean value, n = 6. % Content of gabapentin stated by USP Pharmacopoeia ranges from 90% to 110%*

[b] *% recovery calculated as a function of amount of sample utilized*

[c] *Statistical analyses done between the results obtained from the proposed method and the Reference method*

CONCLUSION

A new visible spectrophotometric method for the assay of gabapentin in bulk and dosage forms has been developed. The new method offers the advantages of being fast, reliable, sensitive and sufficiently accurate to serve as a suitable alternative to reference methods.

REFERENCES

1. Jacobs, K.M.; Kharazia, V.N.; Prince, D.A. Mechanisms underlying epileptogenesis in cortical malformations. *Epilepsy Res.* **1999,** 36(2-3), 165-188.

2. Shafer P.O.; Sirven J.I. 2013. Epilepsy statistics. Retrieved April 18, 2018 from https://www.epilepsy.com/learn/about-epilepsy-basics/epilepsy-statistics

3. WHO 2018. Epilepsy. Retrieved April 18, 2018 from http://www.who.int/mediacentre/factsheets/fs999/en/

4. Goldenberg, M.M. Overview of Drugs Used For Epilepsy and Seizures: Etiology, Diagnosis, and Treatment. *Pharm. Ther.* **2010,** 35(7), 392-415.

5. Ibrahim, G.M.; Rutka, J.T.; Snead, O.C. Epilepsy surgery in childhood: no longer the treatment of last resort. *CMAJ* **2014,** 186(13), 973-974.

6. Williams, T.J.; Cervenka, M.C. The role for ketogenic diets in epilepsy and status epilepticus in adults. *Clin. Neurophysiol. Pract.* **2017,** 2, 154-160.

7. Mattson, R.H. Drug treatment of uncontrolled seizures. *Epilepsy Res.* **1992,** 5, 29-35.

8. Zambon, E.; Giovanetti, R.; Cotarca, L.; Pasquato, L. Mechanistic investigation on 2-aza-spiro [4, 5] decan-3-one formation from 1-(aminomethyl) cyclohexylacetic acid (gabapentin) *Tetrahedron* **2008,** 64(28),6739-6743.

9. Zour, E.; Lodhi, S.A.; Nesbitt, R.U.; Silbering, S.B.; Chaturvedi, P.R. Stability studies of gabapentin in aqueous solutions. *Pharm. Res.* **1992,** 9(5), 595-600.

10. Abdulrahman, S.A.M.; Basavaiah, K. Sensitive and selective spectrophotometric determination of gabapentin in capsules using two nitrophenols as chromogenic agents. *Int. J. Anal. Chem.* **2011,** 2011.

11. Siddiqui, F.A.; Sher, N.; Shafi, N.; Shamshad, H.; Zubair, A. Kinetic and thermodynamic spectrophotometric technique to estimate gabapentin in pharmaceutical formulations using ninhydrin. *J. Anal. Sci. Technol.* **2013,** 4(1), 17.

12. Abdellatef, H.E.; Khalil, H.M. Colorimetric determination of gabapentin in pharmaceutical formulation. *J. Pharm. Biomed. Anal.* **2003,** 31(1),209-214.

13. Ulu, S.T.; Kel, E. Sensitive spectrofluorimetric method of analysis for gabapentin in pure and pharmaceutical preparations. *Chin. J. Chem.* **2011,** 29(3), 562-566.

14. Belal, F.; Abdine, H.; Al-Majed, A.; Khalil, N.Y. Spectrofluorimetric determination of vigabatrin and gabapentin in urine and dosage forms through derivatization with fluorescamine. *J. Pharm. Biomed. Anal.* **2002,** 27(1-2),253-260.

15. Sandhya, S.M.; Jyothisree, G.; Babu, G. Analysis of gabapentin by HPTLC with densitometric measurement after derivatization. *Int. J. Pharm. Pharm.* **2014,** 6,707-710.

16. Martinc, B.; Roškar, R.; Grabnar, I.; Vovk, T. Simultaneous determination of gabapentin, pregabalin, vigabatrin, and topiramate in plasma by HPLC with fluorescence detection. *J. Chromatogr.* B **2014,** 962,82-88.

17. Fonseca, F.; Brito de Barros, R.; Ilharco, L.M.; Garcia, A.R. Spectroscopic methods for quantifying gabapentin: framing the methods without derivatization and application to different pharmaceutical formulations. *Appl. Spectrosc.* **2017,** 71(11),2519-2531.

18. Abdulrahman, S.A.M.; Basavaiah, K. Non-aqueous titrimetric assay of gabapentin in capsules using perchloric acid as titrant. *Chem. Ind. Chem. Eng. Q* **2011,** 17(2), 173-178.

19. Sekar, R.; Azhaguvel, S. Indirect photometric assay determination of gabapentin in bulk drug and capsules by capillary electrophoresis. *J. Pharm. Biomed. Anal.* **2004,** 36(3),663-667.

20. Ulu, S.T.; Kel, K. Highly sensitive determination and validation of gabapentin in pharmaceutical preparations by HPLC with 4-fluoro-7-nitrobenzofurazan derivatization and fluorescence detection. *J. Chromatogr. Sci.* **2011,** 49, 417-421.

21. Lakshmi, B. RP-HPLC method development for the quantitation of gabapentin in formulations. *Int. J. Sci. Techn.* **2012,** 2(1),84-92.

22. Gujral, R.S.; Haque, S.M. Development and validation of a new HPLC method for the determination of gabapentin. *Int. J. Biomed. Sci.* **2009,** 5(1),63-69.

23. Ebrahimzadeh, H.; Yamini, Y.; Firozjaei, H.A.; Kamarei, F.; Tavassoli, N.; Rouini, M.R. Hollow fiber-based liquid phase microextraction combined with high-performance liquid chromatography for the analysis of gabapentin in biological samples. *Anal Chim Acta* **2010,** 665(2), 221-226.

24. Zhu Z.; Neirinck, L. High-performance liquid chromatographic method for the determination of gabapentin in human plasma. *J. Chromatogr. B* **2002,** 779(2), 307-312

25. Chung, T-C; Tai, C-T.; Wu, H-L. Simple and sensitive liquid chromatographic method with fluorimetric detection for the analysis of gabapentin in human plasma. *J Chromatogr A* **2006,** 1119(1-2),294-298.

26. Uboh, C.E.; Liu, Y.; Soma, L.R.; Li, X.; Guan, F.; You, Y.; Rudy; J.A., Chen, J. Analysis of gabapentin in equine plasma with measurement uncertainty estimation by liquid chromatography-tandem mass spectrometry. *J. Anal. Toxicol.,* **2011,** 35, 75-84.

27. Kushnir, M.M.; Crossett, J.; Brown, P.I.; Urry, F.M. Analysis of gabapentin in serum and plasma by solid-phase extraction and gas chromatography-mass spectrometry for therapeutic drug monitoring. *J. Anal. Toxicol.,* **1999,** 23(1), 1-6.

28. Sadones, N.; Bever, E.V.; Bortel, L.V.; Lambert, W.E.; Stove C.P. Dried blood spot analysis of gabapentin as a valid alternative for serum: a bridging study. *J. Pharm. Biomed. Anal.,* **2017,** 132, 72-76.

29. Karnes, H.T.; March, C. Precision, accuracy and data acceptance criteria in biopharmaceutical analysis. *Pharm. Res.* **1993,** 10, 1420-1426.

30. Rose, J., *Advanced Physico-Chemical Experiments*. Pitman: London, **1964**; p 52

31. United States Pharmacopoeia 24/National Formulary 19. US Pharmacopoeial Convention: **1999**; pp 2150-2151.

32. Darweesh, S.A.; Al-Haidari, I. M.A.; Mohammed, A.K.; Dikran, S.B. Spectrophotometric determinations of sulfacetamide following simple diazotization and coupling with chromotropic acid. *Ibn AL-Haitham J. Pure Appl. Sci.* **2017,** 26(3), 281-295.

33. Revanasiddappa, H.D.; Veena, M.A. Spectrophotometric determination of mosapride in pure and pharmaceutical preparations. *Eclét. Quím.* **2007,** 32(4),71-75.

34. Morrison, R.T.; Boyd, R.N., *Organic Chemistry*. 6th ed.; Prentice-Hall: New Jersey, **1992.**

35. Salem, H. Analytical study for the charge-transfer complexes of gabapentin. *Afri. J. Pharm. Pharmacol.* **2008,** 2(7), 136-144.

36. Siddiqui, F.A.; Arayne, M.S.; Sultana, N.; Qureshi, F.; Mirza, A.Z.; Zuberi, M.H.; Bahadur, S.S.; Afridi, N.S.; Shamshad, H.; Rehman, N. Spectrophotometric determination of gabapentin in pharmaceutical formulations using ninhydrin and π-acceptors. *Eur. J. Med. Chem.* **2010,** 45(7), 2761-2767